

TR 85059

UNLIMITED

BR 99456

TR 85059

ICAF Doc No 1613

DTIC FILE COPY



ROYAL AIRCRAFT ESTABLISHMENT

Technical Report 85059

June 1985

**A COMPARISON OF THE FATIGUE
PERFORMANCE OF WOVEN AND
NON-WOVEN CFRP LAMINATES**

by

P. T. Curtis
B. B. Moore

DTIC
ELECTE
JAN 15 1988
S H D

Procurement Executive, Ministry of Defence
Farnborough, Hants

DISTRIBUTION STATEMENT A

Approved for public release;
Distribution Unlimited

UNLIMITED

87 12 29 021

AD-A188 070

UDC 621-419 : 661.66-426 : 678.046 : 539.431

ROYAL AIRCRAFT ESTABLISHMENT

Technical Report 85059

Received for printing 20 June 1985

A COMPARISON OF THE FATIGUE PERFORMANCE OF WOVEN
AND NON-WOVEN CFRP LAMINATES

by

P. T. Curtis

B. B. Moore

SUMMARY

Static and fatigue tests were carried out at room temperature on CFRP laminates with five lay-ups, of both woven and non-woven CFRP. S-N diagrams were produced for both zero-tension and reversed axial loading. Damage development was monitored by optical microscopy, ultrasonic C-scanning, video recording and infra-red thermography.

Carbon fibre reinforced plastics made with woven fabric rather than non-woven material, had significantly poorer static and fatigue performance than non-woven material, due to distortion of the load carrying 0° fibres. When woven fabric was oriented at 45° to the load direction the tensile static and fatigue performance was slightly better than in non-woven ±45° material. Replacing the ±45° layers of a (±45.0) laminate with woven fabric had little effect on the static or fatigue strength.

In non-woven material, notched coupons under fatigue loading did not show the notch sensitivity that was so significant under static loading. However in woven material, because of the additional fatigue degradation processes associated with low crossover points in the weave, holed coupons never quite achieved notch insensitivity in fatigue.

Departmental Reference: Materials/Structures 133

Copyright ©, Controller HMSO, London 1985



By	
Distribution/	
Availability Codes	
Avail and/or	
Special	
A-1	

LIST OF CONTENTS

	<u>Page</u>
1 INTRODUCTION	3
2 EXPERIMENTAL DETAILS	3
3 RESULTS	5
3.1 Static tests	5
3.2 Zero-tension fatigue tests	5
3.2.1 Lay-up A {0,90,90,0} _s	5
3.2.2 Lay-up B {±45,±45} _s	6
3.2.3 Lay-up C {±45,0,90} _s	7
3.2.4 Lay-up D {0,90,±45} _s	7
3.2.5 Lay-up E {±45,02} _s	8
3.3 Reversed axial fatigue	9
3.3.1 Lay-up A {0,90,90,0} _s	9
3.3.2 Lay-up C {±45,0,90} _s	10
3.3.3 Lay-up D {0,90,±45} _s	11
3.3.4 Lay-up E {±45,02} _s	11
4 DISCUSSION	12
4.1 Static tests	12
4.2 Zero-tension fatigue tests	15
4.3 Reversed axial fatigue tests	18
5 CONCLUSIONS	23
Acknowledgment	24
Tables 1 to 14	25
References	37
Report documentation page	
	inside back cover

1 INTRODUCTION

Increasing use is being made of carbon fibre reinforced plastics (CFRP) in the aerospace industry because of their combination of high stiffness and high strength with low density and potentially low unit cost. In addition, the fatigue performance of CFRP has been shown to be very good, being superior to many other materials including metals¹.

At present, most carbon fibre reinforced epoxy resin laminates are made from non-woven unidirectional pre-impregnated sheets. This material is beginning to find extensive use in military aerospace applications, initially in class 2 structures but more recently in class 1 structures as in the McDonnell Douglas AV8B and F-18 aircraft^{2,3}.

Recently, good quality woven carbon fibre cloth has been obtainable and prepreg manufacturers are now able to supply woven carbon fibre prepregs. Many types of weave are available such as, plain, twill and satin, but work on GRP and early work with woven CFRP⁴ has shown that weaves with less fibre distortion, such as satin weaves (in particular five or eight shaft satin weaves for CFRP), result in smaller reductions in mechanical properties.

The main reasons for the use of woven fabric are the ease of handling which lends itself to automation and consequent reductions in labour, the ability of fabric to conform to complex shapes and the fabric has more isotropic in-plane properties compared with unidirectional material. In addition, woven CFRP can result in better containment of impact damage and improved residual properties after impact compared with non-woven material^{5,6}.

At present there is a significant gap in our knowledge of the behaviour of composites made with carbon fibre fabric, particularly compared with non-woven material. In this Report the findings of a programme comparing the fatigue response of laminates fabricated from woven and non-woven CFRP are presented. Since previous work had shown that laminates with only the $\pm 45^\circ$ layers replaced by woven fabric showed superior impact performance to non-woven laminates^{5,6}, these were also included for study in this programme of work. The full S-N behaviour of five lay-ups has been characterised, in both tensile and reversed axial loading in the plain and notched conditions, and damage development studied using optical microscopy, ultrasonic C-scanning and infra-red thermography.

2 EXPERIMENTAL DETAILS

Laminates were moulded from both woven and non-woven pre-impregnated sheets of high strength Toray T300 carbon fibres in Ciba-Geigy BSL914C epoxy resin. The carbon fibre fabric was a balanced five shaft satin weave, woven with 3000 filament tows of the same fibre type used in the non-woven material, but including a fine tracer tow of Kevlar 49 fibres every 50 mm. In this weave about 80% of the fibres in one direction lie on one side of the cloth and correspondingly about 80% of the fibres lie at right angles on the other side of the cloth. Since one prepreg sheet of woven material was approximately twice as thick (0.267 mm) as a ply of non-woven material (0.125 mm), each sheet of cloth was thus similar to two plies of non-woven unidirectional prepreg stacked at 90° to each other as in a (0,90) or (± 45) lay-up.

4

Symmetrical woven and non-woven laminates with equivalent stacking sequences were made up, each approximately 1 mm thick, with five types of lay-up as listed below.

- A (0,90,90,0)_s
- B (±45,±45)_s
- C (±45,0,90)_s
- D (0,90,±45)_s
- E (±45,02)_s

The woven prepreg was stacked so that the dominant fibre direction on each face of the cloth corresponded with the appropriate direction in the non-woven stacking sequence. In (0,90,±45) laminates with 50% 0,90 layers and 50% ±45 layers the stacking sequence was varied so that either the ±45° layers or the 0,90 layers were on the laminate surface. In addition, (±45,0) laminates (lay-up E) were made from both non-woven material and from a mixture of woven and non-woven plies; the 0 layers were of non-woven material and the ±45° layers were of woven material.

The laminates were cured in an autoclave to 170°C and postcured for 4 hours at 190°C. The quality of the laminates was checked using ultrasonic C-scanning equipment. All the laminates with woven carbon fibre fabric were 12-17% thicker than the equivalent non-woven laminates. Approximately 10% of this difference in thickness was due to the lower volume fraction of the woven carbon fibre laminates and the remainder was due to the fabric containing more fibre by weight than two non-woven plies. The laminates were stored in a controlled environment at 23°C and 65% relative humidity for at least 3 months prior to testing. The moisture content after this time was approximately 1%.

Tests were carried out on coupons 250 mm long, with the warp fibres (along the length of the fabric) parallel to the 0 load direction in the 0,90 woven layers (previous work had shown no significant difference between warp and weft properties⁵). Coupons 250 mm long and 20 mm wide were cut from the laminates, except for lay-up B (±45) for which coupons 40 mm wide were used to obtain sufficient loads to preserve fatigue machine controllability. Notched coupons each contained a central 4mm diameter hole. Etched aluminium alloy end plates were bonded to the abraded ends of all coupons using a two part epoxy based adhesive cured at room temperature.

Static tests and constant amplitude fatigue tests were performed using servo-hydraulic fatigue machines, in both zero-tension ($P \pm P$) and reversed axial ($0 \pm P$) loading (except for lay-up B which was tested in tensile loading only). Static tests were performed in position control at a ram speed of between 1.5 mm/min and 2.5 mm/min and fatigue tests in load control at frequencies of between 5 and 20 Hz depending on the sensitivity of the lay-up to hysteresis heating. Ultrasonic C-scan and optical microscopy were used to study the development of damage during fatigue loading. The compression testing was carried out on relatively long coupons supported with an anti-buckling guide which provided continuous edge restraint (Fig 1). Previous work⁷ had shown that this particular anti-buckling guide provided effective restraint against gross buckling and did not induce uncharacteristic failures due to stress concentrations associated with the guides.

The development of damage in some of these specimens during fatigue loading was studied using ultrasonic C-scanning and optical microscopy. Some coupons had their edges polished for examination by optical microscopy. Tests were then performed at the fatigue stress level that gave a mean lifetime of 100000 cycles, and were stopped after 1000, 10000 and 50000 cycles for assessment of the damage state of the coupons. Damage development during the tests was also studied using an optical video camera and an infra-red thermography system.

3 RESULTS

3.1 Static tests

The results of the static tests on all lay-ups, for tensile and compressive loading, of both plain and holed coupons, woven and non-woven, are given in Tables 1 to 5. In all lay-ups the plain coupons, both woven and non-woven, failed at random along their lengths, but holed coupons all failed through the holes. No visible damage was observed before failure except in the tensile tests on lay-up B where both woven and non-woven coupons developed necked regions in the gauge length at approximately 70% of their failure load.

3.2 Zero-tension fatigue tests

3.2.1 Lay-up A {0,90,90,0}_s

Results of the fatigue tests are given in Table 6 and also as a plot of peak stress versus log-life (S-N plot) in Fig 2. Stresses are plotted on a net area basis, as they are throughout this Report. Coupons failed at random positions along their lengths, except for the holed coupons which all failed through the holes. Plain non-woven coupons developed extensive longitudinal splits at their edges in the 0° plies. This became more extensive with increasing numbers of cycles. Holed non-woven coupons also showed evidence of longitudinal splitting of the surface plies at a tangent to the hole edges. Although some longitudinal splitting was also observed at the edges of the woven coupons, it was far less extensive and never developed to the same degree as in the non-woven coupons.

Optical microscopy of plain coupons revealed longitudinal edge cracks along the edges of the non-woven coupons after 1000 cycles at the stress level that gave a mean life of 100000 cycles, but no similar damage was observed in the woven coupons. Both woven and non-woven coupons developed extensive transverse cracks across the 90° layers early in the tests and these tended to initiate delamination after large numbers of fatigue cycles. Delamination was more noticeable in the non-woven material. In the woven coupons there was frequently evidence of the 90° surface tows in the outer 0,90 layers splitting away in places from the 0° tows.

A few coupons from each batch were ultrasonically C-scanned after 1000, 10000 and 50000 cycles at the stress level that gave a mean fatigue life of 100000 cycles, and thereafter at intervals of 50000 cycles until failure. These revealed an overall lightening of the traces with increasing numbers of fatigue cycles, for both woven and non-woven coupons, although the effect was more marked in the woven coupon (Figs 3 and 4) in which light areas developed at the tow crossover points in the weave. After 50000 cycles, woven coupons were frequently white when scanned relative to the same initial panel attenuation

indicating the attenuation of the ultrasonic signal had increased by more than 3 dB throughout the coupon. C-scans of the holed non-woven coupons showed evidence of damage development around the holes, becoming quite extensive after large numbers of cycles, spreading up to half the length of the coupons (Fig 5). The holed woven coupons behaved similarly, except that the damage was less extensive (Fig 6).

3.2.2 Lay-up B ($\pm 45^\circ$, $\mp 45^\circ$)

Results of the fatigue tests on lay-up B are given in Table 7 and also as a plot of peak stress versus log-life (S-N plot) in Fig 7. It is clear that in these S-N curves the percentage loss of static strength with increasing fatigue lifetime was greater than in the 0,90 laminates. All four curves were similar, except that the woven $\pm 45^\circ$ material, both plain and holed, gave longer lifetimes at the lower fatigue stresses. All holed coupons failed through the holes, but plain non-woven coupons showed a tendency to fail 2 cm to 3 cm from either end, although several failures did occur away from the ends. Failure occurred in the non-woven coupons by cracking at $+45^\circ$ and -45° , both along and across fibres, with considerable edge cracking and delamination. Failures were contained, spreading only a few centimetres along the gauge lengths. Woven coupons failed cleanly at $+45^\circ$, with -45° fibres failing along the $+45^\circ$ fracture line. Failures were even more contained than in the non-woven material, there being no visible evidence of damage away from the fracture line.

Optical microscopy of plain coupon edges during testing at the stress level that gave a mean life of 100000 cycles revealed edge delamination cracking in non-woven coupons after 1000 cycles as well as translaminar cracking (Fig 8). This became more extensive after 10000 and 50000 cycles, with delamination being particularly noticeable (Fig 8), failure occurring by the linking of delamination and translaminar cracks. All woven coupons, in particular the $\pm 45^\circ$ coupons, showed poor fibre distribution compared with non-woven material. Fibres were packed closely together in the tows with large resin rich regions between. After 1000 cycles of fatigue loading, cracks had developed around several of the fibre tows, these becoming more extensive by 10000 and 50000 cycles with the development of translaminar cracks (Fig 9). There was no extensive delamination spanning long sections of the gauge length as in the non-woven material. Failure occurred by the linking of translaminar cracks and cracks around fibre tows.

Ultrasonic C-scanning of coupons tested at the stress level that gave a mean life of 100000 cycles revealed the development of damage zones close to the grips in the plain non-woven coupons (Fig 10). Failure frequently occurred at one of these sites. The effect was not observed in the holed non-woven coupons, which showed instead the development of a damage zone around the holes (Fig 11) leading to subsequent failure through the holes. There was no overall lightening of the C-scans with increasing numbers of cycles as observed in the (0,90) coupons. The woven coupons did, however, exhibit a noticeable lightening of the C-scans with increasing numbers of cycles (Fig 12). As in the plain non-woven coupons there was evidence of the development of damage zones close to the ends, but damage also developed more generally, particularly at $+45^\circ$ and -45° to the coupon axis, and failure occurred away from the ends. The holed woven coupons also showed an overall lightening of the C-scans with increasing numbers of cycles, as well as a

lightening close to the coupon ends (Fig 13). Damage was also observed around the holes, this taking the form of a cross shape at $\pm 45^\circ$, failure then occurring along one of the arms of the cross (Fig 13).

3.2.3 Lay-up C ($\pm 45, 0, 90$)_s

Results of the fatigue tests are given in Table 8 and also as a plot of peak net stress versus log-life (S-N plot) in Fig 14. Plain coupons all failed at random positions along their lengths but holed coupons all failed through the holes. Longitudinal edge cracking was visible in some coupons, mainly in the plain non-woven coupons. Woven coupons did develop edge cracks but at greater lifetimes than the non-woven coupons.

Optical microscopy of plain non-woven coupons revealed transverse 90° layer cracks initiated early in the test, probably during the first few loading cycles. These initiated edge cracking between the 0 and 90° layers at larger numbers of cycles (Fig 15). Delamination between the ± 45 layers was also observed at short lifetimes, cracking across the 45° layers occurring at greater numbers of cycles.

Optical microscopy of the woven coupons revealed slightly different behaviour (Fig 16). Transverse cracks formed across individual 90° tows early in the tests followed by edge cracks in the 90° tows and at 0/ 90° interfaces. In addition, because of the woven nature of the plies, the 90° tows were often adjacent to the $\pm 45^\circ$ layers and edge cracking was also observed at these interfaces. Cracking was especially apparent in the resin rich regions between the woven tows. Close to failure, fractured 0° fibres or tows were also observed.

Ultrasonic C-scanning of non-woven coupons tested at the stress level corresponding to failure after 100000 cycles revealed light lines across the coupons after 1000 cycles, probably caused by short lengths of delamination at the ends of transverse cracks (Fig 17). At increased numbers of cycles a lightening of the edges was observed which spread across the coupon width towards the middle. Holed coupons showed less edge whitening and no transverse lightening, but did exhibit lightening around the holes (Fig 18). This eventually linked up with the edge lightening and commenced spreading longitudinally along the coupons.

Ultrasonic C-scanning of plain woven coupons revealed an overall lightening with increasing numbers of cycles and the gradual development of lighter spots at the tow crossover points in the weave (Fig 19). These frequently linked up to form bands, but failure never occurred along these bands. A few transverse light lines were observed as in the non-woven material, as well as edge lightening, although this was not as extensive as in the non-woven material. Holed woven coupons also exhibited some edge lightening (Fig 20) and there was evidence of the development of light spots but less obvious than in the plain woven coupons. Light areas developed around the holes and, as in the non-woven coupons, eventually linked up with the edge lightening.

3.2.4 Lay-up D (0, $90, \pm 45$)_s

Results of the fatigue tests are given in Table 9 and also as a plot of peak net stress versus log-life (S-N plot) in Fig 21. Plain coupons all failed at random positions

along their lengths but holed coupons all failed through the holes. Longitudinal edge cracking was less obvious than in coupons with lay-up C. No other damage was visible during testing.

Optical microscopy of plain non-woven coupons revealed transverse 90° layer cracks, probably initiated during the first few loading cycles, which generated edge cracks in the 90° layers at higher numbers of cycles (Fig 22), but these were less extensive than in lay-up C. Delamination between the $\pm 45^\circ$ layers was also observed, after approximately 10000 cycles, followed by extensive cracking across the 45° layers and 0/90 and 90/45 delamination at greater numbers of cycles.

Optical microscopy of the woven coupons revealed slightly different behaviour (Fig 23). Transverse cracks formed across individual 90° tows early in the tests as well as 0/90 delamination between individual tows. Limited edge cracks developed in the 90° tows and at 0/90 interfaces. After 50000 cycles delamination was visible between $+45^\circ$ and -45° tows and damage in the 90° plies became quite extensive, especially in resin rich regions between the tows. Damage in the 45° plies appeared to be less extensive than in the non-woven coupons.

Ultrasonic C-scanning of non-woven coupons tested at the stress level corresponding to failure after 100000 cycles revealed no transverse lightening as seen in coupons from lay-up C. After 10000 cycles some edge lightening was observed (Fig 24) followed by lightening at 45° across the coupons but by 100000 cycles a more general lightening of the coupons was observed and close to the edge the lightening had extended almost across the full coupon widths in places. Holed coupons exhibited some edge lightening after large numbers of cycles but no transverse lightening, although they did exhibit lightening around the holes (Fig 25). This eventually linked up with the edge lightening and commenced spreading longitudinally along the coupons.

Ultrasonic C-scanning of plain woven coupons revealed an overall lightening with increasing numbers of cycles and the gradual development of lighter spots along the lines of intersection of woven tows (Fig 26), as in coupons from lay-up C, but no transverse light lines. Edge lightening was apparent, but this was very limited and never extended more than 1-2 mm from the coupon edges. Holed coupons showed more interesting behaviour with some edge lightening developing after 50000 cycles (Fig 27) together with evidence of light spots, albeit less obvious than in the plain woven coupons. The light areas that developed around the holes, as in the non-woven coupons, eventually linked up with the edge lightening and spread longitudinally along the coupon edges but not above or below the hole. At large numbers of cycles some intense white spots formed away from the hole area.

3.2.5 Lay-up E ($\pm 45, 02$)_g

Results of the tensile fatigue tests are given in Table 10 and presented as S-N curves in Fig 28. All plain coupons failed at random positions along their lengths and holed non-woven coupons also failed away from the holes. Holed woven coupons failed through the holes at short lifetimes but those coupons surviving to long lifetimes failed away from the holes. Both woven and non-woven coupons showed evidence of edge splitting and delamination at long lifetimes.

Optical microscopy of plain woven and non-woven coupons revealed $\pm 45^\circ$ delamination and translaminar cracking after only 1000 cycles (Fig 29). This became more extensive after 10000 and 100000 cycles (Figs 29 and 30). Above 100000 cycles there was evidence of fibre damage in the 0° fibres (Fig 30).

Ultrasonic C-scanning of plain non-woven coupons revealed little apart from a slight lightening after 1000 cycles and some evidence of damage growth around the coupon ends after large numbers of cycles (Fig 31). Holed non-woven coupons revealed damage around the holes after 10000 cycles (Fig 32) which grew longitudinally to a distance of several hole diameters after one million cycles. Eventually the damage reached the coupon ends and had also grown across the coupon width (Fig 32).

Ultrasonic C-scanning of plain woven coupons revealed only the gradual lightening and development of light spots with increasing numbers of fatigue load cycles observed in the other woven laminates (Fig 33). The holed woven coupons exhibited a similar effect to that observed in the non-woven coupons. Damage was observed around the hole after only 1000 cycles and grew longitudinally to a distance of several hole diameters after 100000 cycles (Fig 34). The damage did not extend quite as far as the grips but did grow across the coupon width.

3.3 Reversed axial fatigue

3.3.1 Lay-up A (0,90,90,0)

Results of the fatigue tests are given in Table 11 and also as a plot of stress amplitude versus log-life (S-N plot) in Fig 35. Stresses are plotted on a net area basis, as they are throughout this Report. All coupons failed at random positions along their lengths, except for the holed coupons which all failed through the holes. Plain non-woven coupons developed longitudinal splits at their edges in the 0° plies. This became more extensive with increasing numbers of cycles. Some longitudinal splitting was also observed at the edges of the woven coupons, but it was far less extensive and never developed to the same degree as in the non-woven coupons.

Optical microscopy of plain coupons revealed longitudinal interlaminar cracks along the edges of the non-woven coupons even before testing (Fig 36) and these became more pronounced after 1000 load cycles. Similar, but less extensive damage was observed in the woven coupons after 1000 cycles (Fig 37). Both woven and non-woven coupons developed transverse cracks across the 90° layers after loading. After 10000 cycles $0/90$ delamination was observed in the non-woven coupons (Fig 36) and fibre damage in the 0° plies. Woven coupons also exhibited $0/90$ delamination after large numbers of load cycles, but this was more localised than in the non-woven coupons being confined to individual tows of fibres by the woven nature of the material. Longitudinal splitting of the 0° edge fibres was also apparent in both woven and non-woven coupons (Figs 36 and 37).

A few coupons from each batch were ultrasonically C-scanned after 1000, 10000 and 50000 cycles at the stress level that gave a mean fatigue life of 100000 cycles, and thereafter at intervals of 50000 cycles until failure. Scans of the non-woven coupons became generally lighter with increasing numbers of fatigue cycles. Light lines developed across the scans after 10000 cycles, these spreading longitudinally at long lifetimes to

give a general lightening along the centre of the coupon width. Some limited edge lightening was also apparent (Fig 38). For woven coupons a slight lightening of the traces for woven coupons with increasing numbers of fatigue cycles was observed (Fig 39). Some edge lightening was observed at large numbers of cycles and also light lines across the scans. Coupons sometimes failed across one of these lines. C-scans of the holed woven coupons showed evidence of damage development around the holes, spreading two to three diameters distant after large numbers of cycles (Fig 40).

3.3.2 Lay-up C ($\pm 45, 0, 90$)

Results of the tension-compression fatigue tests are given in Table 12 and also as a plot of stress amplitude versus log-life (S-N plot) in Fig 41. Plain coupons all failed at random positions along their lengths but holed coupons all failed through the holes. Longitudinal edge cracking was visible, mainly in the plain non-woven coupons, although woven coupons did develop edge cracks but at greater lifetimes than the non-woven coupons.

Optical microscopy of plain non-woven coupons revealed some damage in untested coupons, mainly within the outer $\pm 45^\circ$ plies. Damage in the $\pm 45^\circ$ layers became quite extensive by 1000 cycles leading to 45/0 delamination (Fig 42). Some transverse layer cracks initiated early in the test, probably during the first few loading cycles, and then precipitated edge cracking between the 0° and 90° layers at higher numbers of cycles (Fig 42). Delamination between the 45/0 layers became very pronounced at large numbers of cycles.

Optical microscopy of the woven coupons revealed slightly different behaviour (Fig 43). Some cracking in the outer 45° plies was observed before testing. 0/90 delamination became quite extensive at large numbers of cycles. Transverse cracks formed across individual 90° tows early in the tests. Cracking was especially apparent in the resin rich regions between the woven tows.

Ultrasonic C-scanning of non-woven coupons tested at the stress level corresponding to failure after 10000 cycles revealed light lines across the coupons after 1600 cycles and even a few before testing, probably caused by short lengths of delamination at the ends of transverse cracks (Fig 44). At increased numbers of cycles a lightening of the edges was observed which spread across the coupon width towards the middle. Holed coupons showed less edge whitening and no transverse lightening, but did exhibit lightening around the holes (Fig 45). This eventually linked up with the edge lightening and spread longitudinally along the coupons.

Ultrasonic C-scanning of plain woven coupons revealed an overall lightening with increasing numbers of cycles and the gradual development of lighter spots at the tow crossover points of the weave (Fig 46). These frequently linked up to form bands, but failure never occurred along these bands. A few transverse light lines were observed as in the non-woven material as well as edge lightening, although this was not as extensive as in the non-woven material. Holed woven coupons also exhibited some edge lightening (Fig 47) and there was evidence of the development of light spots but less obvious than in the woven plain coupons. Light areas also developed around the holes and, as in the non-woven coupons, eventually linked up with the edge lightening.

3.3.3 Lay-up D (0,90,±45)

Results of the fatigue tests are given in Table 13 and also as a plot of net stress amplitude versus log-life (S-N plot) in Fig 48. Plain coupons all failed at random positions along their lengths but holed coupons all failed through the holes. No damage was visible in the plain coupons prior to failure but holed coupons, both woven and non-woven, developed short longitudinal cracks at tangents to the edges of the holes. These were most prominent in coupons surviving to long lifetimes.

Optical microscopy of plain non-woven coupons revealed some damage in the 90° plies before testing. Transverse 90° layer cracks were initiated early in the test, probably during the first few loading cycles. These precipitated 90/45 delamination at larger numbers of cycles (Fig 49). Delamination between the ±45° layers was also observed, after approximately 10000 cycles, followed by extensive cracking across the 45° layers.

Optical microscopy of the woven coupons also revealed some damage in the surface 90° tows before testing (Fig 50). Transverse cracks formed across individual 90° tows early in the tests as well as limited edge cracks in the 90° tows and at 0/90 interfaces. After 30000 cycles delamination was visible between +45° and -45° tows and damage in the 90° plies became quite extensive, especially in resin rich regions between the tows. Damage in the 45° plies appeared to be less extensive than in the non-woven coupons. Close to failure the 0° plies developed longitudinal cracks and fibre damage was visible (Fig 50).

Ultrasonic C-scanning of non-woven coupons tested at the stress level corresponding to failure after 100000 cycles revealed no transverse lightening as seen in coupons from lay-up C. After 10000 cycles some edge lightening was observed (Fig 51) and by 100000 cycles the light edge regions extended 1-2 mm in from the coupon edges. Some edge whitening developed in holed coupons after large numbers of cycles but no transverse lightening, although some lightening was visible around the holes (Fig 52). This eventually linked up with the edge lightening and commenced spreading longitudinally along the coupons.

Ultrasonic C-scanning of plain woven coupons revealed an overall lightening with increasing numbers of cycles and the gradual development of lighter spots at the tow crossover points in the weave (Fig 53) as in coupons from lay-up C. Edge lightening was observed, but this was very limited and never extended more than 2-3 mm from the coupon edges. Holed coupons showed similar behaviour with some edge lightening developing after 100000 cycles (Fig 54). There was also evidence of the development of light spots but less obvious than in the plain woven coupons. The light areas that developed around the holes, as in the non-woven coupons, eventually linked up with the edge lightening and spread a short distance longitudinally along the coupon edges.

3.3.4 Lay-up E (±45,02)

Results of the reversed axial fatigue tests are given in Table 14 and presented as S-N curves in (Fig 55). All plain coupons failed at random positions along their lengths. Holed non-woven coupons sometimes failed at the holes but frequently away from the holes. Holed woven coupons also frequently failed away from the holes.

Optical microscopy of plain non-woven coupons revealed $\pm 45^\circ$ delamination after only 1000 cycles (Fig 56). This became more extensive after 10000 and 100000 cycles, and translamellar cracks in the 45° layers were also observed (Fig 56). Woven coupons showed no damage until 10000 cycles when translamellar cracks were visible (Fig 57). These became more extensive after 50000 and 100000 cycles and delamination between the $\pm 45^\circ$ plies was then observed.

Ultrasonic C-scanning of plain non-woven coupons revealed edge damage which initiated from one end and grew along one edge (Fig 58). Eventually light areas were initiated within the coupon width away from the edges through which the coupon failed. Holed non-woven coupons revealed damage around the holes after 10000 cycles (Fig 59) which grew longitudinally to several hole diameters distance after 1 million cycles. Eventually the damage reached the coupon ends and had also grown across the coupon width.

Ultrasonic C-scanning of plain woven coupons revealed the gradual lightening with increasing numbers of fatigue load cycles observed in the other woven laminates (Fig 60). Some edge induced damage was apparent after 50000 cycles. The holed woven coupons exhibited a similar effect to that observed in the non-woven coupons in which damage was observed around the hole after only 1000 cycles and grew longitudinally to extend along half the coupon length after 10000 cycles. The damage then grew transversely from the hole across the width.

Infra-red thermography of holed woven and non-woven coupons revealed an initial heating around the hole, as is common with many holed laminates in fatigue. As the number of load cycles increased however, the regions above and below the hole became hotter and the areas either side of the hole were observed to cool. Further load cycling resulted in the hottest areas moving longitudinally further from the hole until they were within a few centimetres of the coupon ends. An example of this behaviour is given in Fig 61, in which a woven coupon cycled between ± 400 MPa is shown after only 4000 load cycles.

4 DISCUSSION

4.1 Static tests

The results of static tensile tests on the (0,90) laminates, given in Table 1, revealed that the plain woven coupons were 16% weaker than the non-woven coupons. Part of this difference was due to the fibre volume fraction being approximately 10% lower ($V_f = 54\%$) than in the non-woven coupons, an inevitable consequence of the fibre tow distortion in the weave. The additional strength reduction was due to reduced material strength directly associated with the distortion of the fibre tows, indeed similar effects were observed in earlier work on (0,90) laminates^{5,6}. Both woven and non-woven (0,90) laminates were notch sensitive, the strength of the non-woven material falling by 17% in the presence of a 4mm hole and the woven material by 33%. Thus the woven (0,90) material was more notch sensitive than the non-woven material, an observation also made in previous work⁵. This was due to the inhibition of stress relieving and energy absorbing mechanisms at the edge of the hole; in woven material longitudinal splitting at the hole would be restricted to the undistorted length of the weave and delamination would also be contained.

Static compression tests on (0,90) coupons showed the woven material to be just 12% weaker than the non-woven material (Table 1). This could be almost fully attributed to the lower fibre volume fraction in the woven material, although the woven material was expected to be weaker since fibre distortion in the weave should lead to fibre instability at smaller applied stresses. Both woven and non-woven material exhibited significant notch sensitivity in compression, the strength of both materials falling by 38%. The presence of a hole results in local stress concentrations and local biaxial stress distributions. These can be modified by shear cracking and delamination but they will usually cause local fibre instabilities at lower overall applied loads than those in plain coupons, resulting in notch sensitivity.

The woven (± 45) laminates were slightly stronger statically than the non-woven material (Table 2), implying that the lower fibre volume fraction and greater fibre distortion had little effect on strength, although previous work⁵ indicated that the failure strain was reduced. The increased load carrying capacity of the fibres in the woven fabric was probably due to the inhibition of in-plane shear deformation and delamination due to the woven and undulating nature of the fabric, which is also consistent with the reduced failure strain. All (± 45) lay-ups were effectively notch insensitive, a widely reported fact, and similar values of failure stress were obtained for woven and non-woven coupons with 4mm central holes.

Coupons with the ($\pm 45, 0, 90$) lay-up (lay-up C) had lower tensile strengths than either the (0,90) or (0, ± 45) lay-ups, a consequence of the smaller percentage of 0° load bearing fibres. The plain woven material was only 6% weaker than the non-woven material (Table 3), a reduction in keeping with the lower fibre volume fraction. This implies that the fibre distortion had no effect on the strength of the woven material in lay-up C, unlike the (0,90) or (0,90, ± 45) lay-ups. This disparity is difficult to explain but may be associated with anomalous scatter due to the small sample size.

Both the woven and non-woven material with 4mm central holes lost 29% in strength compared with the plain material. The similar notch sensitivity in both materials is in contrast to the (0,90) lay-up in which the woven material proved to be more notch sensitive. This implies that in the 0,90 material the non-woven laminate has the opportunity to stress relieve through the development of longitudinal shear cracks in the 0 layers, a mechanism that is restricted in the woven material by the woven nature of the cloth. In the ($\pm 45, 0, 90$) lay-up the (± 45) layers prevent any possibility of significant longitudinal shear cracks, so similar notch sensitivity was observed in both woven and non-woven material.

Static compression tests on ($\pm 45, 0, 90$) coupons showed the woven material to be 21% weaker than the non-woven material (Table 3). This difference cannot be fully attributed to differences in fibre volume fraction, but must also be due to fibre waviness in the fabric precipitating fibre microbuckling at smaller applied stresses. For this lay-up the measured compressive strengths were greater than the tensile strengths, by 41% for the non-woven material and 18% for the woven material. This is because in this lay-up a large compressive interlaminar normal stress is generated⁸⁻¹⁰, which results in reduced susceptibility to delamination. Fibre instability is initiated at smaller applied

strains in the presence of local delamination, and thus less extensive delamination results in greater compressive strengths. Both materials were notch sensitive, the strength of the woven material being reduced by 29% and the non-woven by 36%.

The results of the static tensile tests on the (0,90,±45) lay-up (lay-up D), given in Table 4, showed that the plain woven material was 24% weaker than the non-woven material. This is due to the combination of lower fibre volume fraction and greater fibre distortion, already discussed in connection with lay-up A. Both woven and non-woven material exhibited similar notch sensitivity, as observed in lay-up C, the strength of the woven material being reduced by 22% due to a central 4mm hole and the non-woven material by 26%. However lay-up D was generally stronger than lay-up C, by up to 29%. This difference can be attributed to the different ply stacking sequences, which result in large interlaminar normal stresses at the edges of coupons⁸⁻¹⁰ with lay-up C but only small stresses for lay-up D. As a result, longitudinal edge cracks developed in coupons with lay-up C but not lay-up D, and these led to different failure processes and reduced tensile strength.

Static compression tests on (0,90,±45) coupons showed the woven material to be 23% weaker than the non-woven material (Table 4). This was again due to the combined effects of lower fibre volume fraction and greater fibre distortion in the woven material. In this lay-up the compression strength was slightly less than the tensile strength and also less than in lay-up C. This was because the interlaminar normal stress is small in lay-up D, so delamination could occur more readily than in lay-up C. In addition, one surface of the load bearing 0 layers was unsupported at the laminate surface, which would lead to instability at smaller applied stresses. Both materials were notch sensitive, the strength of the non-woven material falling 24% and the woven material 15% in the presence of a hole. The effect of the hole was less than in lay-up C, indeed the actual notched stresses were similar in lay-ups C and D. This implies that although the interlaminar normal stress was an important factor in determining plain strength, it had little effect on notched compressive strength. Perhaps instabilities associated with the complex stress field at the notch were of overriding importance.

The tensile strengths of plain (±45,0) coupons, (lay-up E), were similar for both non-woven and mixed woven coupons (with only the ±45 layers replaced by woven fabric), as shown in Table 5. This observation has been made in previous work with (±45,0) lay-ups^{5,6,11,12}. A slightly reduced strength would have been expected from the mixed woven coupons because of their lower fibre volume fraction, but this may have been absorbed by the scatter in the results. Both materials were notch sensitive, the non-woven material losing 27% of its strength and the mixed woven 31% due to the action of a 4mm central hole. The degree of notch sensitivity was similar to that observed in lay-ups C and D which also contained ±45° layers. It is apparent that these layers can seriously limit stress relieving mechanisms such as 0° longitudinal splitting around stress concentrators and lead to high notch sensitivity in composite materials.

Static compression tests on (±45,0) coupons showed the mixed woven material was 15% stronger than the plain non-woven material, (Table 5). This was probably an anomaly associated with the small number of tests, since the notched strength was apparently

greater than the plain strength, an observation not recorded in previous work with the same material^{5,6}. The mixed woven material was slightly notch sensitive, the strength falling 13% in the presence of a hole. Thus this lay-up was less notch sensitive in compression than in tension.

4.2 Zero-tension fatigue tests

In the tensile fatigue loading of the (0,90) material (lay-up A), both plain non-woven and woven coupons suffered losses in strength with increasing numbers of fatigue cycles, but the effect was more pronounced in the woven material (Fig 2). Thus the static strength difference observed between the non-woven and woven material, due to a combination of lower fibre volume fraction and greater fibre distortion in the woven material, became greater in fatigue loading. Optical microscopy and ultrasonic C-scanning revealed extensive transverse cracks across the 90° layers and delamination between layers, increasing with increasing numbers of fatigue cycles. In the non-woven material this effectively uncoupled the 90° layers from the 0° layers and the behaviour was then typical of unidirectional CFRP in fatigue. In the woven material however, the 90° tows remain interwoven with the 0° tows and thus continue to exert a stress concentrating influence on them. The C-scan revealed areas of damage at tow crossovers, probably involving 0° tow degradation, and this resulted in a steeper S-N curve than observed in the non-woven material.

The strength of the (0,90) holed coupons, both woven and non-woven, increased at first with increasing numbers of fatigue cycles, but fell after greater numbers of cycles (Fig 2). The initial increase in strength was only possible because of the manner in which the fatigue tests were performed, which involved the gradual increase of peak load from zero to maximum over about 2000 fatigue cycles. There was sufficient cyclic loading to develop damage zones around the holes and relieve the stress concentration leading to initially greater strengths. After only 10000 cycles the holed non-woven coupons were as strong as the plain coupons, but the holed woven coupons never quite attained the strength of the plain coupons, even after 10 million load cycles. Ultrasonic C-scanning revealed the development of longitudinal splitting and 0/90 delamination around the holes, this being the cause of the initial reduction in notch sensitivity. This was more apparent in the non-woven material, explaining why this material recovered more of its plain strength than the woven material. In the holed woven material the 90° tows can never become completely uncoupled from the 0° tows, because of their woven nature, and they continue to exert a stress concentrating influence at the tow crossover points. Indeed these points were the site of additional damage observed experimentally.

The (±45) coupons behaved similarly in fatigue, in both the plain and holed state, the notch insensitivity apparent statically being preserved in fatigue. The woven coupons did appear slightly stronger and this became more noticeable at long lifetimes when woven coupons outlasted non-woven ones by almost one decade in life (Fig 7). The major micro-structural difference observed was less extensive damage in the woven material, presumably a consequence of the damage growth restrictions imposed by the woven nature of the material, and this resulted in survival to longer lifetimes. The woven material also

exhibited an overall C-scan lightening associated with damage development at tow cross-overs, but this did not appear detrimental in the (± 45) material, unlike other lay-ups.

Tensile fatigue tests on coupons with a ($\pm 45, 0, 90$) lay-up (lay-up C) showed a substantial loss in strength with increasing numbers of cycles, for both woven and non-woven material (Fig 14). Ultrasonic C-scanning and optical microscopy revealed extensive longitudinal edge cracking, growing from the coupon edges towards the centres of their widths, probably the cause of the significant strength losses observed. The plain woven material appeared to suffer an even greater loss in strength at high lifetimes. This implies that the static differences attributed to lower fibre volume fraction and greater fibre distortion in the woven material continued to account for the lower fatigue strength except at long lifetimes when additional strength degradation mechanisms were operative in the woven material. The microstructural analysis again revealed considerable damage at the tow crossover points in the woven material, particularly at long lifetimes, and this undoubtedly resulted in a further reduction in the load bearing capacity of the 0° tows. This caused an additional loss in strength compared with the non-woven material in which the 0° and 90° plies became uncoupled and the stress concentrating effects of the 90° plies on the 0° plies relieved.

The holed woven and non-woven coupons with the ($\pm 45, 0, 90$) lay-up (lay-up C) also increased in strength initially in the tensile fatigue tests, for the same reason as discussed for lay-up A. Between 100000 and 1 million cycles the strengths of the holed coupons approached those of the plain coupons and the notch sensitivity disappeared completely in the non-woven material, but remained to a small extent in the woven material. The C-scan revealed extensive damage growth around holes during fatigue, this linking up with edge cracking caused by the high interlaminar normal stresses in this particular lay-up⁸⁻¹⁰. As a consequence, layers became uncoupled, causing considerable stress relief, resulting in the loss of notch sensitivity in the non-woven material. Although the $\pm 45^\circ$ layers can become uncoupled from the $0, 90$ layers, leading to stress relaxation, the woven material never became completely notch insensitive as the 0° tows can never become totally uncoupled from the stress concentrating influence of the 90° tows, being intimately woven together. Indeed, woven coupons with the ($0, 90$) lay-up (lay-up A) remained partially notch sensitive for identical reasons.

Coupons with the ($0, 90, \pm 45$) lay-up (lay-up D) also showed a significant loss in strength with increasing numbers of tensile fatigue cycles (Fig 21). Microstructural analysis revealed less extensive longitudinal edge cracking than in lay-up C, but transverse cracks were formed across the 90° plies and initiated some layer delamination at large numbers of cycles. Considerable damage was also developed in the $\pm 45^\circ$ layers adding to the loss in strength observed. The strength of the woven material remained a similar fraction of that of the non-woven material even up to 1 million fatigue cycles. This implies that the principal cause for the difference between the strength of the plain woven and non-woven material remained greater fibre distortion and lower fibre volume fraction. This is somewhat surprising since the microstructural analysis revealed, as in coupons with lay-up C, the development of significant damage at the tow crossover points in the woven material after large numbers of fatigue cycles. The effect

was most noticeable in lay-up C at lifetimes exceeding 1 million load cycles, but no coupons with lay-up D survived for longer than 1 million cycles, simply because of the experimental selection of stress levels. It is possible that a reduction in the strength of the woven material would have been observed at greater numbers of fatigue cycles.

As in lay-up C, the holed non-woven coupons with lay-up D became notch insensitive after about 100000 load cycles, but the holed woven coupons, although approaching the strength of the plain coupons, never quite became totally notch insensitive. Similar types and degrees of damage were observed around the holes as in coupons with lay-up C, and the main difference between the holed non-woven and woven coupons remained the additional damage developed at tow crossover points in the woven material and the inability of the 90° tows to become completely uncoupled from the 0° tows.

Coupons with lay-up C had greater static strengths than those with lay-up D, but this difference became less obvious during fatigue. This difference was attributed to the extensive longitudinal edge cracking developed in coupons with lay-up C, due to the particular ply stacking sequence, and not observed statically in coupons with lay-up D. The improvement in the fatigue performance of coupons with lay-up C, relative to those with lay-up D, may be because coupons from both lay-ups developed longitudinal edge cracking in fatigue, although this was always more extensive in coupons with lay-up C.

The static tests on coupons with the $(\pm 45, 0_2)$ lay-up (lay-up E) showed there to be little difference in strength between the non-woven and mixed woven coupons, and a similar observation was made in the tensile fatigue tests (Fig 28). The plain coupons suffered a loss in strength of nearly 25% after 1 million load cycles in both the non-woven and mixed woven cases. Previous work had found a greater loss in strength in the non-woven material^{11,12}, but this was not the case in the present work. Microstructural analysis revealed the damage to be confined mainly to the $\pm 45^\circ$ layers, which carry only a small fraction of the applied load. Thus the coupons behaved in a similar manner to unidirectional material, and indeed the loss in strength during fatigue was comparable with that observed in unidirectional material. C-scans of the plain mixed woven coupons did reveal damage at tow crossover points in the $\pm 45^\circ$ layers, but since these layers carried only small loads the damage had no significant effect on the material strength.

Tensile fatigue tests on holed coupons with the $(\pm 45, 0_2)$ lay-up (lay-up E) showed both the non-woven and mixed woven coupons increased initially in strength, for reasons discussed earlier in this section in connection with coupons with lay-up A. The fatigue strengths of both the non-woven and mixed woven coupons remained similar at all lifetimes and between 100000 and 1 million cycles the holed coupons became notch insensitive, their strengths matching those of the plain coupons. The ultrasonic C-scan revealed damage development around the holes at low lifetimes, this taking the form of delamination between the $\pm 45^\circ$ and 0° layers with longitudinal shear cracks at the edges of the holes. As the tests proceeded, these shear cracks and the associated delamination grew longitudinally towards the coupon ends. The 0° layers thus became uncoupled from the $\pm 45^\circ$ layers and behaved in the notch insensitive manner typical of unidirectional material. This behaviour was readily apparent in infra-red thermography studies of the coupons in

which the hottest areas were initially either side of the holes but rapidly migrated to above and below the holes and then moved away from the holes towards the coupon ends.

4.3 Reversed axial fatigue tests

The damage processes in composite materials during compressive loading and their relationship to compressive mechanical properties are still not well understood. Much work reported in the literature has referred to different failure modes in compression including fibre buckling, shear failure and interfacial failure. Models based on other mechanisms have also been proposed. A useful review of compressive damage mechanisms is provided in Ref 13, and a study of the effects of moisture content is described in Ref 14. However, assuming that the test method employed obviates any macro-instability of the test coupon¹⁵, the wide range of failure processes and models aimed at describing the compressive failure process can probably be reduced to just two principle mechanisms; fibre instability and material failure of the fibre. In the latter case the fibres may fail in compression, or in shear, but this failure mode will only occur if fibre instability is avoided, and this therefore represents the upper bound to composite compressive strength. The avoidance of fibre instability thus provides a key to the potential improvement of composite compressive strength.

Within the group of failures covered by the fibre instability mode come those usually attributed to fibre microbuckling, interfacial failure and shear failure. All of these involve fibre instability, triggered by different factors. To avoid fibre instability, it is necessary to eliminate or minimise the importance of these factors. These include fibre/matrix debonding, ply delamination, poor fibre support due to low resin stiffness or reduced resin integrity and poor fibre alignment as well as certain contributory factors such as the use of small diameter fibres, low stiffness fibres and possible adverse thermal effects resulting from the cure schedule. Fibre/matrix debonding can be initiated in materials with a poor interfacial bond strength^{16,17}, in materials degraded by environmental exposure or fatigue loading, or adjacent to misaligned fibres due to the large shear stresses induced, and will trigger failure by local fibre instability. Ply delamination can be caused by large interlaminar stresses at free edges⁸⁻¹⁰, holes or defects, as a part of impact induced damage, through loading in fatigue, or from severe environmental exposure. Delamination reduces the support offered by one layer to another and can also trigger fibre instability, although this mechanism frequently induces macrobuckling type failures. The resin performs an important function in supporting the fibres against local buckling. Thus limitations in resin performance may result in resin failure, frequently in shear, which triggers fibre instability before the full fibre strength can be realised¹⁸. Degradation of the resin due to environmental or fatigue exposure frequently leads to failure in this manner. Poor fibre alignment, such as in woven fabrics, misalignment of fibres in prepregs, or ply misorientation induced during fabrication can reduce measured compressive strengths since fibre instability is triggered at smaller applied stresses¹⁹. It is likely that the use of low stiffness fibres, or the increasing trend to smaller diameter fibres, as in recent carbon fibre developments, could also precipitate fibre instability at smaller applied stresses.

Finally, certain polymer fibres may defibrillate through exposure to fatigue loading and severe environments²⁰ and subsequently also fail by fibre instability triggered by the defibrillation.

In fatigue the resin and the fibre/matrix interface become damaged and are less able to support the fibres, thus fibre instability occurs at smaller applied stresses. Consequently resin and interface damage, and also delamination, are critical damage processes in compressive fatigue loading and the susceptibility of a material to these processes will greatly influence the material's fatigue performance.

During the reversed axial fatigue loading of plain coupons from lay-up A (0,90), a significant loss in strength was observed (Fig 35), much greater than observed during zero-tension loading. The loss in strength was greatest in the woven coupons, where after 1 million cycles the peak fatigue stress was less than half the static strength. Edge cracking was observed in plain non-woven coupons as well as translaminal 90° layer cracks early in the life, which spread to form 0/90 delamination at greater numbers of cycles. Although the plain woven coupons suffered a greater strength loss in reversed axial fatigue than the non-woven coupons, they developed less extensive damage; some edge cracking was visible and also 90° cracks, followed at long lifetimes by local 0/90 delamination confined to individual 0 fibre tows by the weave of the fabric. Damage was also visible at the tow crossover points as observed during the tensile fatigue work.

The compressive failure process dominated in the reversed axial fatigue tests, but was modified by damage incurred during the tensile excursion. The crucial difference between the woven and non-woven material was perhaps the large initial 0° fibre misalignment in the woven material, which led to overall fibre instability at smaller applied stresses than in the non-woven material with its better fibre alignment. In reversed axial fatigue loading, the resin and interfaces in the regions of distorted 0° fibres must carry greater shear stresses than in the better aligned non-woven material. This causes more rapid local degradation of the resin interface than in non-woven material, accentuating the effect of the fibre misalignment and precipitating 0° fibre instability at even lower applied stresses.

Holed coupons with lay-up A showed a smaller loss in strength than the plain coupons, indeed the non-woven material increased in strength initially. After 1 million cycles the difference between the non-woven and woven material was dramatic, the peak fatigue stresses in the non-woven material being about 370 MPa but only 170 MPa in the woven material. This latter figure corresponds to a coupon strain of less than 0.25%. After large numbers of fatigue cycles, the holed coupons approached the lifetimes of their respective non-woven coupons. Thus the static notch sensitivity almost disappeared in reversed axial fatigue, as in zero-tension fatigue, a consequence of local damage around the hole, probably initiated during the tensile excursions, relieving stress concentrations. At large numbers of cycles the bulk damage accumulation became dominant and the limiting damage processes were then the same as observed in the plain material and discussed above.

Reversed axial fatigue tests on coupons with lay-up C (±45,0,90) yielded the S-N curves given in Fig 41. Since the tensile static strengths were less than the compressive

strengths these have also been plotted in Fig 41 as circled values. Thus in the reversed axial case the tensile excursion dominated at very short lifetimes. After only a small number of cycles however, compression behaviour prevailed and all coupons failed in compression at smaller stresses than in the tensile fatigue tests. All coupons exhibited steeply sloping S-N plots with a greater loss in strength than observed in tension alone. Static differences between plain woven and non-woven coupons were preserved in reversed axial fatigue, and indeed increased at long lifetimes. The peak fatigue stress for the plain non-woven material was reduced to about 195 MPa after 1 million cycles and 150 MPa for the plain woven material.

Plain non-woven coupons from lay-up C developed longitudinal edge cracks in the 90 layer and translaminar cracks in the $\pm 45^\circ$ and 90° layers early in their lives. This led to 0/90 and 0/45 delamination at longer lifetimes, when edge cracks grew from the coupon edges towards the centre of the coupon widths. Plain woven coupons developed similar damage, except that additional damage was initiated at the tow crossover points.

The particular stacking sequence of lay-up C gave rise to a large interlaminar normal stress at the edges of coupons subjected to tensile loading⁸⁻¹⁰ which resulted in the formation of edge cracking. This was not observed in the static compression tests as the interlaminar normal stresses were then compressive, hence the static compressive strength was greater than the tensile strength. In reversed axial fatigue however, edge cracks formed and grew in the tensile fatigue part of the cycle. These reduced the stability of the 0° fibres on the compressive part of the loading cycle, hence smaller applied stresses were required to trigger fibre instability and the compressive strength thus fell with increasing numbers of fatigue cycles. Fatigue damage in the woven and non-woven materials was similar, thus similar reductions in compressive strength were observed, except at long lifetimes when the additional damage at the tow crossover points led to greater reductions in the compressive strength of the woven material.

Holed non-woven coupons with lay-up C demonstrated a significant static notch sensitivity but this disappeared in fatigue after only a few cycles. Holed non-woven coupons were significantly stronger than the holed woven coupons. The damage observed was similar, but less extensive, to that in the plain coupons except that the C-scan revealed damage around the holes which grew and linked with the edge cracking and then grew longitudinally along the coupons. Holed woven coupons were also notch sensitive statically, the effect being significantly reduced but never disappearing completely in fatigue. Damage was similar to that observed in the plain woven material, although less extensive, but as in the holed non-woven material damage was also observed around the hole. This also grew to link with the edge damage and then grew longitudinally along the coupon length. It is clear that the holed coupons behaved similarly in fatigue to the plain coupons, the stress concentrating influence of the hole quickly being almost completely nullified by damage generated around the holes.

Unlike lay-up C, the static compressive strengths of plain coupons with lay-up D (0,90, ± 45) were similar to, perhaps slightly lower than, their tensile strengths. This was because lay-up D was not susceptible to the serious edge delamination effect observed in coupons with lay-up C. Hence the reversed axial fatigue S-N plots in Fig 41 were

drawn conventionally to include the static compressive strengths of the materials. All coupons exhibited steeply sloping S-N plots with a greater loss in strength than observed in tensile fatigue. The static compressive differences between the strengths of the woven and non-woven materials decreased slightly at short lifetimes but increased again at longer lifetimes. Peak fatigue stresses for plain non-woven coupons were about 180 MPa after 1 million cycles compared with 135 MPa for the woven coupons.

Plain non-woven coupons from lay-up D developed 90° translaminal cracks after small numbers of reversed axial fatigue cycles, which led to delamination between the 90° and 45° layers at greater numbers of cycles. Delamination was also observed between the $+45^\circ$ and -45° layers and translaminal cracks formed across these layers after large numbers of cycles. Plain woven coupons developed similar damage, with 90° layer cracks forming early in the tests followed by local $0/90$ and ± 45 delamination between tows and damage within the 45° layers. Close to failure however, some longitudinal splitting was observed within the 0° plies.

The fatigue performance of coupons with lay-up D was very similar to those with lay-up C, despite the static differences associated with the large interlaminar normal stress in lay-up C. Indeed the degradation processes of delamination and translaminal cracking were similar in both lay-ups and resulted in similar reversed axial fatigue behaviour. The woven material was less strong statically due to the greater initial fibre misalignment in the fabric. This difference was generally reflected in the fatigue performance, perhaps increasing at long lifetimes due to the additional damage initiated at the tow crossover points in the woven material which reduced support for the 0 fibres and thus reduced the applied stress required to trigger fibre instability.

Holed non-woven coupons with lay-up D exhibited static notch sensitivity, but this disappeared in reversed axial fatigue loading after about 100000 cycles. Holed non-woven coupons were stronger at all fatigue lives than the holed woven coupons. Holed woven coupons were also notch sensitive statically, the effect being reduced in fatigue and notch insensitivity was achieved after long lifetimes. The general damage development was similar to that observed in coupons with lay-up C. In both woven and non-woven holed coupons, damage quickly developed around the hole in fatigue, relieving the stress concentrating influence of the hole in both the tensile and compressive phases of the fatigue cycle and leading to notch insensitive behaviour similar to that in the plain coupons.

Reversed axial fatigue tests on coupons with lay-up E ($\pm 45, 0$), presented in Fig 55, yielded steep S-N plots with coupons failing in compression at significantly smaller stresses than in the tensile fatigue tests. Peak fatigue stresses were reduced to about 350 MPa after 1 million cycles for both the non-woven and mixed woven materials, which corresponds to a coupon strain of approximately 0.5%.

The damage visible by ultrasonic C-scan and at edges by optical microscopy of coupons with lay-up E was confined to the $\pm 45^\circ$ layers in both the plain non-woven and mixed woven materials. Indeed similar damage developed in both materials except that extra damage was observed at the tow crossover points in the $\pm 45^\circ$ layers of the mixed woven material. The compression strength of this lay-up in reversed axial fatigue loading

was dependent on the rate at which the stress for the onset of 0° fibre microbuckling decayed with increasing numbers of fatigue cycles. This was determined by the nature and rate of the damage developed which essentially fell into two categories. Firstly resin and fibre/matrix interface degradation within the 0° layers, which locally reduced support for the 0° fibres and was similar for both the non-woven and mixed woven materials. Secondly damage within the $\pm 45^\circ$ layers and delamination at the $45/0$ interface which influenced the support provided for the 0° layers by the adjacent $\pm 45^\circ$ layers. This latter mechanism, although potentially different in the two materials, proved to be similar in both materials, thus the reversed axial fatigue performance of both the non-woven and mixed woven materials was very similar.

Any differences between the static compressive strengths of the non-woven and mixed woven holed coupons with lay-up E disappeared after only short lifetimes of reversed axial fatigue loading. Behaviour became totally notch insensitive in both materials, to the extent that most coupons failed away from the holes. Damage was observed around the holes early in the fatigue lives. This took predominantly the form of longitudinal shear splits in the 0° plies at tangents to the holes which rendered the hole ineffective as a stress concentrator, resulting in notch insensitive behaviour. Infra-red thermography and ultrasonic C-scanning revealed the growth of these shear splits and associated delamination for a considerable distance longitudinally away from the holes. Apart from rendering the hole ineffective, it is unlikely that these splits had any effect on the ultimate compressive strength, which would be controlled by the same factors as for the plain material discussed above.

It is worth emphasising that there was no significant difference between the reversed axial fatigue performance of the mixed-woven and non-woven materials, indeed the superior damage tolerance of the mixed-woven material^{5,6} could invite its widespread use in composite structures.

It can be concluded that there is a significant fatigue effect in the reversed axial loading of carbon fibre composite materials. This fatigue degradation is affecting one of the key properties, that is notched compression, which in the hot/wet condition currently determines aircraft design stress levels. It is possible that the combined effects of notching, elevated temperature, moisture AND reversed axial fatigue loading could lead to further reductions in the residual strength at long fatigue lifetimes. Aerospace designers would do well to reconsider designs based on the assumption that the static strength represents the worst case. Further investigations into the effects of hot/wet compressive fatigue are continuing at RAE. Current efforts by resin and fibre manufacturers must be directed towards improvements in the basic compressive strength of carbon fibre composites, as well as reducing its susceptibility to temperature and environmental effects and reversed axial fatigue loading. This will only be forthcoming through material improvements based on a sound knowledge of the key factors controlling the compressive failure process in carbon fibre composite materials.

5 CONCLUSIONS

- (1) The static strengths of the laminates tested were reduced by two stress concentrating effects, that due to tow crossover points in the woven fabric and that due to machined notches in all the laminates. The relative magnitude of these effects varied with both lay-up and loading mode, but both served to reduce strengths. 0,90 lay-ups were most sensitive to these stress concentrations and $\pm 45^\circ$ lay-ups least sensitive. Other lay-ups exhibited intermediate behaviour. In general the woven materials were the most notch sensitive.
- (2) Replacing the $\pm 45^\circ$ layers of a laminate with woven fabric had little effect on the static tensile or compressive strengths.
- (3) In tensile fatigue loading, degradation processes led to further reductions in strength. Stress concentrations at notches were reduced after large numbers of tensile fatigue cycles and non-woven material became notch insensitive. However the stress concentrating effect of tow crossover points in the woven material was generally increased as fatigue induced damage was initiated at these points. The combined effect of these degradation processes was to reduce the stresses in the 0,90 and both 0,90, ± 45 lay-ups to the equivalent of less than 0.6% strain. The tensile strength of ± 45 material was also reduced by fatigue loading, although the woven material gave greater fatigue lifetimes than the non-woven material. Thus where ± 45 material is used in isolation, as in many aircraft trailing-edge applications, the use of woven fabric will lead to greater fatigue lives.
- (4) In reversed axial fatigue loading, the initial differences between the woven and non-woven materials, which were associated with fibre misalignment at tow crossover points in the woven material, were generally increased at long lifetimes as damage developed in the woven materials at these points. In the three 0,90 and 0,90, ± 45 lay-ups, the strengths of the holed woven coupons after 1 million cycles were reduced to the equivalent of 0.3% strain or less. In the worst case, the 0,90 lay-up, the equivalent sustainable strain in the holed woven material was reduced to just 0.25%, whereas the holed non-woven material gave a strain of almost 0.6%. This effectively excludes the use of woven fabric to replace load bearing 0° fibres in aerospace structure.
- (5) Replacing the ± 45 layers in 0, ± 45 lay-ups with woven fabric had little effect on fatigue behaviour, in tensile or reversed axial loading. This, combined with the good damage tolerance of this configuration, could invite the widespread use of mixed woven material in composite aerospace structures.
- (6) Reversed axial fatigue loading was more detrimental than tensile fatigue and led to greater losses in strength. This fatigue degradation affects one of the key properties, that is notched compression, which in the hot/wet condition currently determines aircraft design strain levels. Aerospace designers would do well to reconsider designs based on the assumption that the static compressive strength represents the worst case. Additional work is required to establish whether the combined effects of reversed axial fatigue loading and hot/wet notched compression testing lead to further reductions in composite strength.

(7) Resin and fibre manufacturers must direct their efforts towards improving the basic compressive strength of carbon fibre composites as well as reducing the effects of temperature, environmental exposure and reversed axial fatigue loading. This will be forthcoming only through material improvements based on a sound knowledge of the key factors controlling the compressive failure process.

Acknowledgment

The authors wish to acknowledge Mr D. Whitehead and Mr J. Coleman for their contribution in performing many of the mechanical tests.

Table 1
STATIC TESTS ON LAY-UP A (C,90,90,0)

Specimen number	Type	Loading	Failure stress MPa
WUA-3	Non-woven plain	Tension	697
WUA-37	" "	"	731
WUA-9	Non-woven holed	"	586
WUA-31	" "	"	605
WUA-17	Non-woven plain	Compression	626
WUA-51	" "	"	599
WUA-23	Non-woven holed	"	437
WUA-45	" "	"	325
WXA-3	Woven plain	Tension	571
WXA-37	" "	"	623
WXA-9	Woven holed	"	425
WXA-31	" "	"	377
WXA-17	Woven plain	Compression	541
WXA-51	" "	"	542
WXA-23	Woven holed	"	363
WXA-45	" "	"	312

Table 2
STATIC TESTS ON LAY-UP B ($\pm 45, \mp 45$)

Specimen number	Type	Loading	Failure stress MPa
WUB-2	Non-woven plain	Tension	174
WUB-19	" "	"	205
WUB-3	Non-woven holed	"	208
WUB-20	" "	"	205
WXB-2	Woven plain	"	217
WXB-19	" "	"	210
WXB-3	Woven holed	"	216
WXB-20	" "	"	214

Table 3
STATIC TESTS ON LAY-UP C ($\pm 45, 0, 90$)_s

Specimen number	Type	Loading	Failure stress MPa
WUC-3	Non-woven plain	Tension	441
WUC-37	" "	"	476
WUC-9	Non-woven holed	"	288
WUC-31	" "	"	363
WUC-17	Non-woven plain	Compression	635
WUC-51	" "	"	656
WUC-23	Non-woven holed	"	421
WUC-45	" "	"	402
WXC-3	Woven plain	Tension	422
WXC-37	" "	"	442
WXC-9	Woven holed	"	304
WXC-31	" "	"	306
WXC-17	Woven plain	Compression	542
WXC-51	" "	"	480
WXC-23	Woven holed	"	389
WXC-45	" "	"	338

Table 4
STATIC TESTS ON LAY-UP D (0, 90, ± 45)_s

Specimen number	Type	Loading	Failure stress MPa
WUD-3	Non-woven plain	Tension	546
WUD-37	" "	"	584
WUD-9	Non-woven holed	"	428
WUD-31	" "	"	410
WUD-17	Non-woven plain	Compression	505
WUD-51	" "	"	570
WUD-23	Non-woven holed	"	345
WUD-45	" "	"	474
WXD-3	Woven plain	Tension	434
WXD-37	" "	"	429
WXD-9	Woven holed	"	336
WXD-31	" "	"	339
WXD-17	Woven plain	Compression	406
WXD-51	" "	"	426
WXD-23	Woven holed	"	359
WXD-45	" "	"	349

Table 5
STATIC TESTS ON LAY-UP E ($\pm 45, 0_2$)_s

Specimen number	Type	Loading	Failure stress MPa
WUE-3	Non-woven plain	Tension	799
WUE-37	" "	"	825
WUE-9	Non-woven holed	"	590
WUE-31	" "	"	603
WUE-17	Non-woven plain	Compression	776
WUE-51	" "	"	633
WUE-23	Non-woven holed	"	799
WUE-45	" "	"	690
WXE-3	Woven plain	Tension	800
WXE-37	" "	"	809
WXE-9	Woven holed	"	565
WXE-31	" "	"	542
WXE-17	Woven plain	Compression	896
WXE-51	" "	"	742
WXE-23	Woven holed	"	786
WXE-45	" "	"	629

Table 6

ZERO-TENSION FATIGUE DATA FOR LAY-UP A (0,90,90,0)

Frequency = 20 Hz unless otherwise stated

Coupon number	Coupon type	Stress range MPa	Cycles to failure
2	Non-woven plain	200 \pm 200	5476200 run-out
34	" "	"	5302800 "
18	" "	250 \pm 250	10233300 "
49	" "	"	10000000 "
25	" "	300 \pm 300	2229800
43	" "	"	755400
7	" "	325 \pm 325	1779500
29	" "	"	79900
1	" "	337.5 \pm 337.5	19200
4	" "	"	35100
10	Non-woven holed	275 \pm 275	8512000 run-out
21	" "	287.5 \pm 287.5	3436000
41	" "	"	518600
5	" "	300 \pm 300	4034300
15	" "	312.5 \pm 312.5	3255900
47	" "	325 \pm 325	409900
32	" "	"	1771200
39	" "	337.5 \pm 337.5	7600
24	Woven plain	225 \pm 225	1173800
49	" "	"	1209700
1	" "	250 \pm 250	15600
27	" "	"	121000
2*	" "	"	15600
34*	" "	"	50500
7	" "	275 \pm 275	2600
29	" "	"	3000
10	Woven holed	175 \pm 175	8690000 run-out
21	" "	200 \pm 200	3180000
41	" "	"	830200
5	" "	212.5 \pm 212.5	58500
39	" "	"	708600
15	" "	225 \pm 225	1700
47	" "	"	3700
32	" "	"	380500

* At 10 Hz

Table 7

ZERO-TENSION FATIGUE DATA FOR LAY-UP B ($\pm 45, \pm 45$)_s

Frequency = 5 Hz unless otherwise stated

Coupon number	Coupon type	Stress range MPa	Cycles to failure
10	Non-woven plain	30 \pm 30	4573000 run-out
26	" "	40 \pm 40	1442000
22	" "	" "	1592200
5	" "	50 \pm 50	178600
28	" "	" "	203100
1*	" "	60 \pm 60	32000
7	" "	" "	25400
18*	" "	" "	46200
13	" "	70 \pm 70	2800
23	" "	" "	4700
10	Non-woven holed	30 \pm 30	4341200 run-out
27	" "	40 \pm 40	1172300
24	" "	" "	713700
4	" "	50 \pm 50	154900
14	" "	" "	94500
16	" "	60 \pm 60	25300
9	" "	" "	16700
21	" "	70 \pm 70	5700
12	" "	" "	5200
5	Woven plain	30 \pm 30	4278000 run-out
13	" "	40 \pm 40	7659000
26*	" "	" "	5296200
10	" "	50 \pm 50	290600
28	" "	" "	301700
1*	" "	60 \pm 60	44300
7	" "	" "	41400
18*	" "	" "	59100
13	" "	70 \pm 70	8900
23	" "	" "	8900
9	Woven holed	40 \pm 40	7814300
21	" "	" "	4786400
4	" "	50 \pm 50	358300
24	" "	" "	397600
6	" "	60 \pm 60	64000
16	" "	" "	65700
27	" "	70 \pm 70	2900
12	" "	" "	10100

* At 10 Hz

Table 8

ZERO-TENSION FATIGUE DATA FOR LAY-UP C ($\pm 45, 0, 90$)

Frequency = 20 Hz

Coupon number	Coupon type	Stress range MPa	Cycles to failure
2	Non-woven plain	125 \pm 125	10342200 run-out
25	" "	150 \pm 150	6547800
43	" "	" "	6166800
18	" "	175 \pm 175	218300
7	" "	" "	78000
34	" "	200 \pm 200	42600
49	" "	" "	28100
29	" "	212.5 \pm 212.5	12600
36	" "	" "	100
15	Non-woven holed	150 \pm 150	1067700
47	" "	" "	1206400
21	" "	175 \pm 175	419100
41	" "	" "	27900
5	" "	187.5 \pm 187.5	48000
39	" "	" "	1300
10	" "	200 \pm 200	1500
32	" "	" "	2000
49	Woven plain	129.5 \pm 129.5	1477300
29	" "	" "	2925600
2	" "	150 \pm 150	294000
18	" "	162.5 \pm 162.5	120600
7	" "	" "	99200
34	" "	175 \pm 175	667700
25	" "	" "	137300
43	" "	" "	42000
4	" "	200 \pm 200	1300
27	" "	" "	12600
10	Woven holed	125 \pm 125	1109700
32	" "	" "	2228900
21	" "	137.5 \pm 137.5	676400
41	" "	" "	569200
5	" "	150 \pm 150	56100
39	" "	" "	183400
15	" "	162.5 \pm 162.5	1300
47	" "	" "	900

Table 9
ZERO-TENSION FATIGUE DATA FOR LAY-UP D (0,90,±45)
Frequency = 20 Hz unless otherwise stated

Coupon number	Coupon type	Stress range MPa	Cycles to failure
4	Non-woven plain	175 ± 175	582200
1	" "	200 ± 200	49900
43	" "	212.5 ± 212.5	65400
25	" "	" "	64200
29	" "	225 ± 225	22600
7	" "	" "	34600
49	" "	237.5 ± 237.5	25700
18	" "	" "	8900
34	" "	257.5 ± 257.5	2200
2	" "	" "	2600
24	Non-woven holed	175 ± 175	520000
47	" "	187.5 ± 187.5	277500
15	" "	" "	125200
39	" "	200 ± 200	112200
5	" "	" "	117300
41	" "	212.5 ± 212.5	13500
21	" "	" "	34200
32	" "	225 ± 225	8100
10	" "	" "	1000
43	Woven plain	137.5 ± 137.5	775800
25	" "	" "	615200
29	" "	150 ± 150	369000
7	" "	" "	127400
49	" "	162.5 ± 162.5	71700
18	" "	" "	50000
34	" "	182.7 ± 182.7	15300
1	" "	" "	9300
47	Woven holed	125 ± 125	1000100
15	" "	" "	1000100
4	" "	137.5 ± 137.5	243900
39	" "	150 ± 150	11000
5	" "	" "	3600
41	" "	175 ± 175	600
24	" "	" "	900
32	" "	190 ± 190	600
10	" "	" "	600

* At 10 Hz

Table 10
ZERO-TENSION FATIGUE DATA FOR LAY-UP E ($\pm 45, 02$)
Frequency = 20 Hz

Coupon number	Coupon type	Stress range MPa	Cycles to failure
2	Non-woven plain	300 \pm 300	9176100
7		315 \pm 315	1922900
29		"	1854600
25		320 \pm 320	3336400
34		325 \pm 325	5063700
18		"	1300
49		"	20300
43		350 \pm 350	1600
1		"	1800
4		"	1100
21	Non-woven holed	300 \pm 300	2572400 (tl)
41		"	748900 (te)
5		315 \pm 315	1162300 (te)
39		"	580800 (be)
15		325 \pm 325	1600 (th)
47		"	373500 (te)
10		"	259300 (te)
32		"	2100 (th)
2	Woven plain	325 \pm 325	68100
34		"	1684600
18		350 \pm 350	2300
49		"	174700
7		375 \pm 375	6200
29		"	2300
25		337.5 \pm 337.5	25400
43		"	1226900
47	Woven holed	300 \pm 300	5457400 (le)
15		"	1300 (th)
41		"	3995600 "
21		"	2200 "
39		315 \pm 315	900 "
5		"	1600 "
32		325 \pm 325	700 "
10		"	456000 "

le = failure at lower end of coupon. th = failure through the hole.
te = failure across the top end of the coupon.

Table 11
REVERSED AXIAL FATIGUE DATA FOR LAY-UP A (0,90,90,0)
Frequency = 10 Hz

Coupon number	Coupon type	Stress range MPa	Cycles to failure
12	Non-woven plain	0 ± 200	9995900 run-out
30	" "	0 ± 300	10000000 run-out
16	" "	0 ± 400	8930200
24	" "	"	1451000
27	" "	0 ± 425	670000
8	" "	0 ± 450	393500
50	" "	"	274400
26	" "	0 ± 500	121500
35	" "	"	97800
44	" "	0 ± 525	14600
20	" "	"	162000
36	" "	0 ± 550	76300
28	Non-woven holed	0 ± 400	898700
6	" "	"	547700
46	" "	0 ± 425	372300
22	" "	"	35600
14	" "	0 ± 450	19300
42	" "	"	5000
33	" "	0 ± 475	27400
11	" "	0 ± 500	700
12	Woven plain	0 ± 212.5	1209700
30	" "	"	2855100
44	" "	0 ± 250	162100
26	" "	"	728500
36	" "	0 ± 300	13500
8	" "	"	23300
50	" "	0 ± 350	3400
16	" "	0 ± 400	2100
46	Woven holed	0 ± 200	382600
22	" "	"	178600
14	" "	0 ± 212.5	697100
42	" "	"	80500
28	" "	0 ± 250	13000
6	" "	"	21400
33	" "	0 ± 300	2100
11	" "	"	6300

Table 12
REVERSED AXIAL FATIGUE DATA FOR LAY-UP C ($\pm 45, 0, 90$)
Frequency = 10 Hz

Coupon number	Coupon type	Stress range MPa	Cycles to failure
35	Non-woven plain	0 \pm 170	4188500
8	" "	"	1746000
30	" "	0 \pm 200	757500
12	" "	"	494700
50	" "	0 \pm 250	97800
16	" "	"	48700
44	" "	0 \pm 300	23700
26	" "	"	29700
11	Non-woven holed	0 \pm 100	10000000 run-out
6	" "	0 \pm 150	8919300
46	" "	0 \pm 170	2056200
28	" "	0 \pm 200	647000
33	" "	"	618100
42	" "	0 \pm 250	56600
14	" "	"	47800
52	" "	0 \pm 300	13800
4	" "	"	700
44	Woven plain	0 \pm 130	5216500
50	" "	"	4971100
30	" "	0 \pm 170	499700
12	" "	"	508000
16	" "	0 \pm 200	162100
8	" "	"	324500
26	" "	0 \pm 250	47600
35	" "	"	66800
46	Woven holed	0 \pm 130	2472800
22	" "	"	3156500
33	" "	0 \pm 150	525800
42	" "	"	693300
22	" "	0 \pm 170	130800
11	" "	"	117800
20	" "	0 \pm 200	53800
28	" "	"	22500

Table 13
REVERSED AXIAL FATIGUE DATA FOR LAY-UP D (0,90,±45)
Frequency = 10 Hz

Coupon number	Coupon type	Stress range MPa	Cycles to failure
52	Non-woven plain	0 ± 170	2120400
48	" "	" "	2357600
27	" "	0 ± 200	328400
44	" "	0 ± 250	49600
26	" "	" "	33700
35	" "	0 ± 300	2500
8	" "	0 ± 350	2500
50	" "	" "	1700
16	" "	0 ± 400	2100
30	" "	" "	1000
12	" "	0 ± 450	400
46	Non-woven holed	0 ± 170	1639800
42	" "	" "	1148000
22	" "	0 ± 200	659000
14	" "	" "	401700
28	" "	0 ± 250	26900
11	" "	" "	15200
33	" "	0 ± 300	3400
6	" "	0 ± 450	300
26	Woven plain	0 ± 130	1808500
50	" "	0 ± 170	259700
16	" "	" "	208300
30	" "	0 ± 200	61500
12	" "	" "	66700
35	" "	0 ± 250	8500
8	" "	" "	5200
22	Woven holed	0 ± 130	1351200
33	" "	" "	1771200
46	" "	0 ± 150	290200
27	" "	" "	244600
11	" "	0 ± 170	49500
28	" "	" "	85900
6	" "	" "	87600
42	" "	0 ± 200	16500
14	" "	" "	11900

Table 14
REVERSED AXIAL FATIGUE DATA FOR LAY-UP E ($\pm 45, 0$)
Frequency = 10 Hz

Coupon number	Coupon type	Stress range MPa	Cycles to failure
35	Non-woven plain	0 \pm 350	1246700
8	" "	"	554100
44	" "	0 \pm 400	200
26	" "	"	309600
20	" "	0 \pm 450	49100
50	" "	"	10900
16	" "	0 \pm 500	3400
30	" "	"	12400
12	" "	0 \pm 600	400
52	Non-woven holed	0 \pm 350	1381500 (th)
22	" "	"	1248700 (th)
46	" "	0 \pm 400	100 (th)
33	" "	"	398900 (le)
11	" "	0 \pm 450	101600 (th)
42	" "	"	84700 (th)
14	" "	0 \pm 500	28900 (te)
28	" "	"	16900 (th)
6	" "	0 \pm 600	500 (th)
48	Woven plain	0 \pm 350	2248500
35	" "	"	317000
44	" "	0 \pm 400	198100
26	" "	"	82700
8	" "	0 \pm 450	36700
50	" "	"	45300
16	" "	0 \pm 500	12600
30	" "	"	7900
12	" "	0 \pm 600	800
24	Woven holed	0 \pm 350	44800 (th)
46	" "	"	585100 (th)
1	" "	0 \pm 400	184700 (te)
22	" "	"	130300 (th)
33	" "	0 \pm 450	1300 (th)
11	" "	"	40600 (th)
42	" "	0 \pm 500	1500 (th)
14	" "	"	800 (th)
28	" "	0 \pm 550	300 (th)
6	" "	0 \pm 600	5500 (le)

le = failure at lower end of coupon. th = failure through the hole.
 te = failure across the top end of the coupon.

REFERENCES

- | <u>No.</u> | <u>Author</u> | <u>Title, etc</u> |
|------------|--|---|
| 1 | B. Harris | Fatigue and accumulation of damage in reinforced plastics.
<i>Composites</i> , <u>9</u> (4), p 214 (1977) |
| 2 | R.A. Weinberger
A.R. Somoroff
B.L. Riley | US Navy certification of composite wings for the F-18 and advanced Harrier aircraft.
<i>AIAA Journal</i> , <u>17</u> , p 477 (1977) |
| 3 | J.C. Watson | AV-8B composite fuselage design.
Paper presented at AIAA 19th Aerospace Sciences Meeting, St. Louis, Mo., January 1981 |
| 4 | S. Hanaqud
et al | Comparative evaluation of woven graphite epoxy composites.
NASA CR 159001, Georgia Institute of Technology, July 1979 |
| 5 | S.M. Bishop
P.T. Curtis | An assessment of the potential of woven carbon fibre reinforced plastics for aerospace use.
RAE Technical Report 83010 (1983) |
| 6 | P.T. Curtis
S.M. Bishop | An assessment of the potential of woven carbon fibre reinforced plastics for high performance applications.
<i>Composites</i> , <u>15</u> (4), pp 259-266 (1984) |
| 7 | P.T. Curtis
B.B. Moore | The effect of environmental exposure on the fatigue behaviour of CFRP laminates.
RAE Technical Report 84027 (1984) |
| 8 | P.T. Curtis | The effect of edge stresses on the failure of (0, 45, 90) CFRP laminates.
RAE Technical Report 80054 (1980) |
| 9 | P.T. Curtis | The effect of edge stresses on the failure of (0, 45, 90) CFRP laminates.
<i>Journal of Materials Science</i> , <u>19</u> , pp 167-182 (1984) |
| 10 | P.T. Curtis | The tensile behaviour of (0, 45, 90) CFRP laminates - effects of material type and layer thickness.
RAE Technical Report 83011 (1983) |
| 11 | W. Cantwell
P.T. Curtis
J. Morton | Post-impact fatigue performance of carbon fibre laminates with mixed-woven layers.
<i>Composites</i> , <u>14</u> (3), pp 301-306 (1983) |
| 12 | W. Cantwell
P.T. Curtis
J. Morton | Impact and subsequent fatigue damage growth in carbon fibre laminates.
<i>International Journal of Fatigue</i> , <u>6</u> (2), pp 113-118 (1984) |
| 13 | T.W. Chou
W.B. Stewart
M.G. Bader | On the compression strength of glass/epoxy composites.
Met. Soc. AIME, pp 331-346 (1979) |

REFERENCES (concluded)

<u>No.</u>	<u>Author</u>	<u>Title, etc</u>
14	D. Pulew R.T. Potter	The effect of environment on the compression strength of notched CFRP - a fractographic investigation. RAE Technical Report 84032 (1984)
15	P.T. Curtis	CRAG test methods for the measurement of the engineering properties of fibre reinforced plastics. RAE Technical Report 84102 (1984)
16	P.T. Curtis J. Morton	The effect of fibre surface treatment on the compressive strength of CFRP laminates. RAE Technical Report 82047 (1982)
17	P.T. Curtis J. Morton	The effect of fibre surface treatment on the compressive strength of CFRP laminates. Proc. ICCM IV, Tokyo, 1982
18	A.S.D. Wang	A non-linear microbuckling model predicting the compressive strength of unidirectional composites. ASME Meeting, San Francisco, USA, December 1978
19	M.A. Crannage	The flexural strength of unidirectional composite materials - an analytical investigation. Final Report under MOD Contract A91a, 1278, November 1984
20	C.J. Jones R.F. Dickson T. Adam H. Reiter B. Harris	The environmental fatigue behaviour of reinforced plastics. Proc. Roy. Soc., London, A396, pp 315-338, 1984

Fig 1

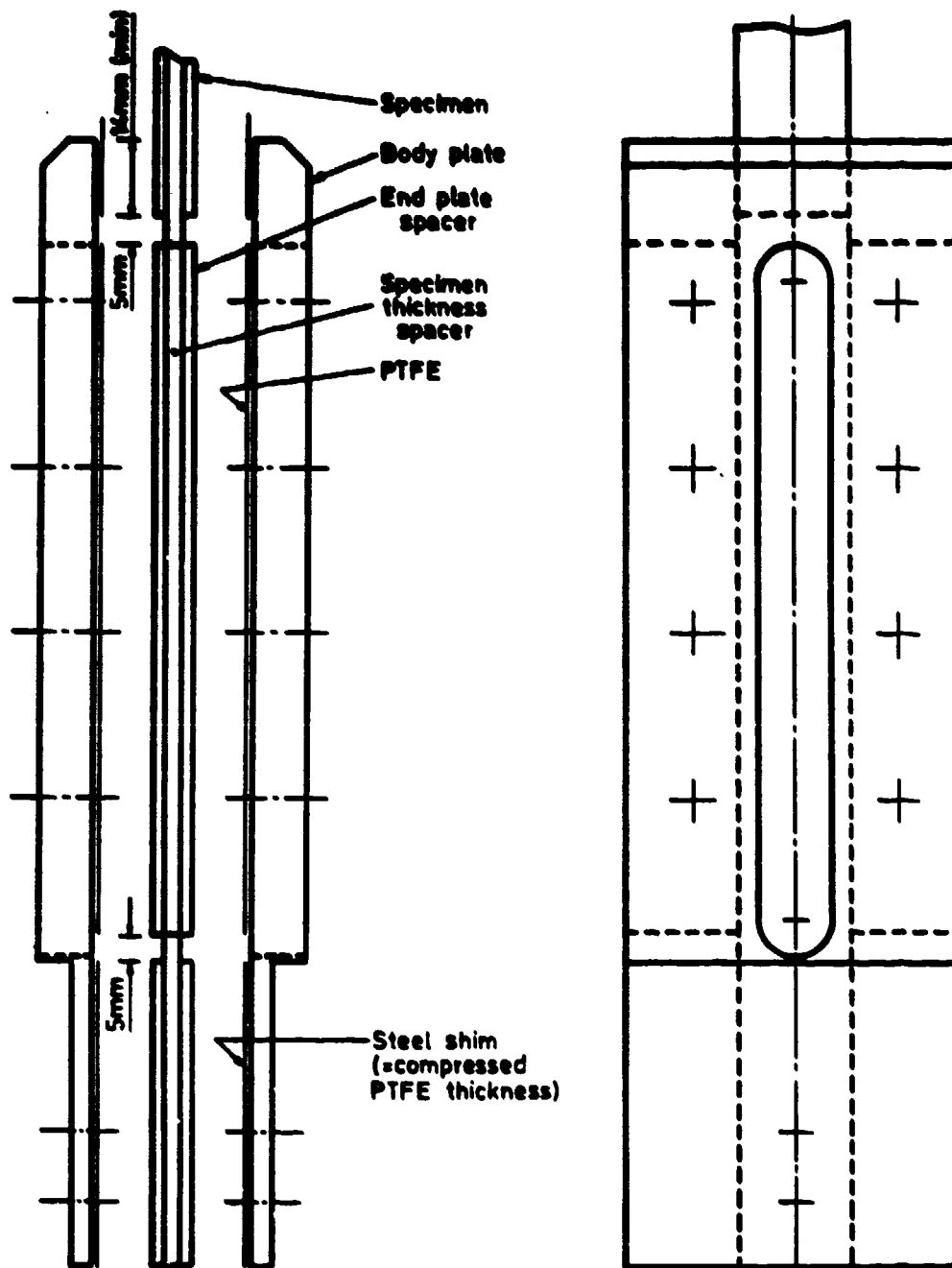


Fig 1 Anti-buckling guide used to support coupons during compressive testing

Fig 2

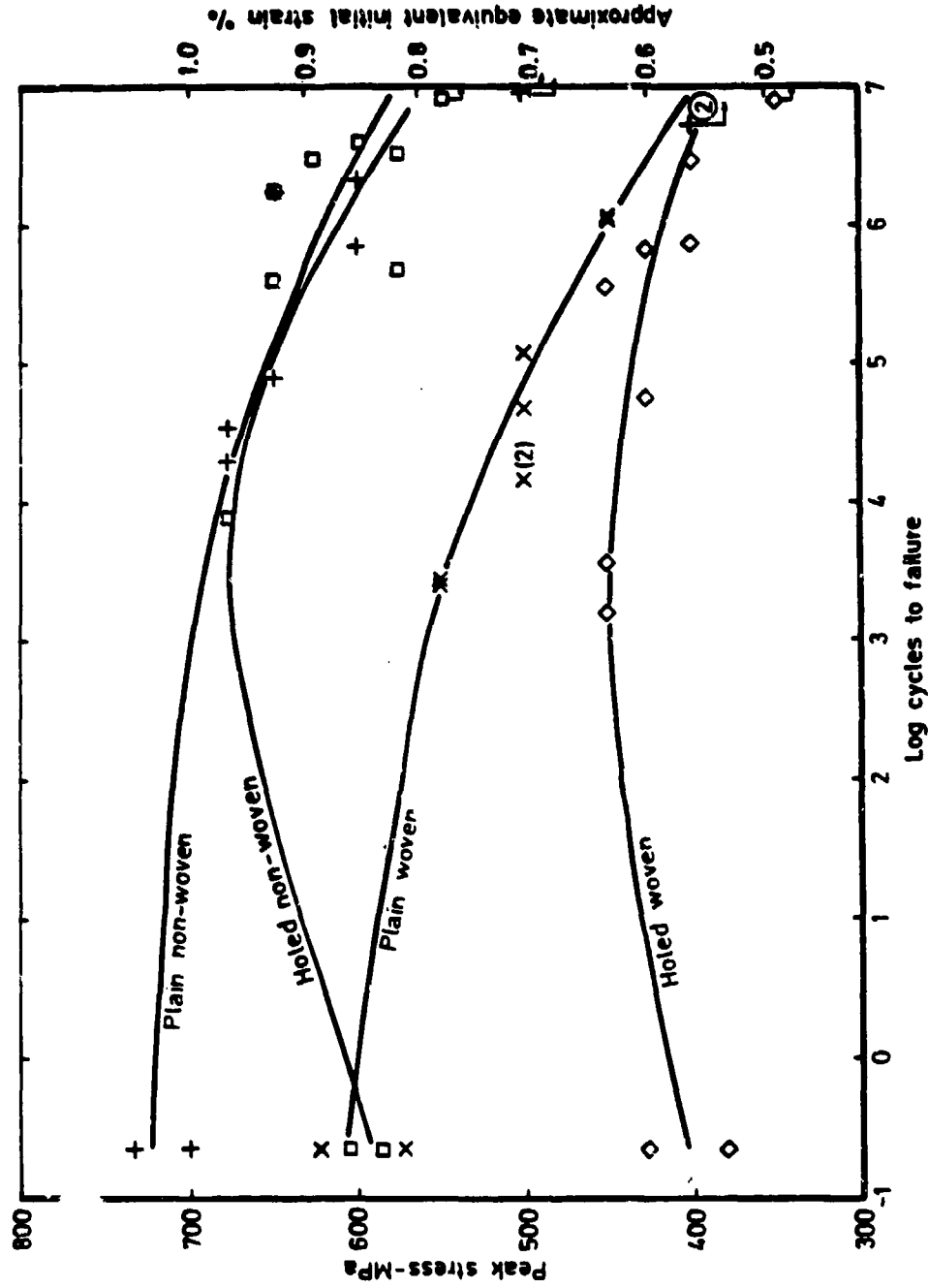


Fig 2 S-N plots of zero-tension fatigue data for layup A (0,90).
Horizontal arrows denote run-outs

TR 88059

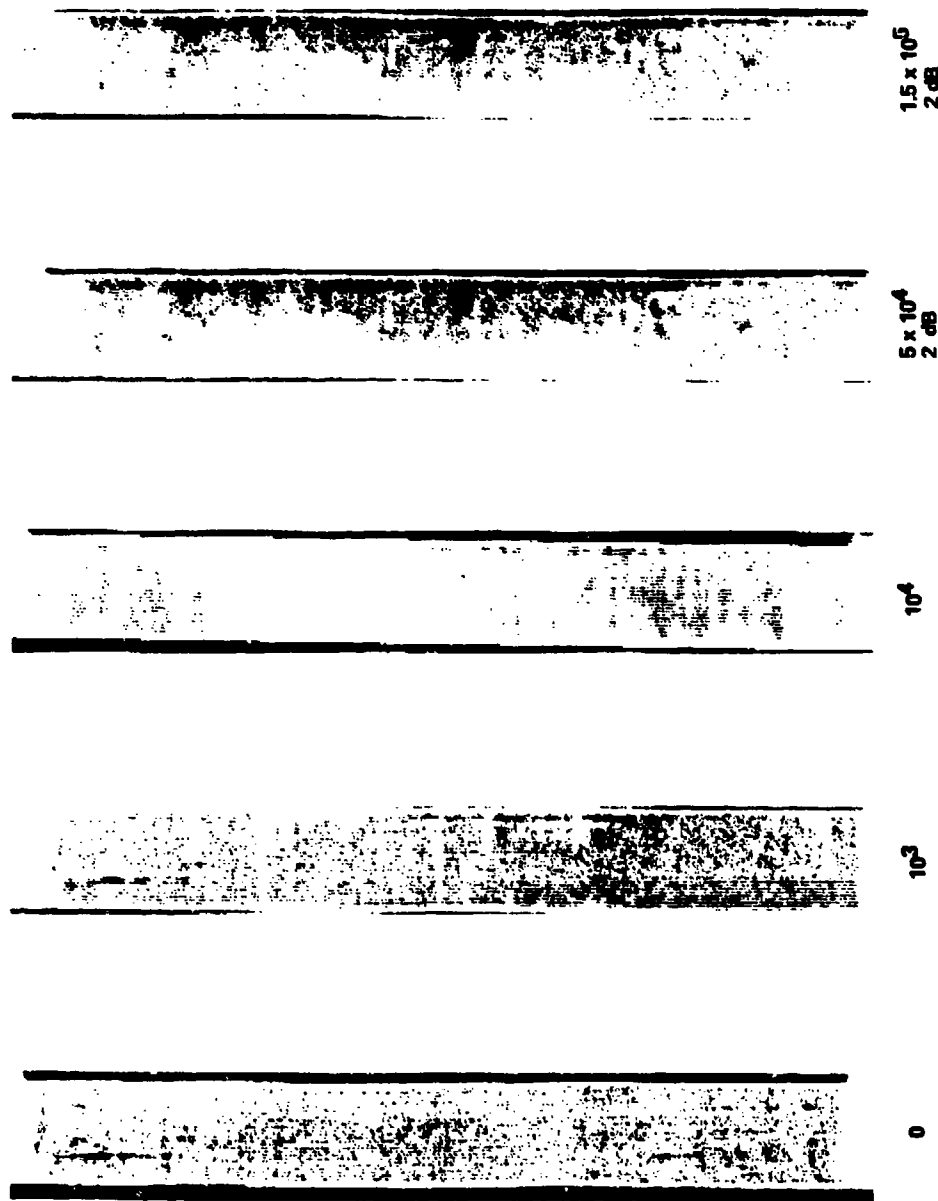


Fig 3 Ultrasonic C-scans of a non-woven plain coupon with layup A (0.90) tested in tensile fatigue at the stress level giving a mean life of 100000 cycles. Left to right, scans after: 0 cycles at 1 dB steps, 1000 cycles at 1 dB steps, 10000 cycles at 1 dB steps, 50000 cycles at 2 dB steps, 150000 at 2 dB steps

Fig 4

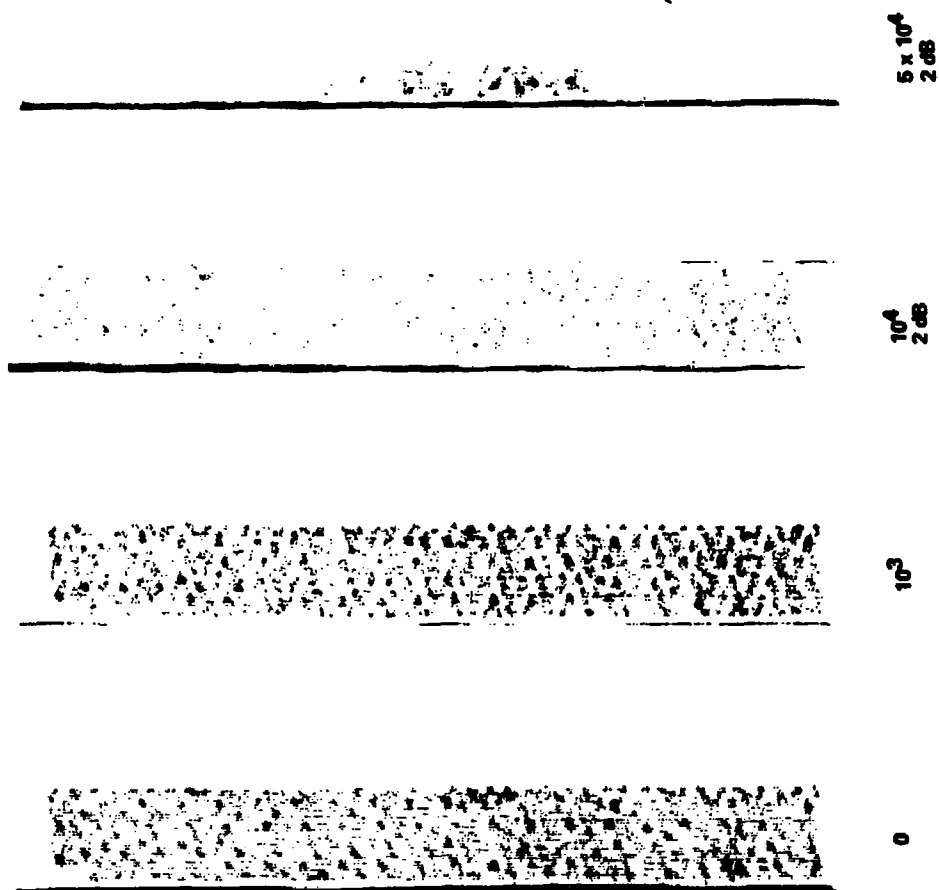


Fig 4 Ultrasonic C-scans of a woven plain coupon with layup A (0/90) tested in tensile fatigue at the stress level giving a mean life of 100000 cycles. Left to right, scans after: 0 cycles at 1 dB steps, 1000 cycles at 1 dB steps, 10000 cycles at 2 dB steps, 50000 cycles at 2 dB steps

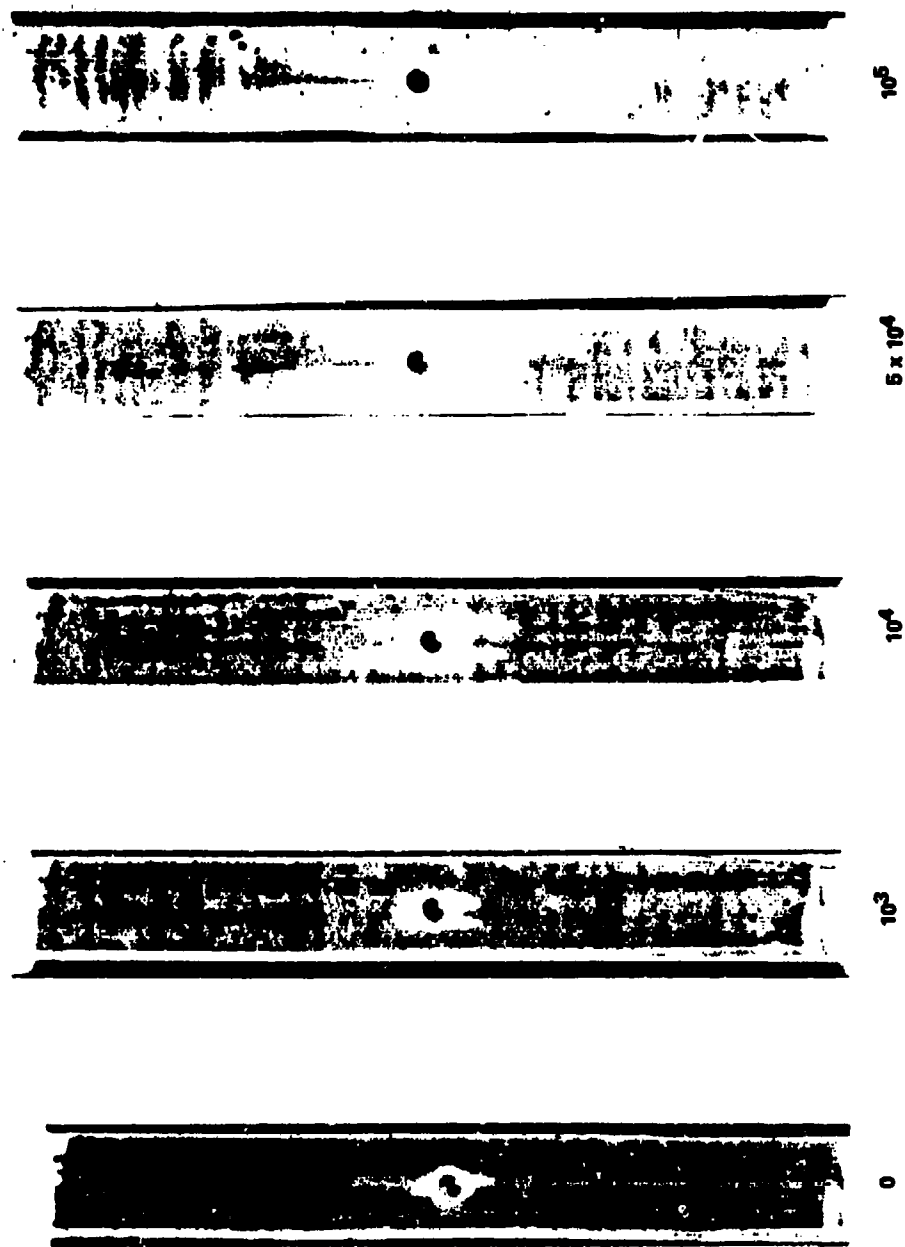


Fig 5

Fig 5 Ultrasonic C-scans of a non-woven holed coupon with layup A (0.90) tested in tensile fatigue at the stress level giving a mean life of 100,000 cycles. Left to right, scans after: 0 cycles at 1 dB steps, 1000 cycles at 1 dB steps, 10,000 cycles at 1 dB steps, 50,000 cycles at 1 dB steps, 100,000 cycles at 1 dB steps

Fig 6

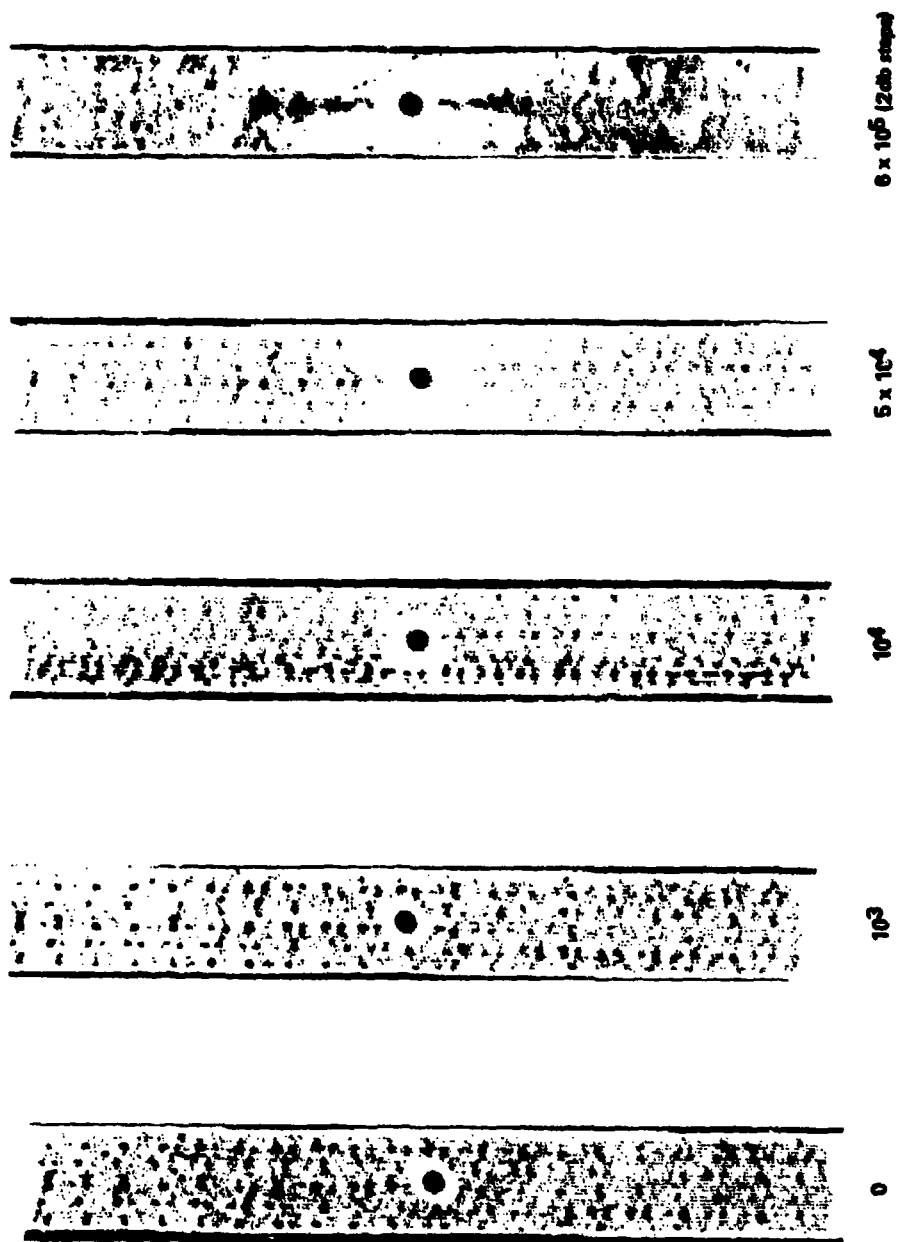


Fig 6 Ultrasonic C-scans of a woven hole coupon with layout A (0.90) tested in tensile fatigue at the stress level giving a mean life of 100000 cycles. Left to right, scans after: 0 cycles at 1 db steps, 1000 cycles at 1 db steps, 10000 cycles at 1 db steps, 50000 cycles at 1 db steps, 600000 cycles at 2 db steps

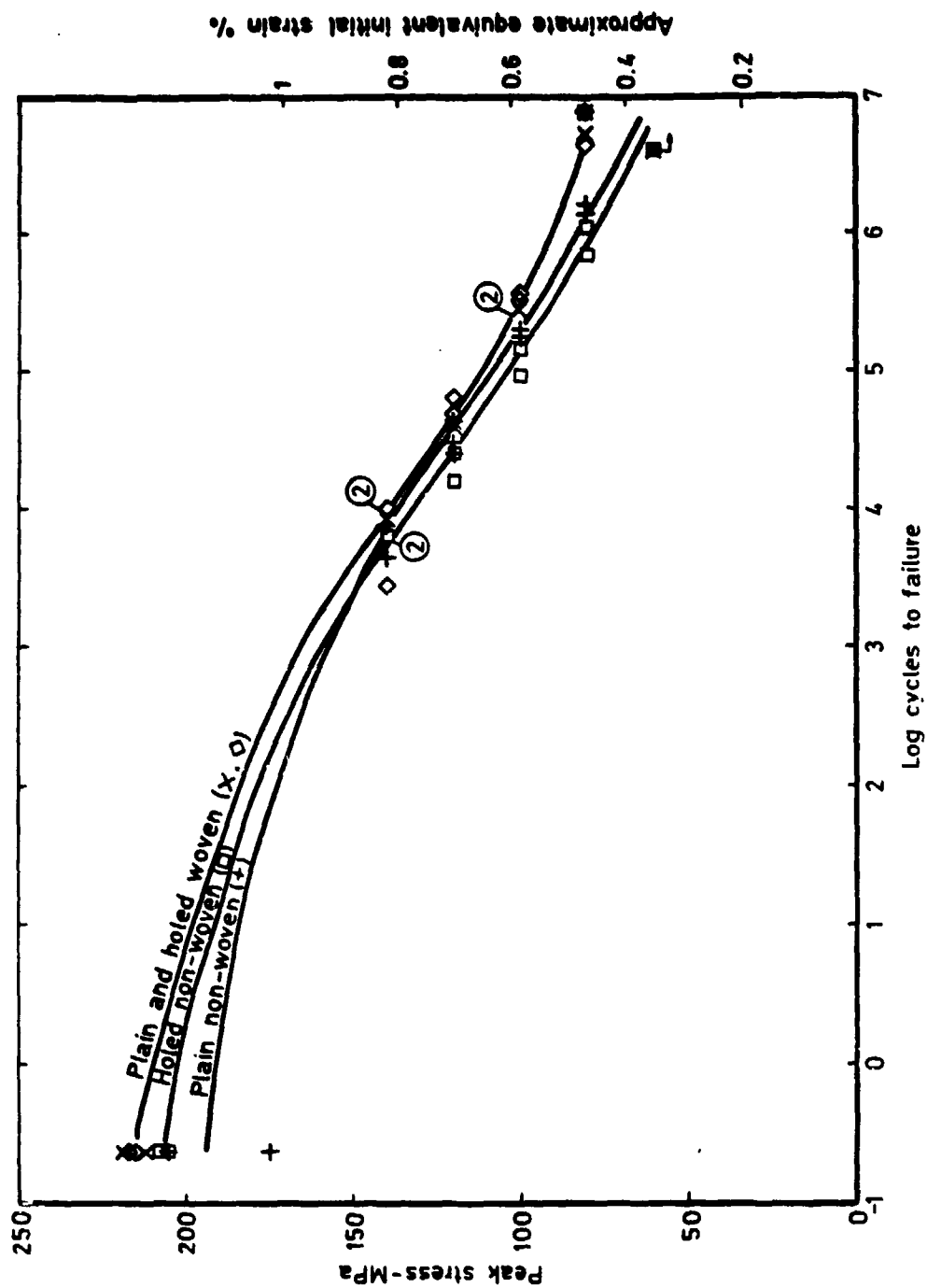
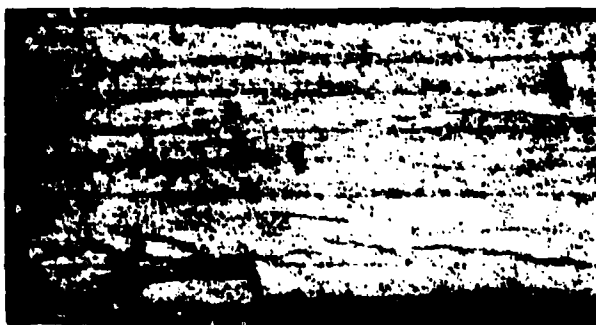


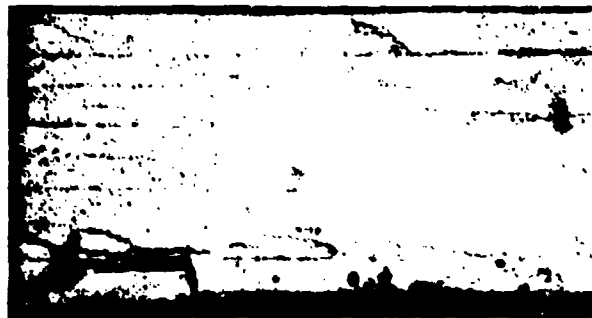
Fig 7 S-N plots of tensile fatigue data for layout B (1.45). Horizontal arrows denote run-outs

Fig 7

Fig 8



10^3



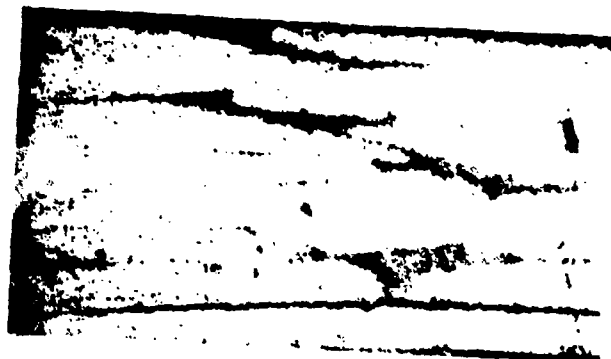
5×10^4



failed

Fig 8 Optical micrographs of non-woven plain coupons with layup B (± 45) tested in tensile fatigue at the stress level giving a mean life of 10000 cycles. Left to right, micrographs after: 1000 cycles, 5000 cycles, failure

TR 33099



10^3



10^4



1.49×10^5
failed

Fig 9 Optical micrographs of woven plain coupons with layup B (1:45) tested in tensile fatigue at the stress level giving a mean life of 100,000 cycles. Left to right, micrographs after: 1000 cycles, 10,000 cycles, failure

Fig 10

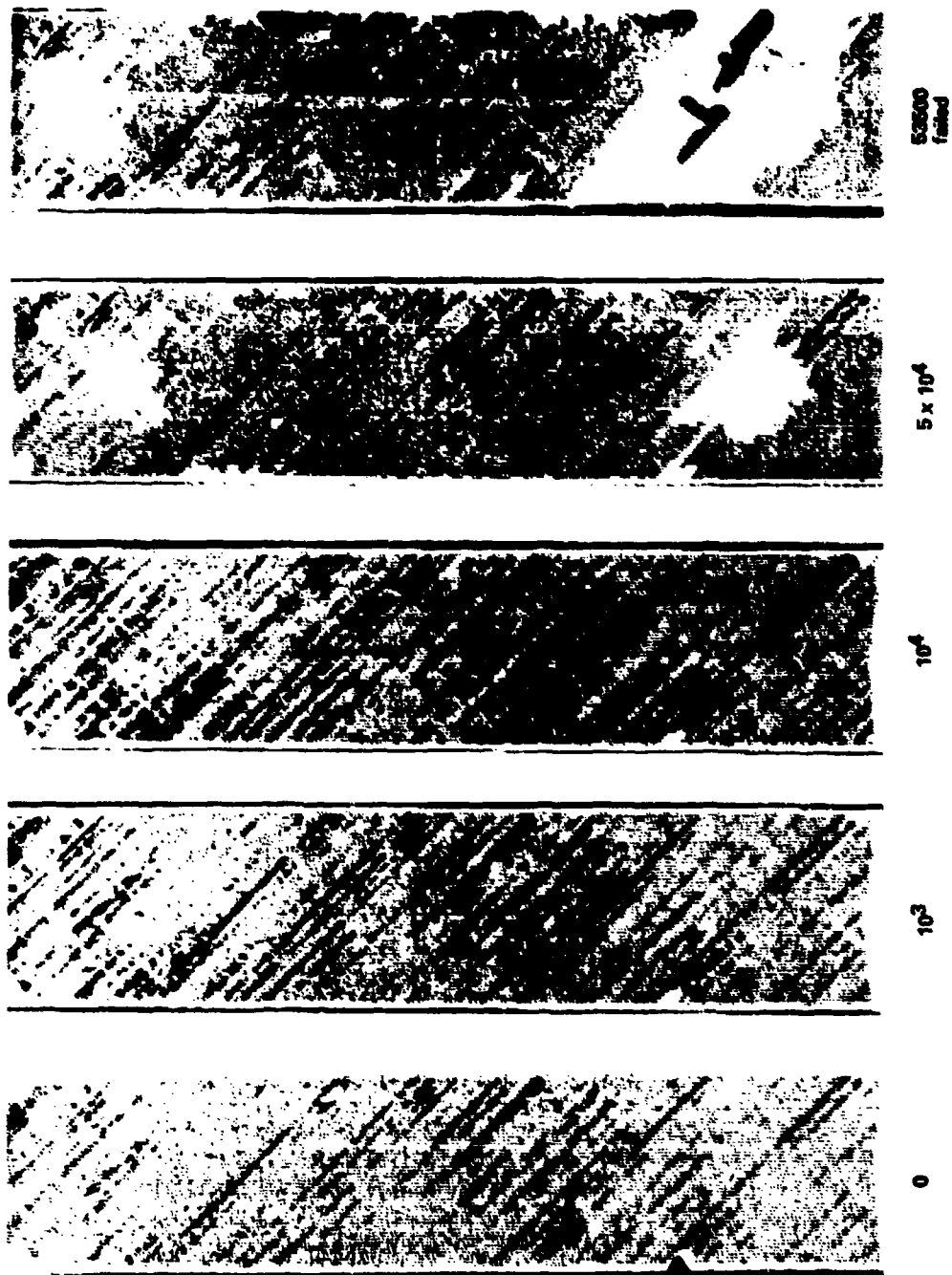
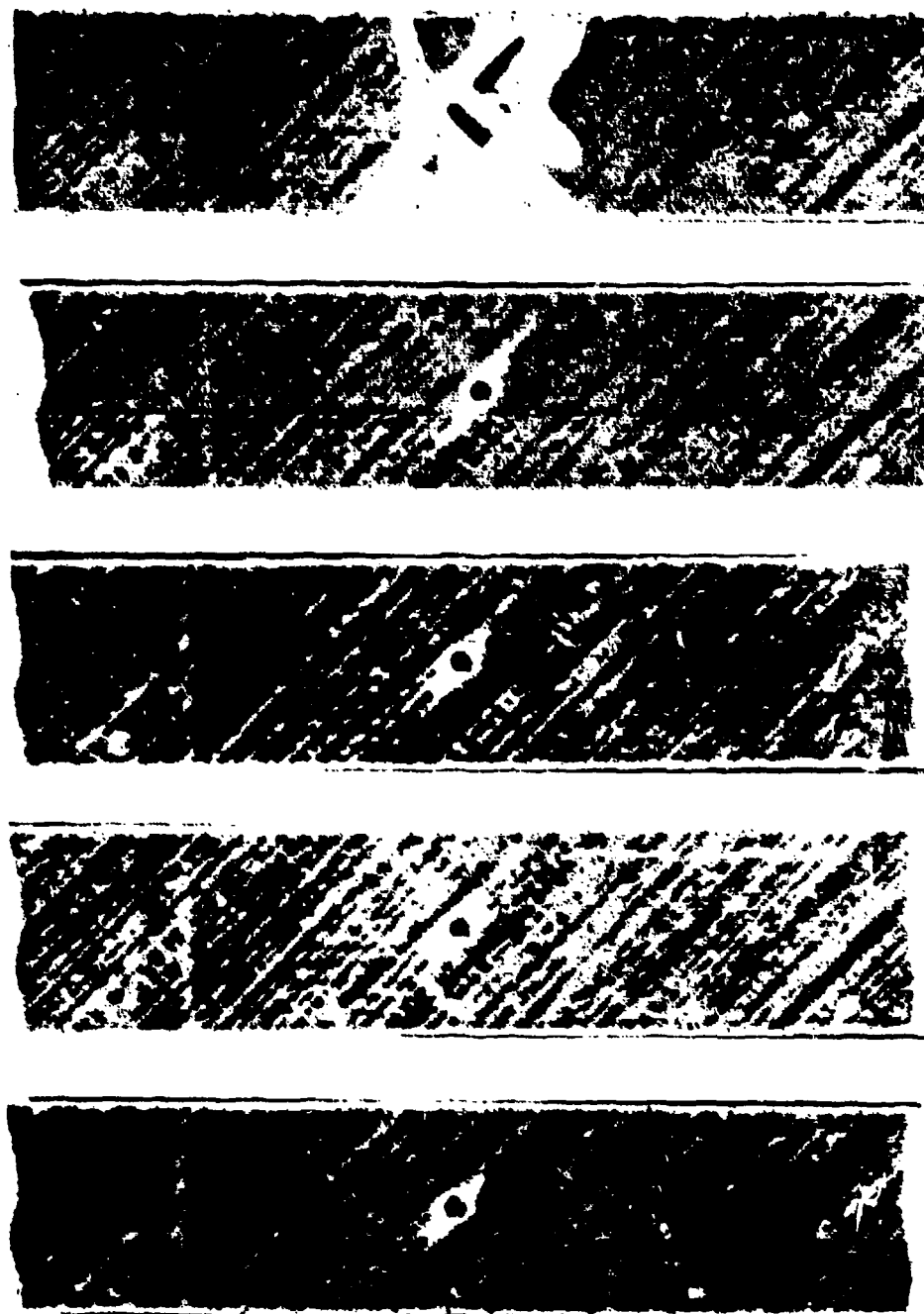


Fig 10 Ultrasonic C-scans of a non-woven plain coupon with layup B (± 45) tested in tensile fatigue at the stress level giving a mean life of 10000 cycles. Left to right, scans after: 0 cycles at 1 dB steps, 1000 cycles at 1 dB steps, 10000 cycles at 1 dB steps, 50000 cycles at 1 dB steps, 53500 cycles at 1 dB steps - failure

TR 20050



1.289×10^6
failed

10^5

10^4

10^3

0

Fig 11 Ultrasonic C-scans of a non-crown holed coupon with layout B ($\pm 45^\circ$) tested in tensile fatigue at the stress level giving a mean life of 100000 cycles. Left to right, scans after: 0 cycles at 1 dB steps, 1000 cycles at 1 dB steps, 10000 cycles at 2 dB steps, 100000 cycles at 2 dB steps, 138900 cycles at 2 dB steps - failed

Fig 12

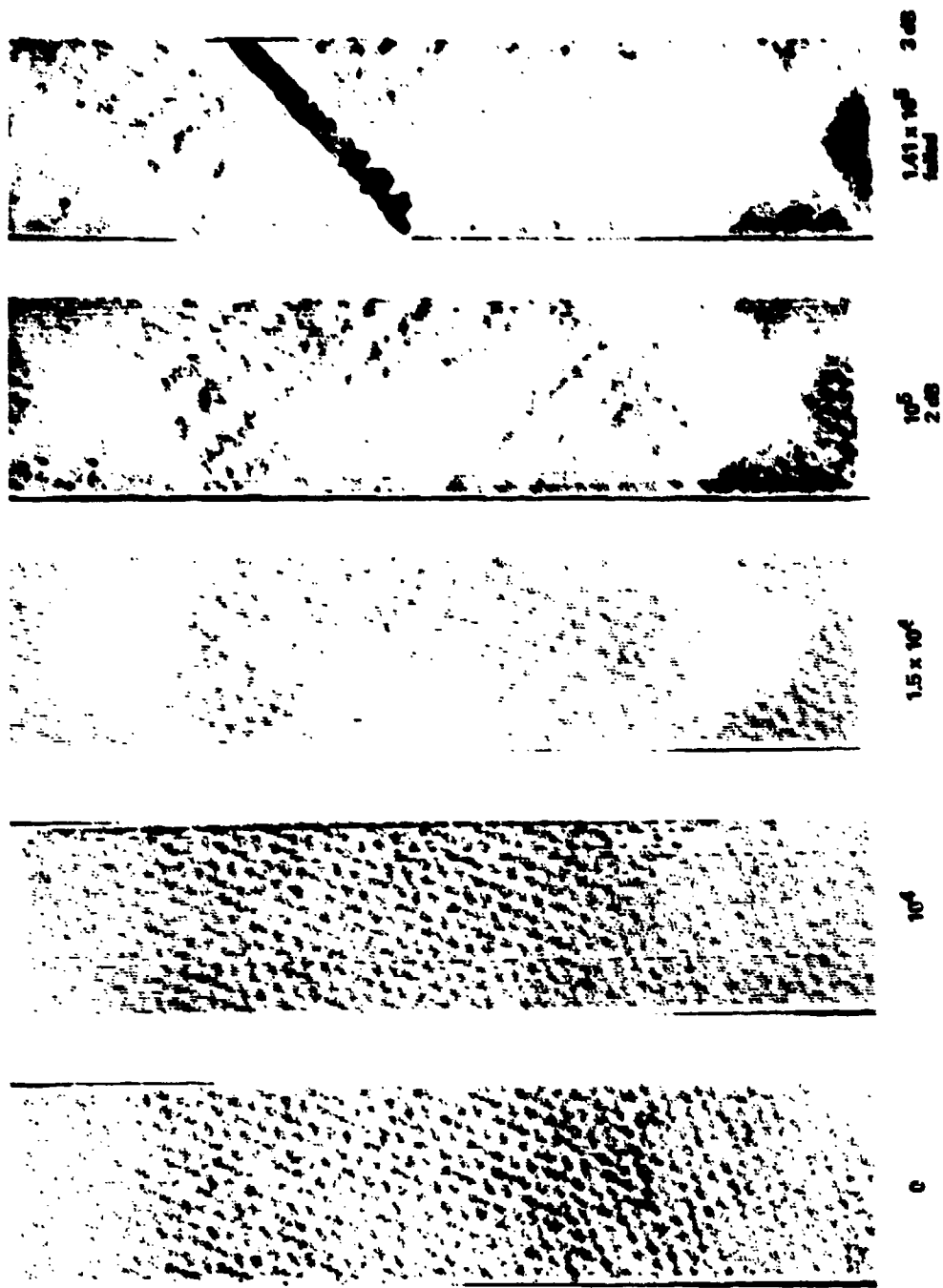


Fig 12 Ultrasonic C-scans of a woven plain coupon with layup B ($\pm 95^\circ$) tested in tensile fatigue at the stress level giving a mean life of 100000 cycles. Left to right, scans after: 0 cycles at 1 dB steps, 10000 cycles at 1 dB steps, 50000 cycles at 1 dB steps, 100000 cycles at 2 dB steps, 149000 cycles - failure at 3 dB steps

TR 00000

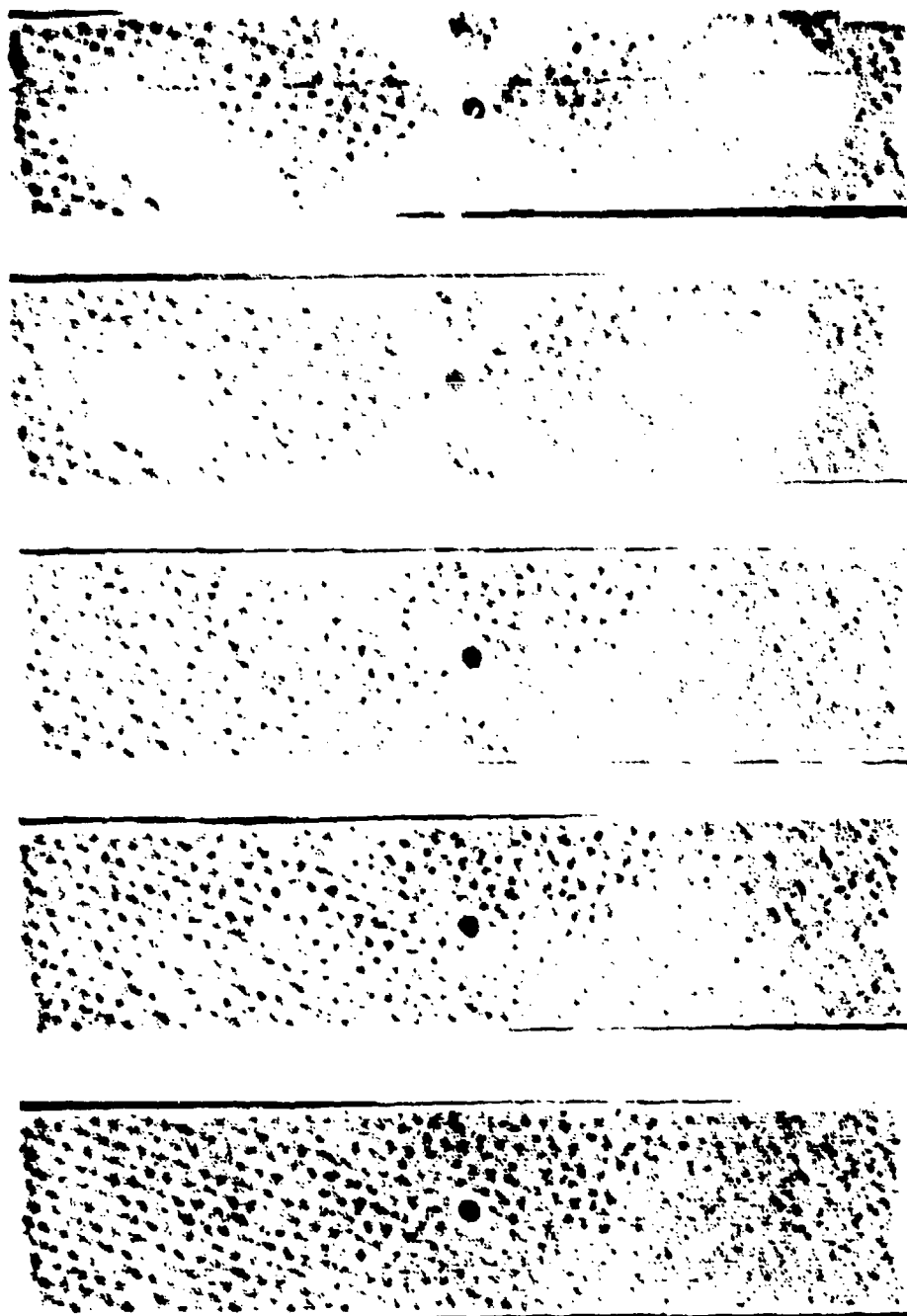


Fig 13 Ultrasonic C-scans of a woven hole coupon with layup B (± 45) tested in tensile fatigue at the stress level giving a mean life of 100000 cycles. Left to right, scans after: 0 cycles at 1 dB steps, 1000 cycles at 1 dB steps, 10000 cycles at 1 dB steps, 50000 cycles at 1 dB steps, failure

Fig 14

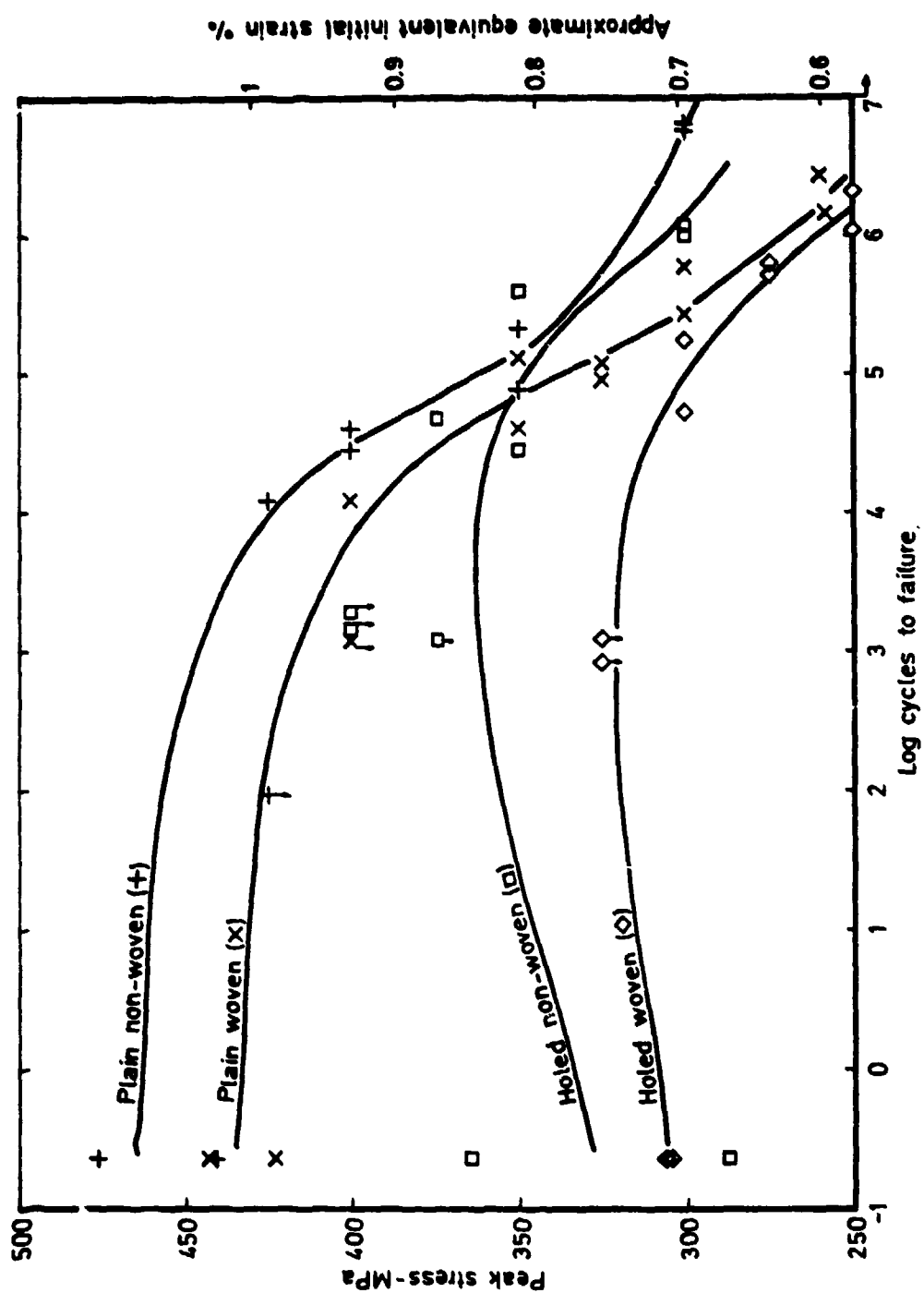


Fig 14 S-N plots of tensile fatigue data for layout C ($\pm 45,0,90$). Vertical arrows denote run-outs and horizontal arrows run-outs

Fig 15

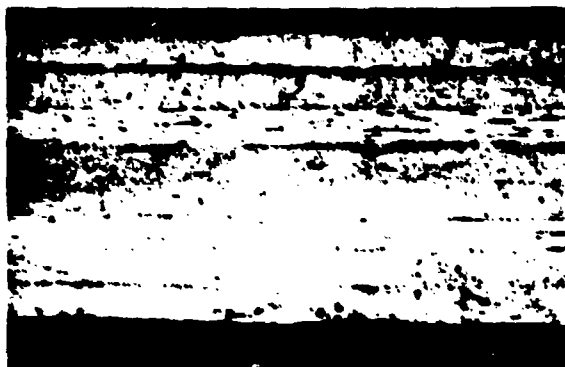
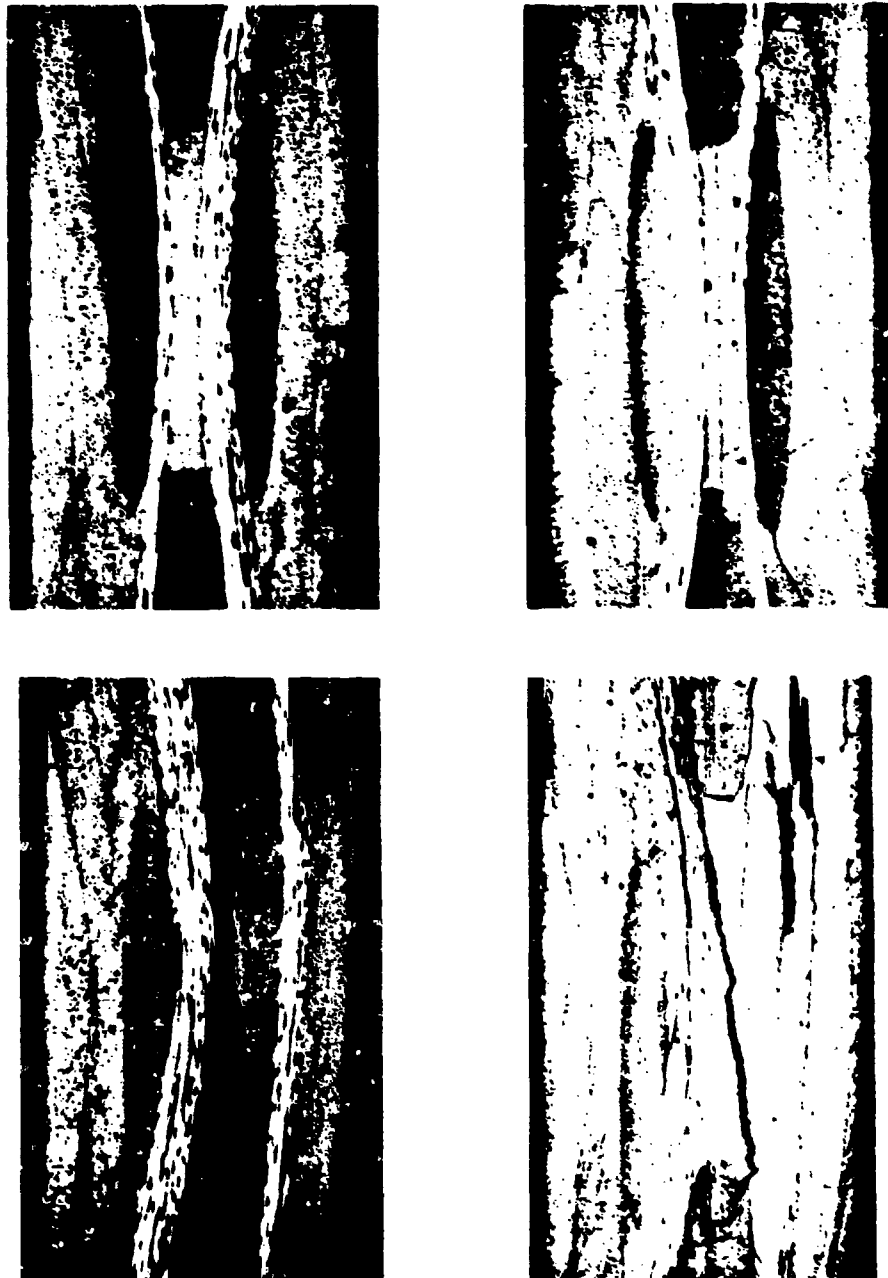


Fig 15 Optical micrograph of a non-woven plain coupon with layup C ($\pm 45,0,90$) after 10000 cycles, tested in tensile fatigue at the stress level giving a mean life of 100000 cycles

Fig 16



WXC-19 O-T plan (a) 10^3 (b) 10^4 (c) 5×10^4 (d) 1.5×10^5

Fig 16 Optical micrographs of woven plain coupons with layup C ($\pm 45,0,90$) tested in tensile fatigue at the stress level giving a mean life of 100000 cycles. Top left to bottom right, micrographs after: 1000 cycles, 10000 cycles, 50000 cycles, 150000 cycles

Fig 17

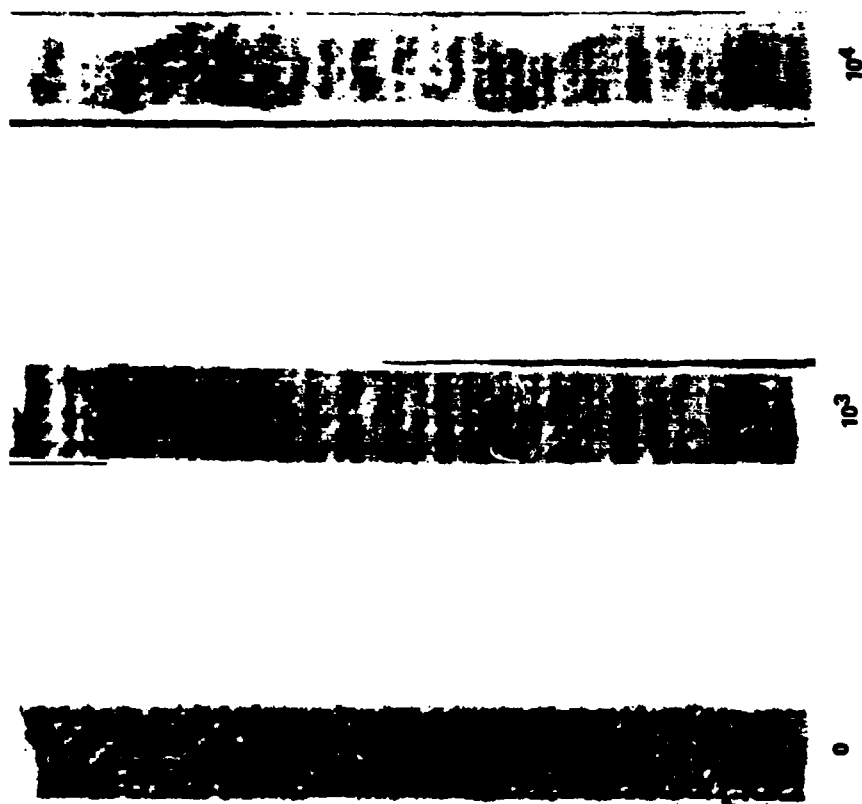


Fig 17 Ultrasonic C-scans of a non-woven plain coupon with layout C ($\pm 45, 0, 90$) tested in uniaxial fatigue at the stress level giving a mean life of 100,000 cycles. Left to right, scans after: 0 cycles at 1 dB steps, 1000 cycles at 1 dB steps, 10,000 cycles at 1 dB steps

Fig 18

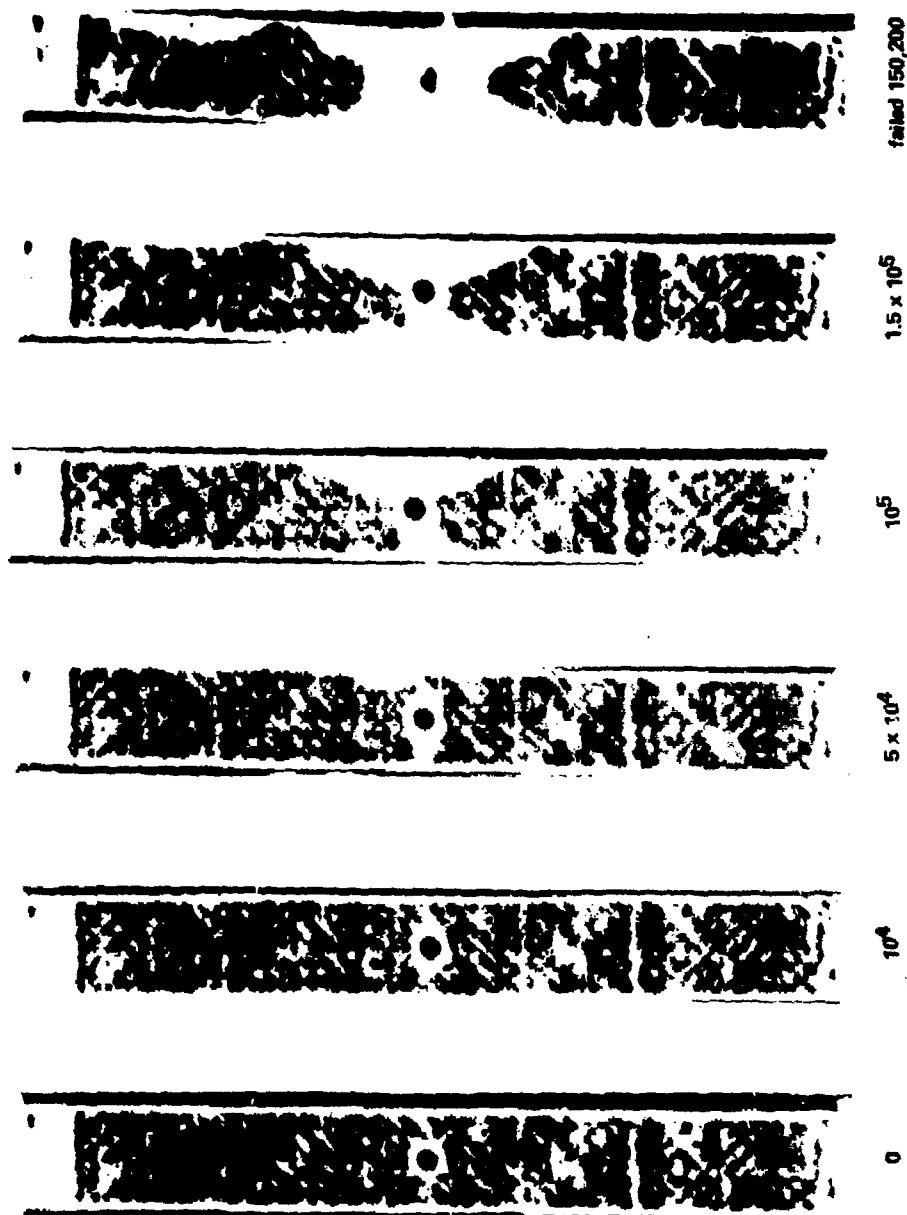


Fig 18 Ultrasonic C-scans of a non-woven holed coupon with $\log_{10} C (\pm 45, 0.90)$ tested in tensile fatigue at the stress level giving a mean life of 100,000 cycles. Left to right, scans after: 0 cycles at 1 dB steps, 10,000 cycles at 1 dB steps, 50,000 cycles at 1 dB steps, 100,000 cycles at 1 dB steps, 150,000 cycles at 1 dB steps, 150,200 cycles — failure, at 1 dB steps

TR 85060

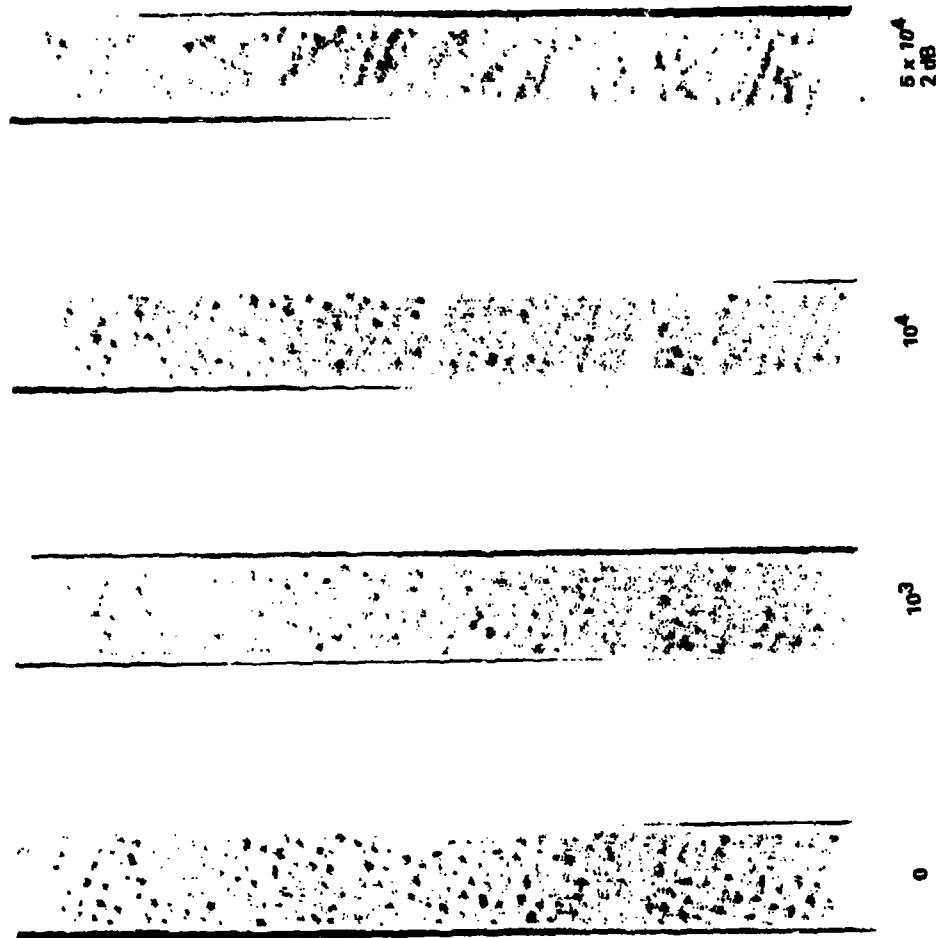


Fig 19

Fig 19 Ultrasonic C-scans of a woven plain coupon with layout C ($\pm 45, 0, 90$) tested in transverse fatigue at the stress level giving a mean life of 100000 cycles. Left to right, scans after: 0 cycles at 1 dB steps, 10000 cycles at 1 dB steps, 50000 cycles at 2 dB steps

Fig 20

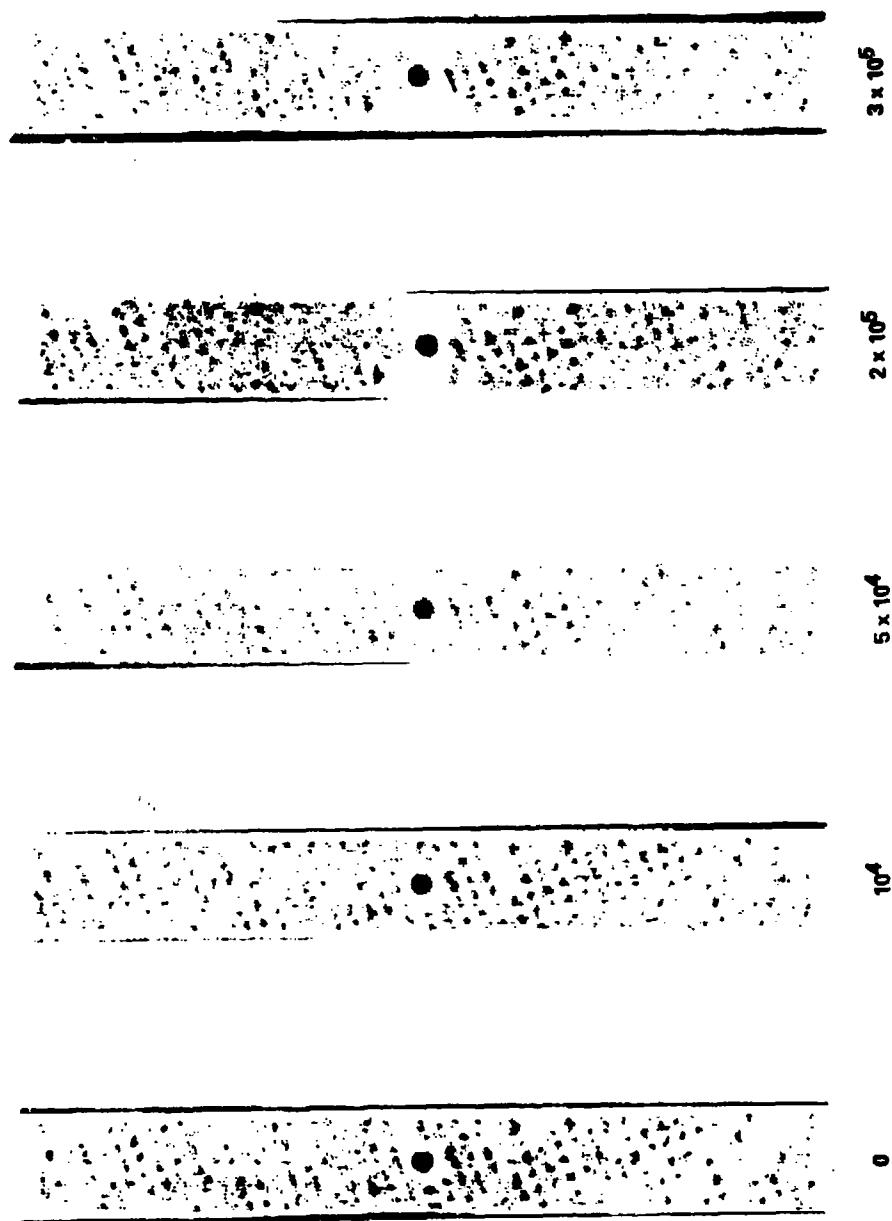


Fig 20 Ultrasonic C-scans of a woven holed coupon with layup C ($\pm 45,0,90$) tested in tensile fatigue at the stress level giving a mean life of 100000 cycles. Left to right, scans after: 0 cycles at 1 dB steps, 10000 cycles at 1 dB steps, 50000 cycles at 1 dB steps, 200000 cycles at 1 dB steps, 300000 cycles at 1 dB steps

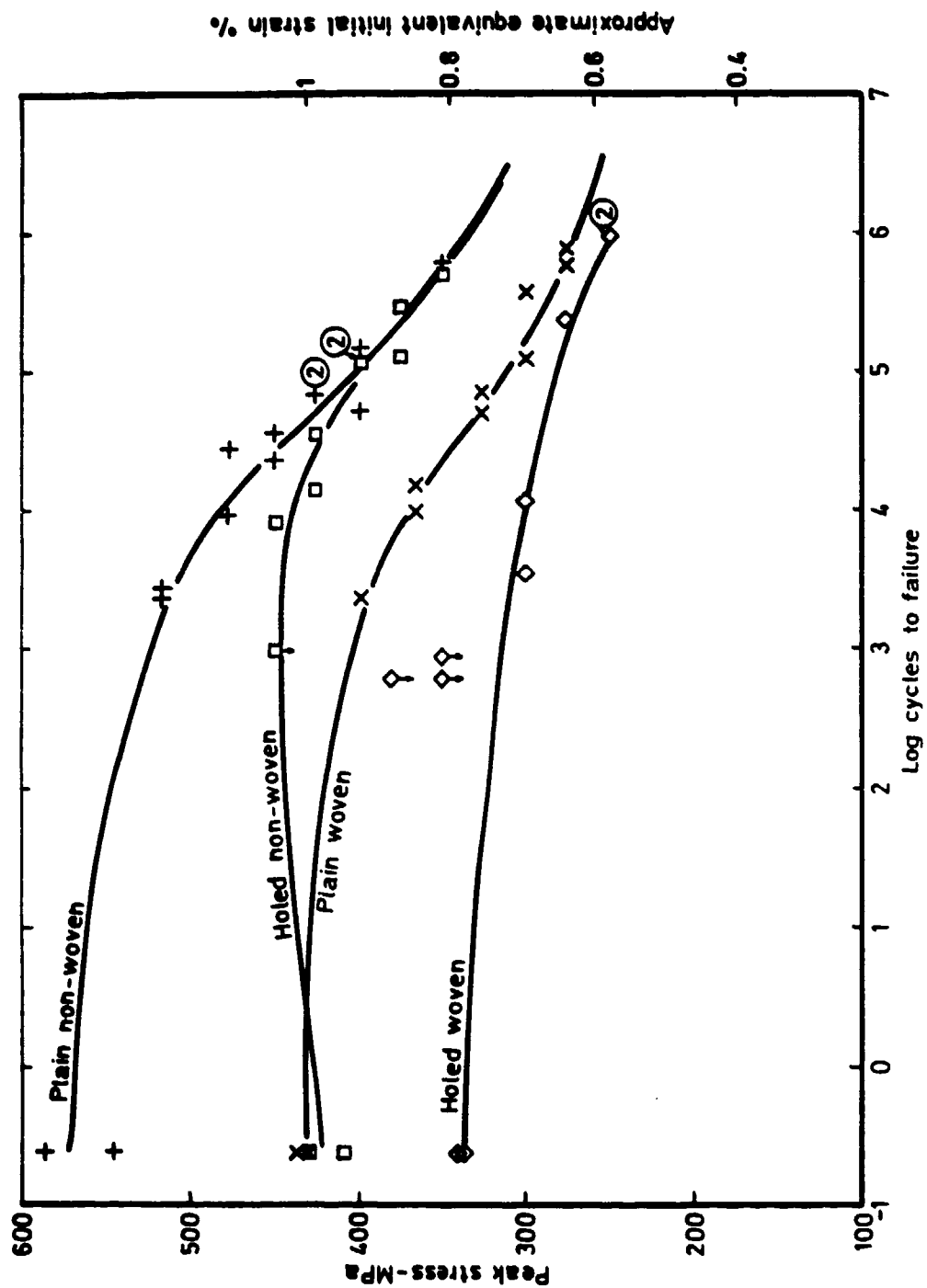
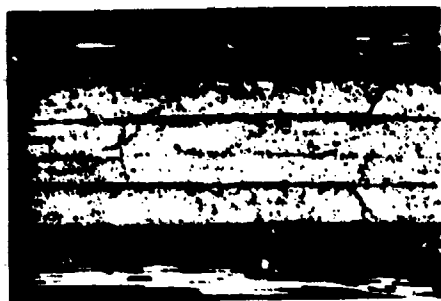


Fig 21 S-N plots of tensile fatigue data for layup D (0,90,45). Optical arrows denote run up failures

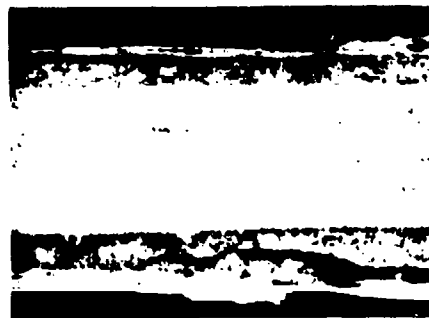
Fig 22



10^5



5×10^4



10^3

Fig 22 Optical micrographs of non-woven plain coupons with layup D (0.90, ± 45) tested in tensile fatigue at the stress level giving a mean life of 100000 cycles. Left to right, micrographs after: 1000 cycles, 50000 cycles, 100000 cycles

Fig 23



5×10^4

Fig 23 Optical micrograph of a woven plain coupon with layup D (0,90, ±45) after 50000 cycles, tested in tensile fatigue at the stress level giving a mean life of 100000 cycles

Fig 24

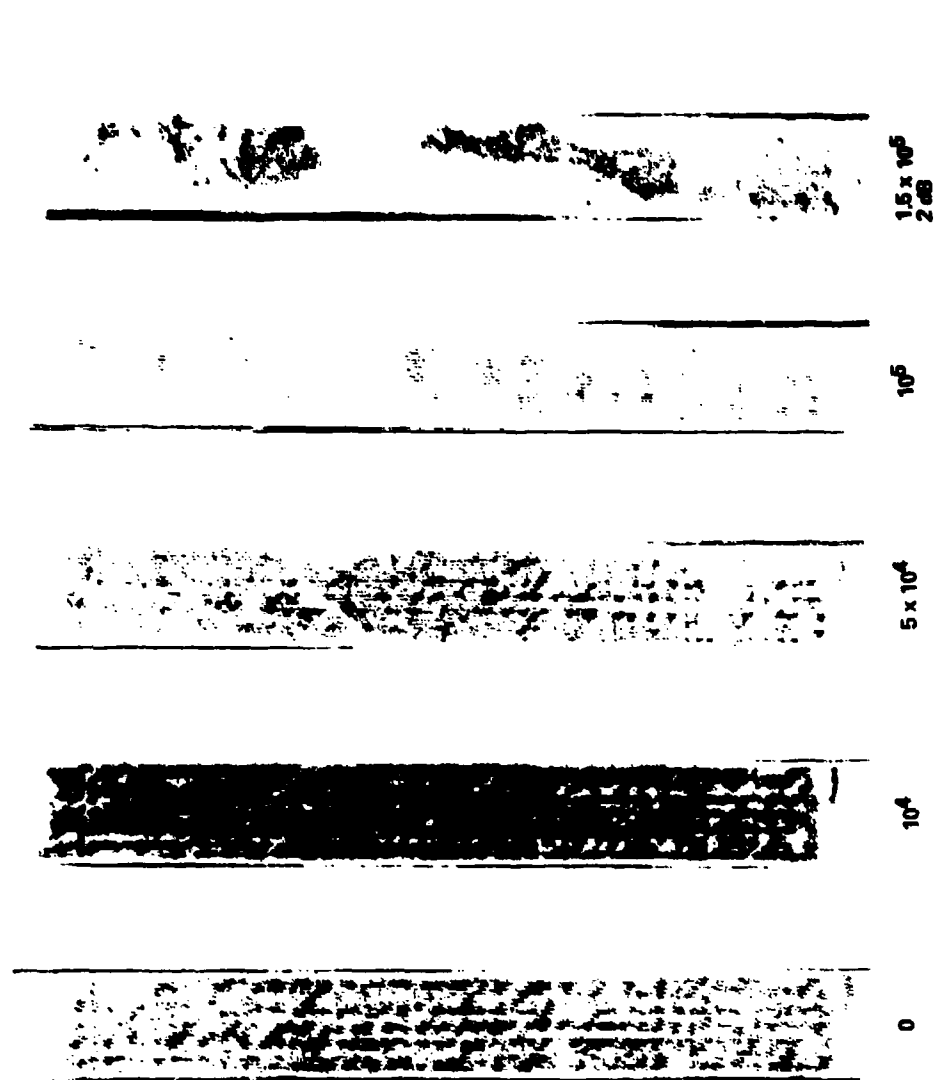


Fig 24 Ultrasonic C-scans of a non-woven plain coupon with layup D (0.90, ± 45) tested in tensile fatigue at the stress level giving a mean life of 100000 cycles. Left to right, scans after: 0 cycles at 1 dB steps, 10000 cycles at 1 dB steps, 50000 cycles at 1 dB steps, 100000 cycles at 1 dB steps, 150000 cycles at 2 dB steps

TR 00020

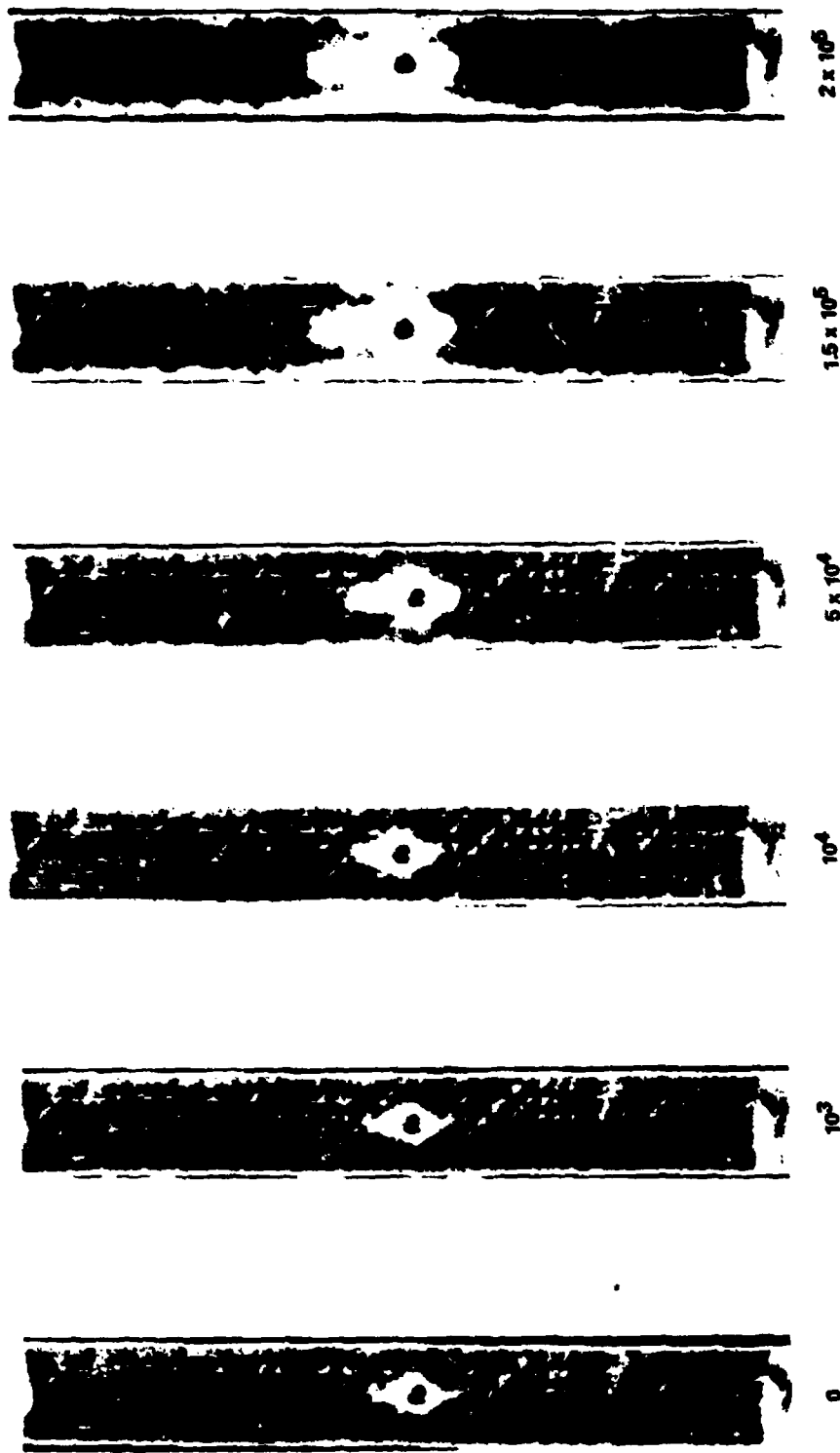


Fig 25 Ultrasonic C-scans of a non-woven holed coupon with layup D (0.90, ±45) tested in tensile fatigue at the stress level giving a mean life of 100000 cycles. Left to right, scans after: 0 cycles at 1 dB steps, 1000 cycles at 1 dB steps, 10000 cycles at 1 dB steps, 50000 cycles at 1 dB steps, 150000 cycles at 1 dB steps, 200000 cycles at 1 dB steps

Fig 26

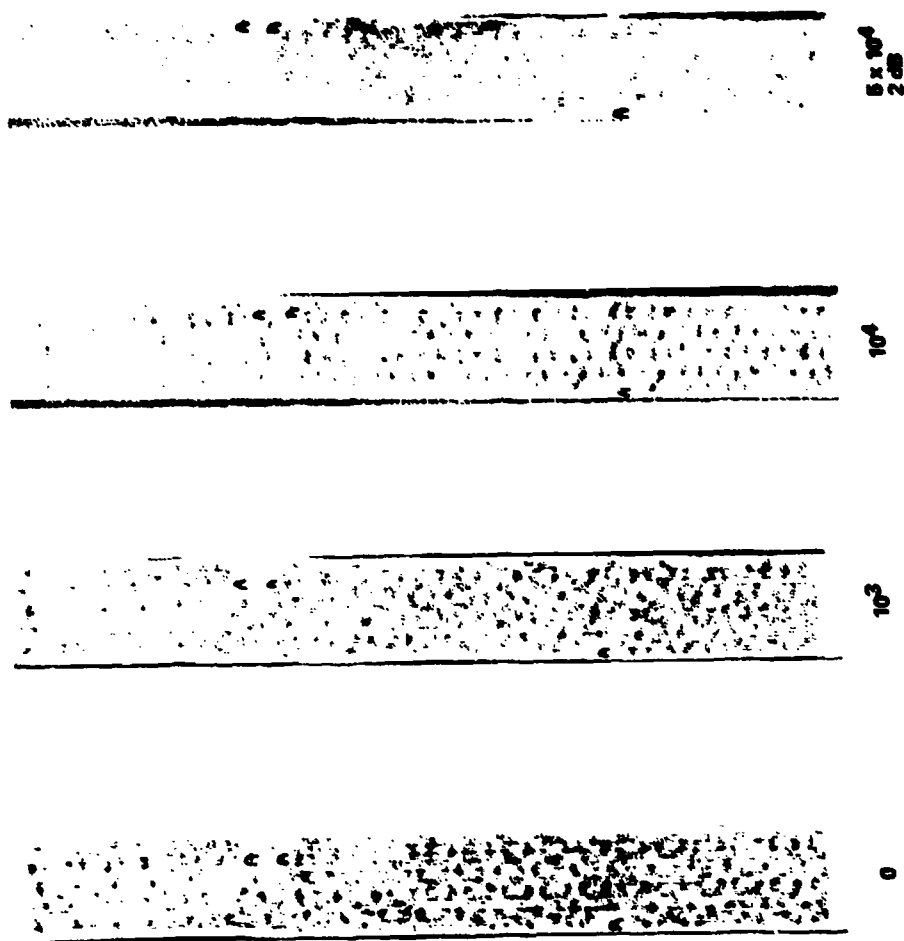


Fig 26 Ultrasonic C-scans of a woven plain coupon with layup D (0.90, ± 45) tested in tensile fatigue at the stress level giving a mean life of 100000 cycles. Left to right, scans after: 0 cycles at 1 dB steps, 10000 cycles at 1 dB steps, 50000 cycles at 2 dB steps

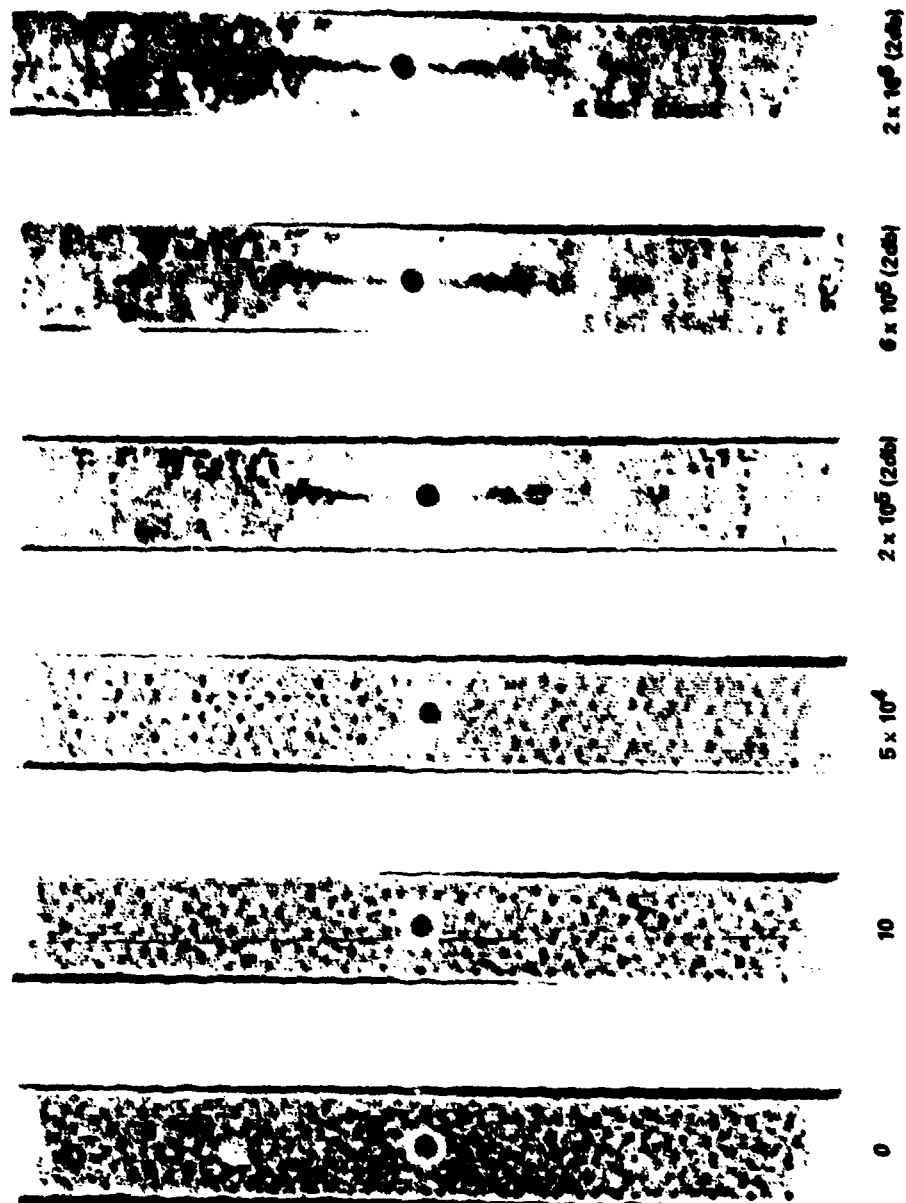


Fig 27 Ultrasonic C-scans of a woven hole coupon with layup D (0,90,±45) tested in tensile fatigue at the stress level giving a mean life of 100000 cycles. Left to right, scans after: 0 cycles at 1 dB steps, 10000 cycles at 1 dB steps, 50000 cycles at 1 dB steps, 200000 cycles at 2 dB steps, 600000 cycles at 2 dB steps, 2000000 at 2 dB steps

Fig 28

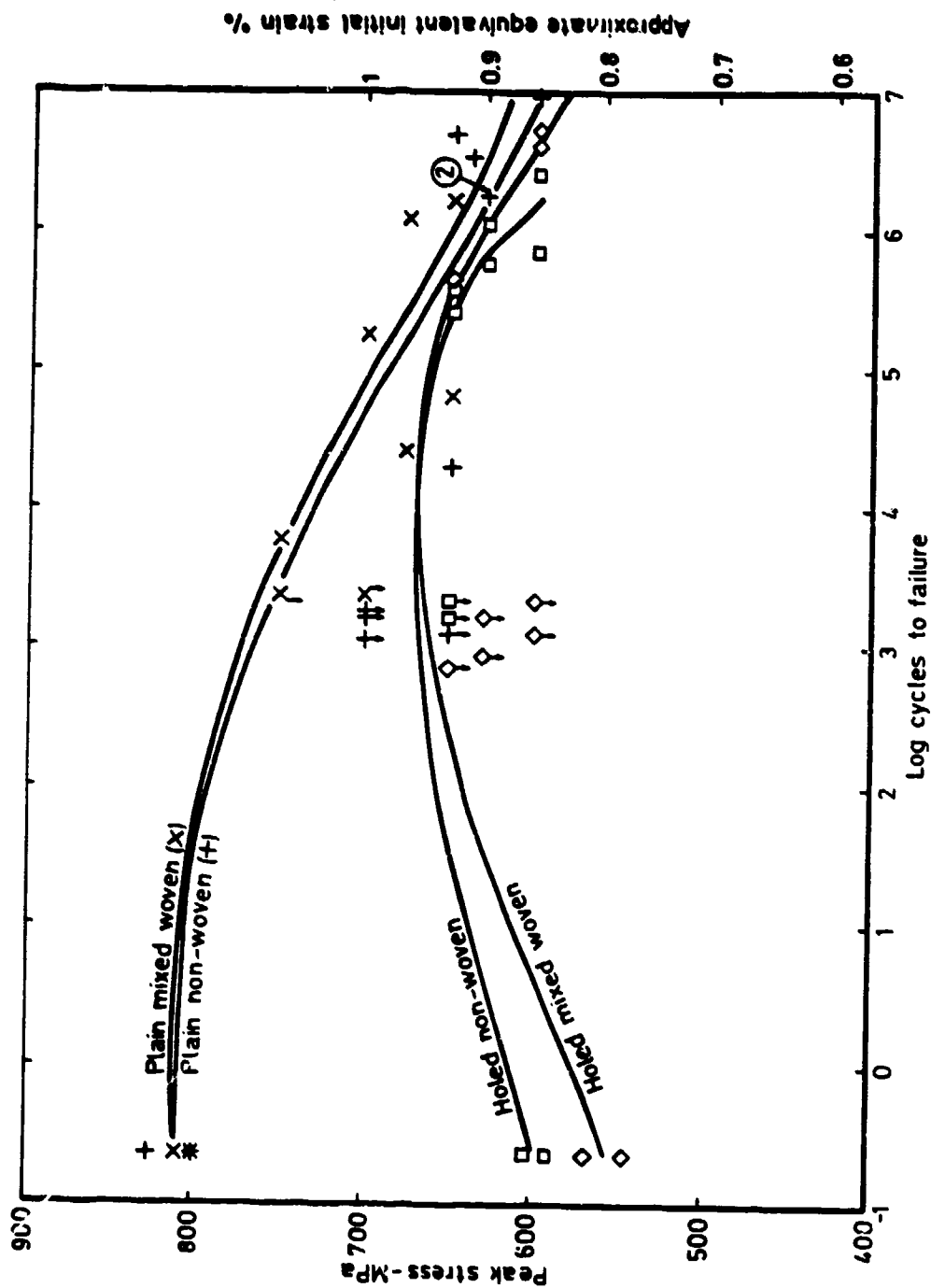
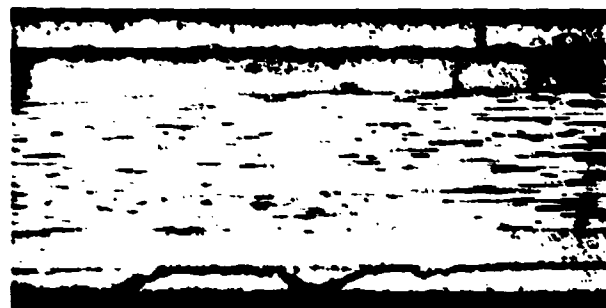


Fig 28 S-N plots of tensile fatigue data for layout E (145,02). A vertical arrow denotes run up failure



10^4



10^5



1.5×10^5

Fig 29 Optical micrographs of non-woven plain coupons with layup E (± 45.02) tested in tensile fatigue at the stress level giving a mean life of 100000 cycles. Left to right micrographs after: 10000 cycles at 1 dB steps, 100000 cycles at 1 dB steps, 150000 cycles at 1 dB steps

Fig 30

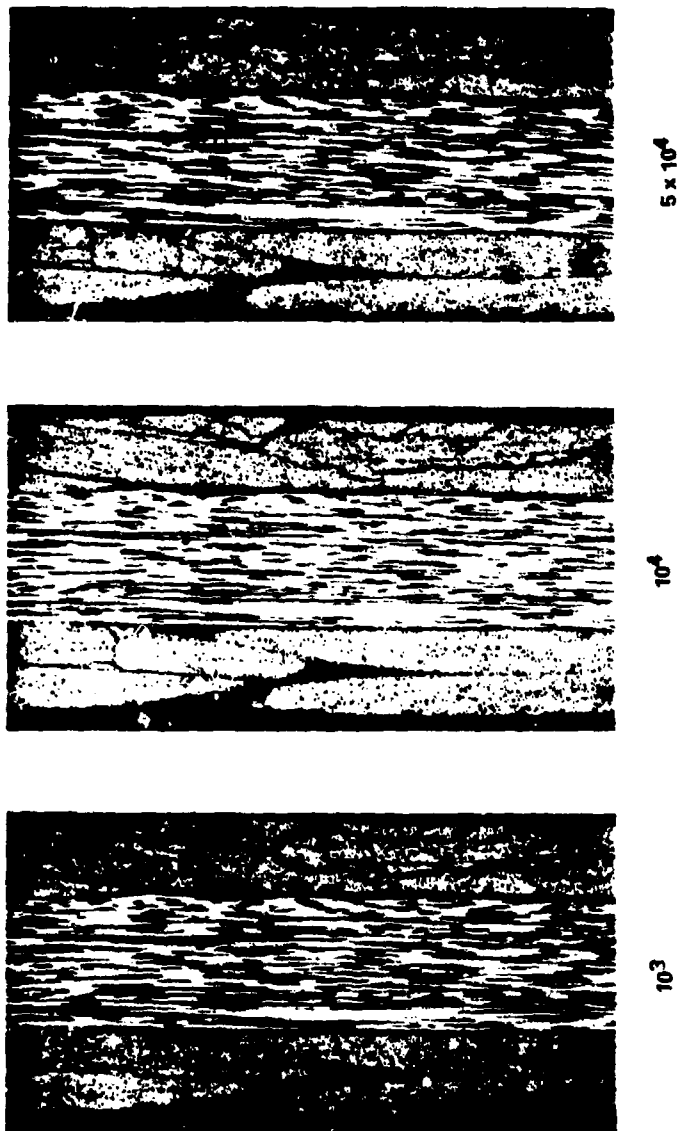


Fig 30 Optical micrographs of woven plain coupons with layup E (±45,02) tested in tensile fatigue at the stress level giving a mean life of 100000 cycles. Left to right, micrographs after: 1000 cycles, 10000 cycles, 50000 cycles

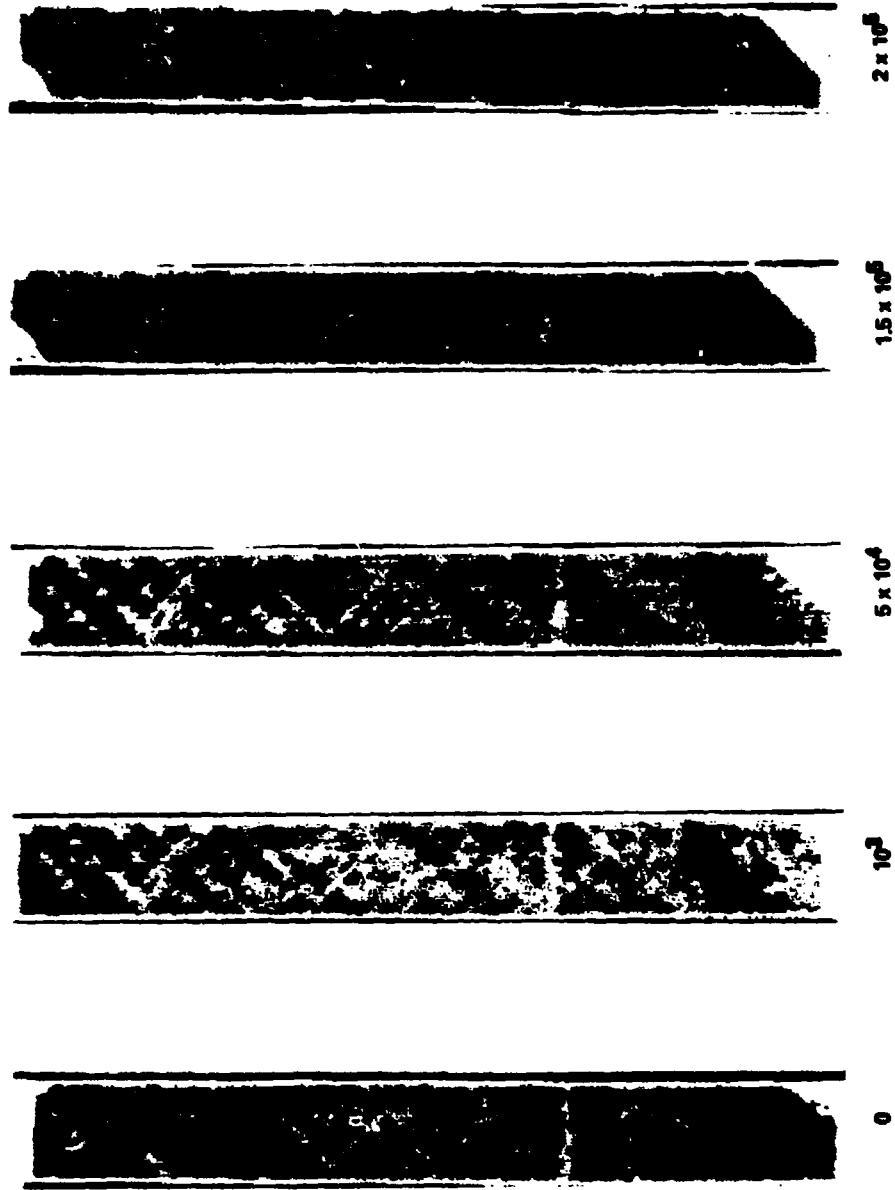


Fig 31 Ultrasonic C-scans of a non-woven plain coupon with layout E ($\pm 45,02$) tested in tensile fatigue at the stress level giving a mean life of 100,000 cycles. Left to right, scans after: 0 cycles at 1 dB steps, 1000 cycles at 1 dB steps, 50,000 cycles at 1 dB steps, 150,000 cycles at 1 dB steps, 200,000 cycles at 1 dB steps

Fig 32

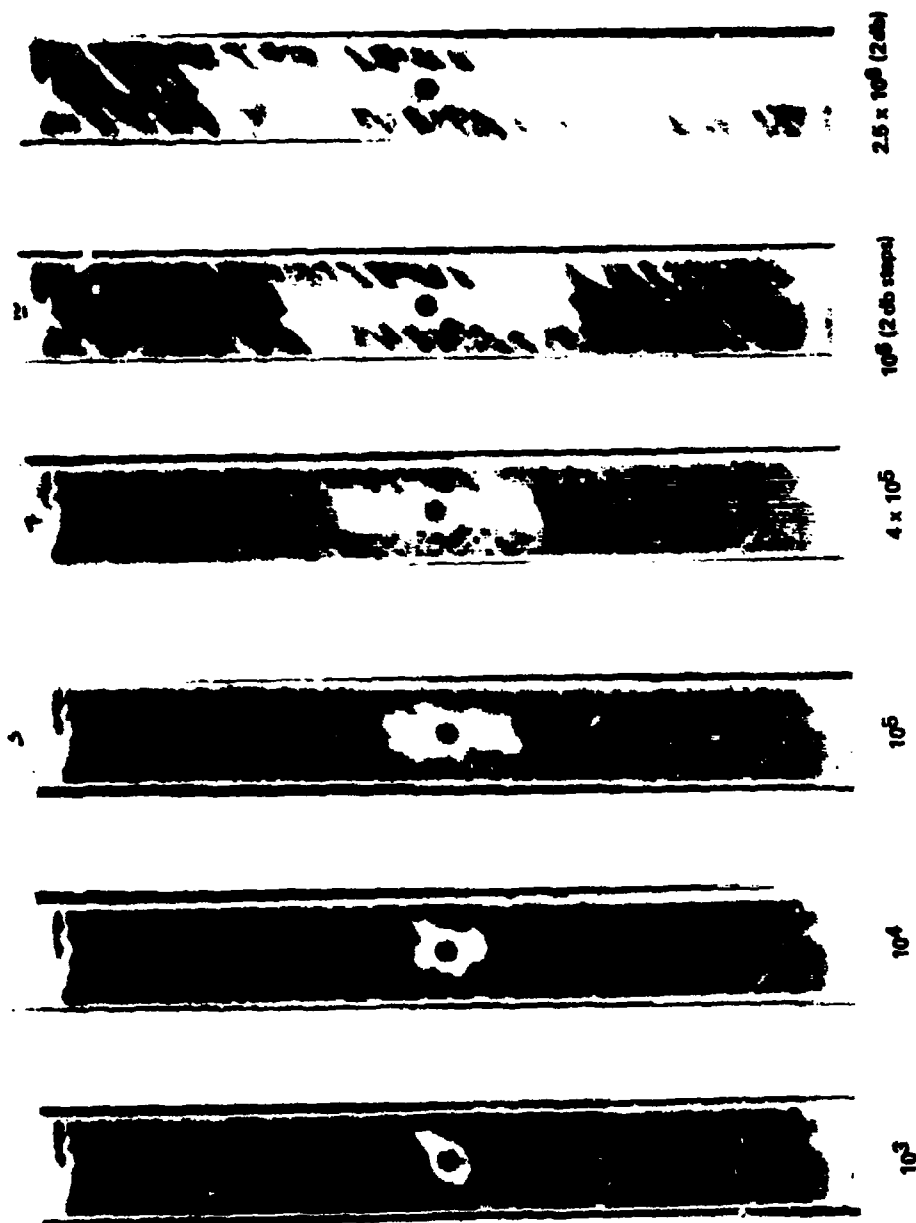


Fig 32 Ultrasonic C-scans of a non-woven holed coupon with layup E ($\pm 45, 0/2$) tested in tensile fatigue at the stress level giving a mean life of 1000000 cycles. Left to right, scans after: 1000 cycles at 1 db steps, 10000 cycles at 1 db steps, 100000 cycles at 1 db steps, 400000 cycles at 1 db steps, 1000000 cycles at 2 db steps, 2500000 cycles at 2 db steps

TR 82000

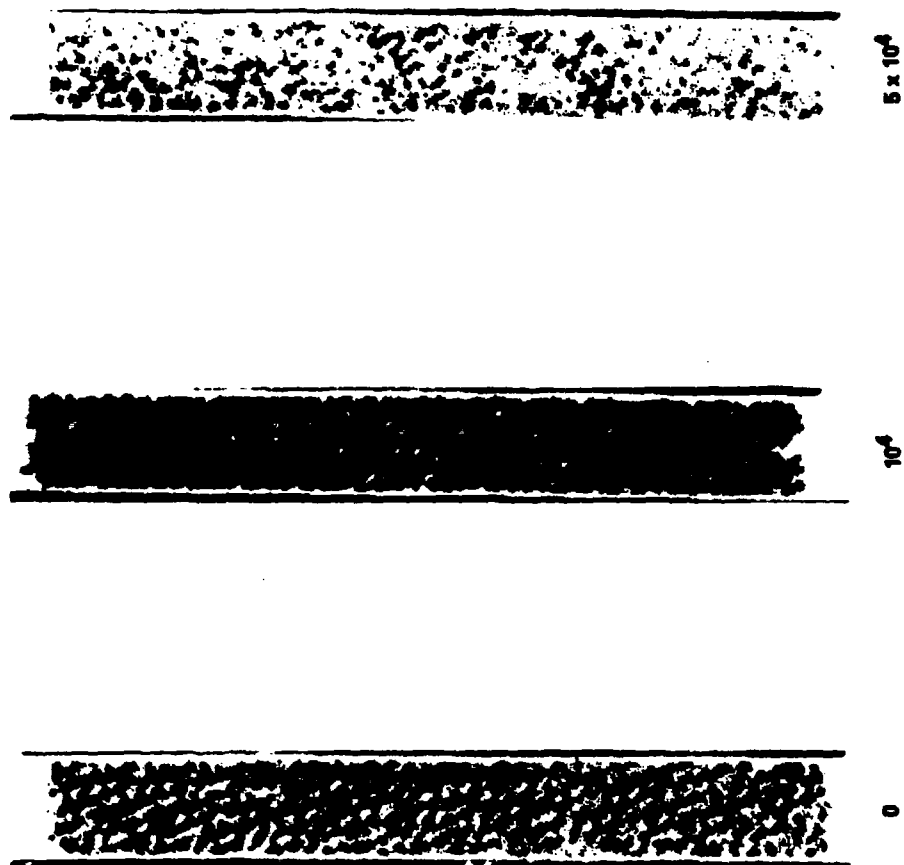


Fig 33 Ultrasonic C-scans of a woven plain coupon with layout E ($\pm 45, 0/2$) tested in tensile fatigue at the stress levels indicated. The mean life of 100,000 cycles. Left to right, scans after: 0 cycles at 1 dB steps, 10,000 cycles at 1 dB steps, 50,000 cycles at 1 dB steps

Fig 34

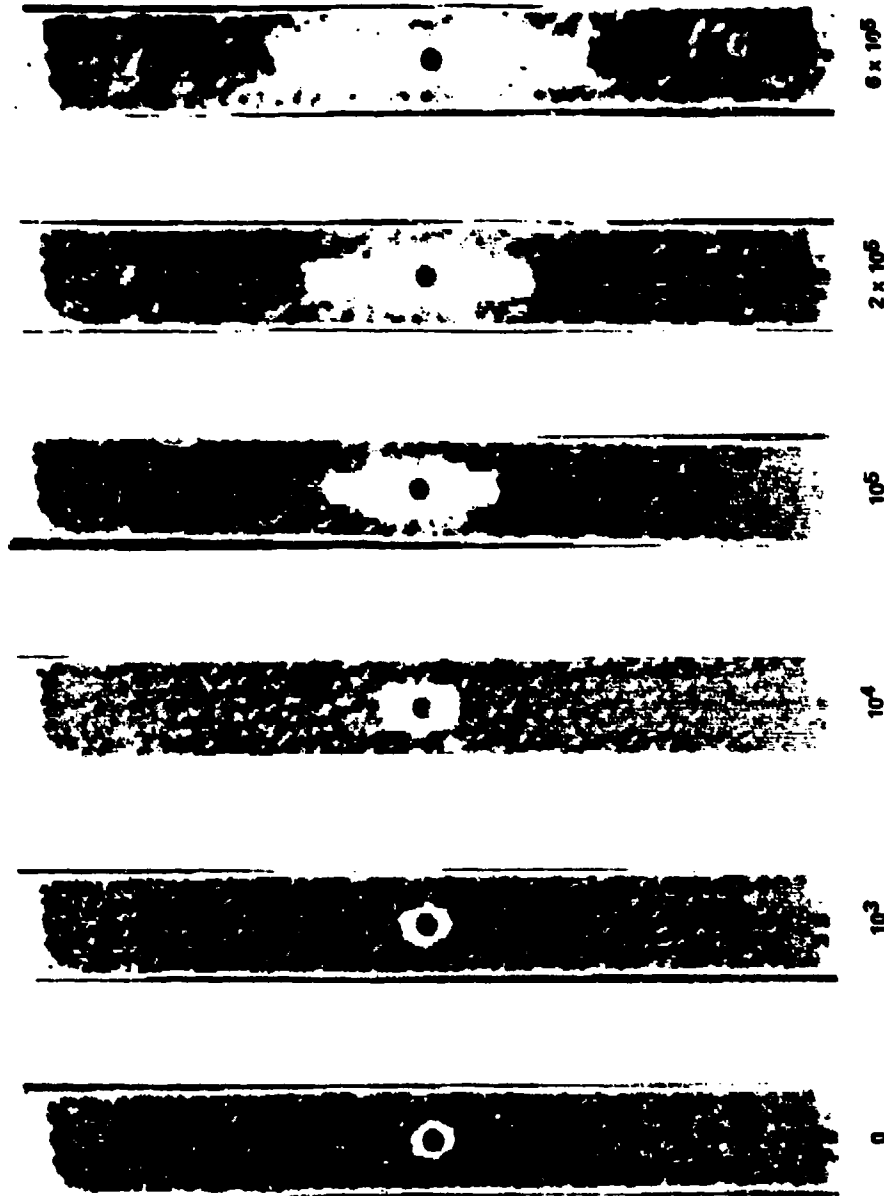


Fig 34 Ultrasonic C-scans of a woven hole coupon with layup E ($\pm 45, 02$) tested in tensile fatigue at the stress level giving a mean life of 100000 cycles. Left to right, scans after: 0 cycles at 1 dB steps, 1000 cycles at 1 dB steps, 10000 cycles at 1 dB steps, 100000 cycles at 1 dB steps, 200000 cycles at 1 dB steps, 600000 cycles at 1 dB steps

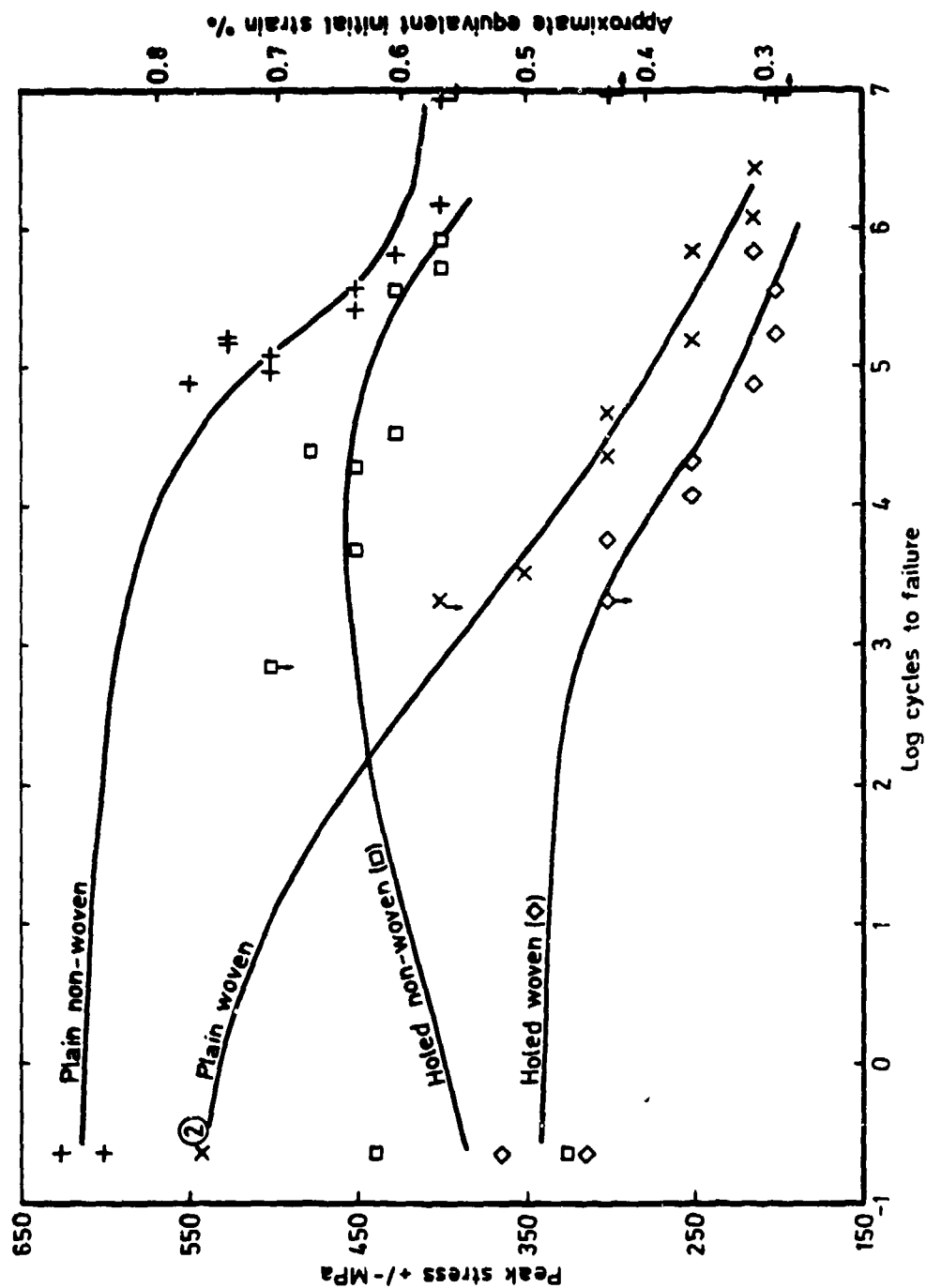


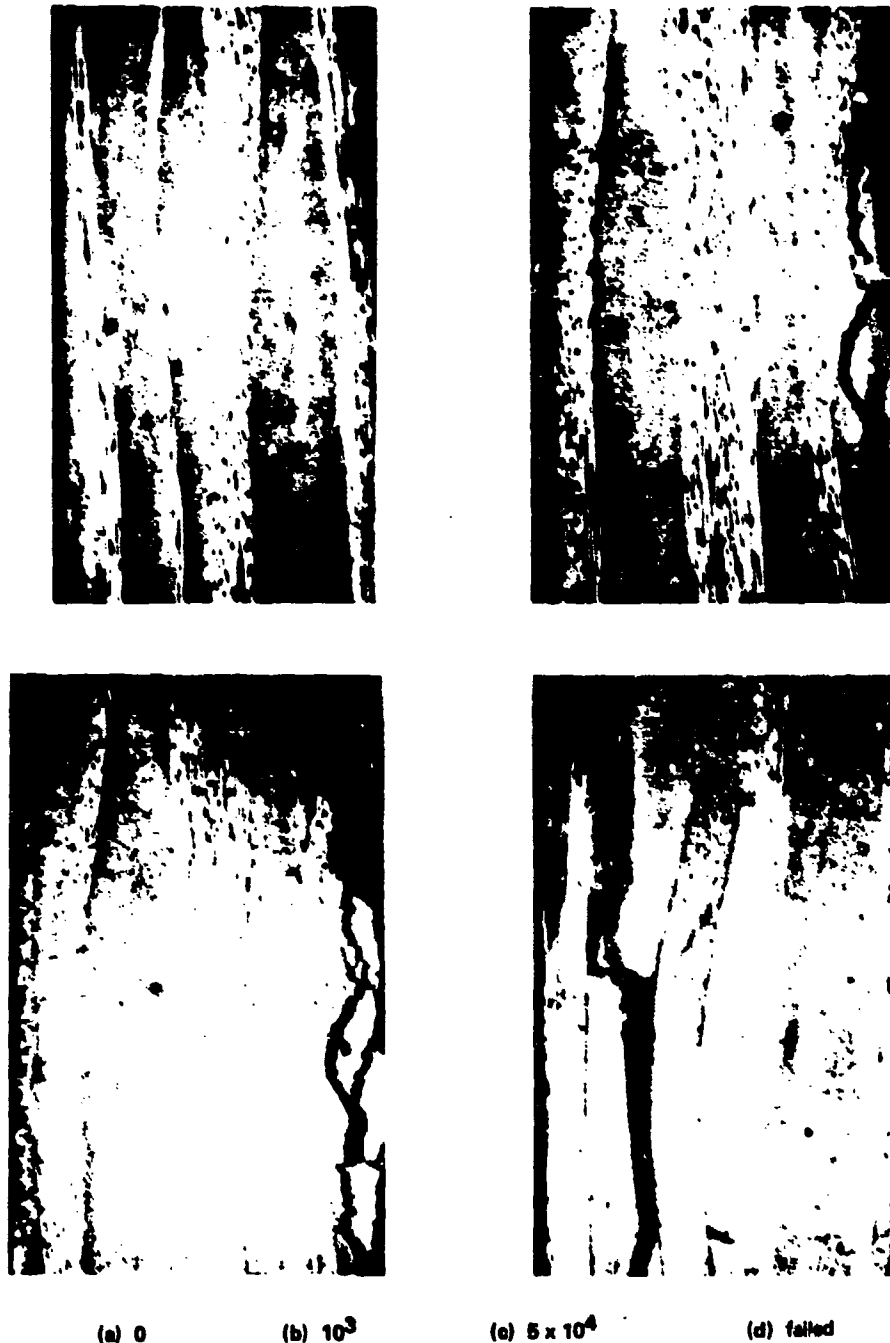
Fig 35 S-N plots of reversed axial fatigue data for layout A (0,90). Vertical arrows denote run up failures and horizontal arrows run-outs

Fig 36



Fig 36 Optical micrographs of non-woven plain coupons with layup A (0.90) tested in reversed axial fatigue at the stress level giving a mean life of 10000 cycles. Left to right, micrographs after: 0 cycles, 1000 cycles, 10000 cycles

Fig 37



(a) 0 (b) 10^3 (c) 5×10^4 (d) failed

Fig 37 Optical micrographs of woven plain coupons with layup A (0,90) tested in reversed axial fatigue at the stress level giving a mean life of 100000 cycles. Top left to bottom right, micrographs after: 0 cycles, 1000 cycles, 50000 cycles, failure

Fig 38

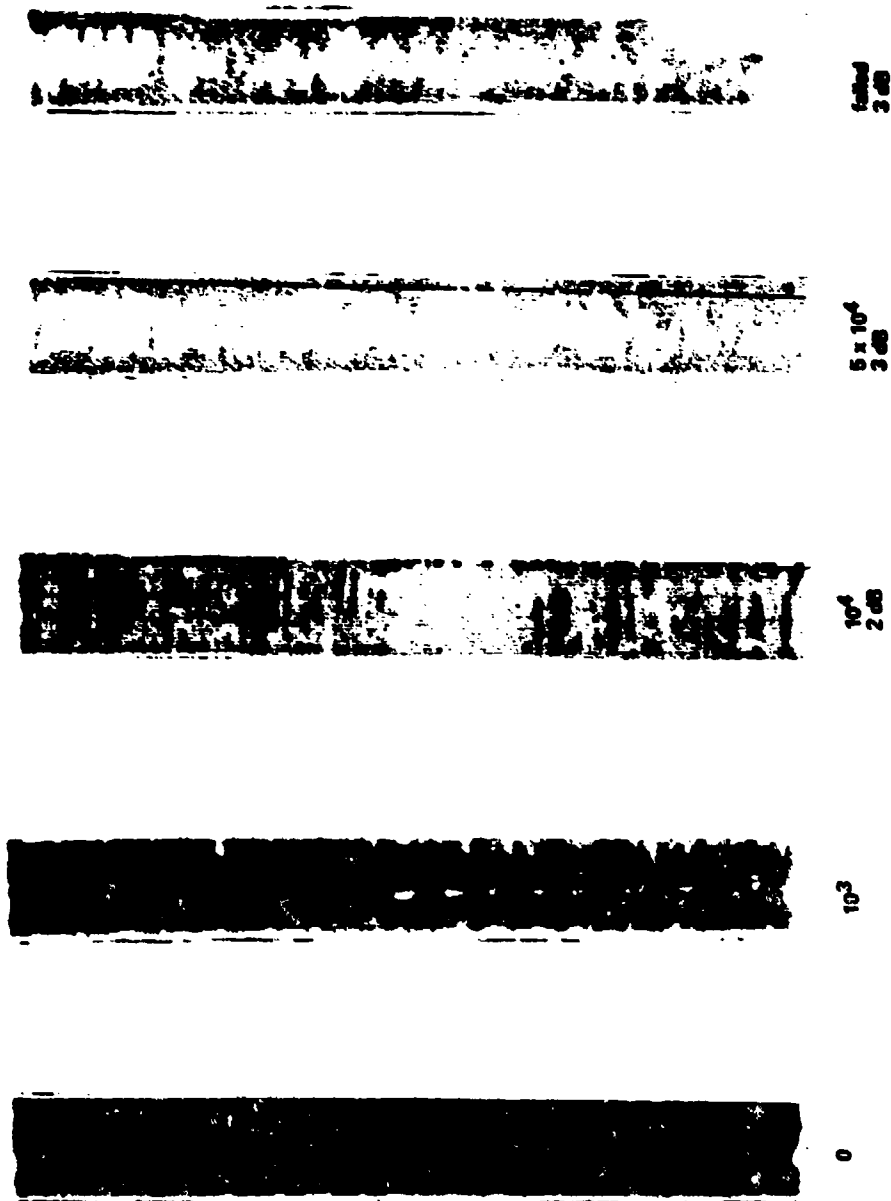


Fig 38 Ultrasonic C-scans of a non-woven plain coupon with layup A (0.90) tested in reversed axial fatigue at the stress level giving a mean life of 100000 cycles. Left to right, scans after: 0 cycles at 1 dB steps, 1000 cycles at 1 dB steps, 10000 cycles at 2 dB steps, 50000 cycles at 3 dB steps, failure at 3 dB steps

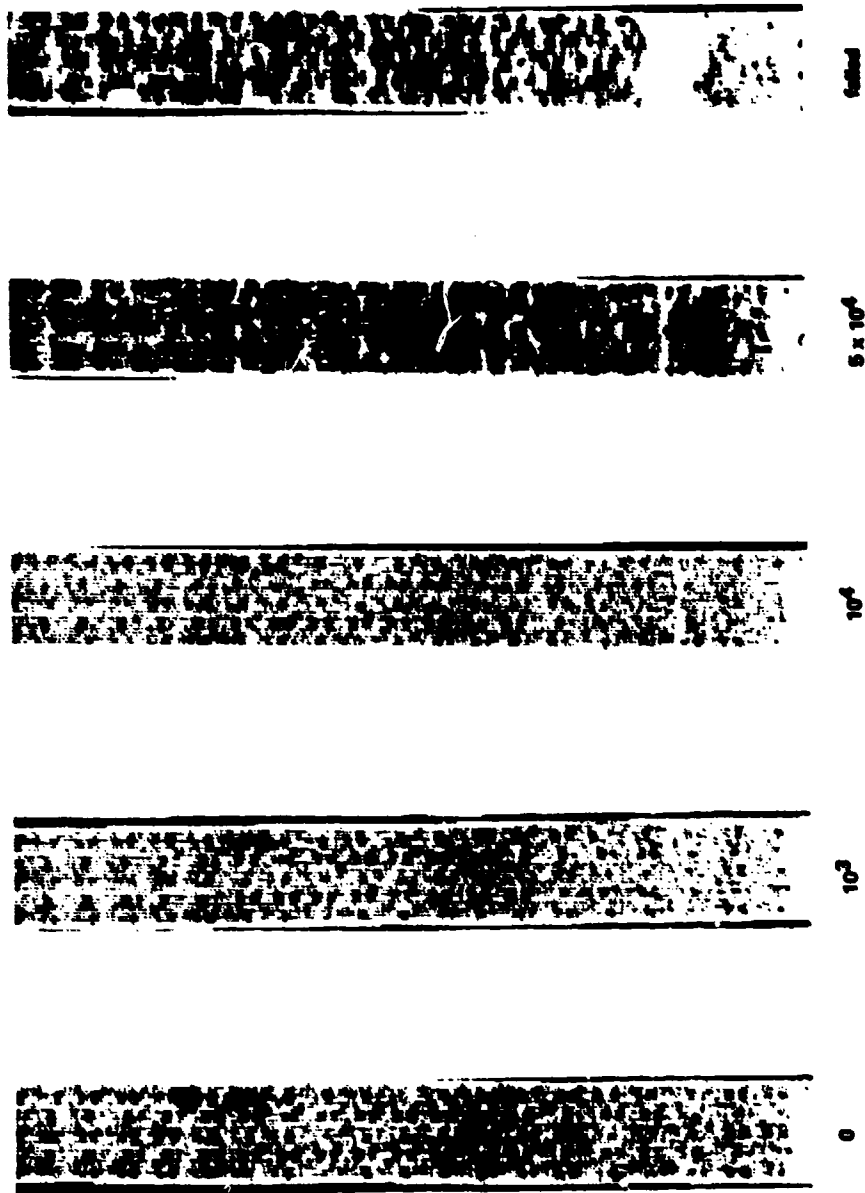


Fig 38 Ultrasonic C-scans of a woven plain coupon with layup A (0,90) tested in reversed axial fatigue at the stress level giving a mean life of 100000 cycles. Left to right, scans after: 0 cycles at 1 dB steps, 1000 cycles at 1 dB steps, 10000 cycles at 1 dB steps, 50000 cycles at 1 dB steps, failure

Fig 40

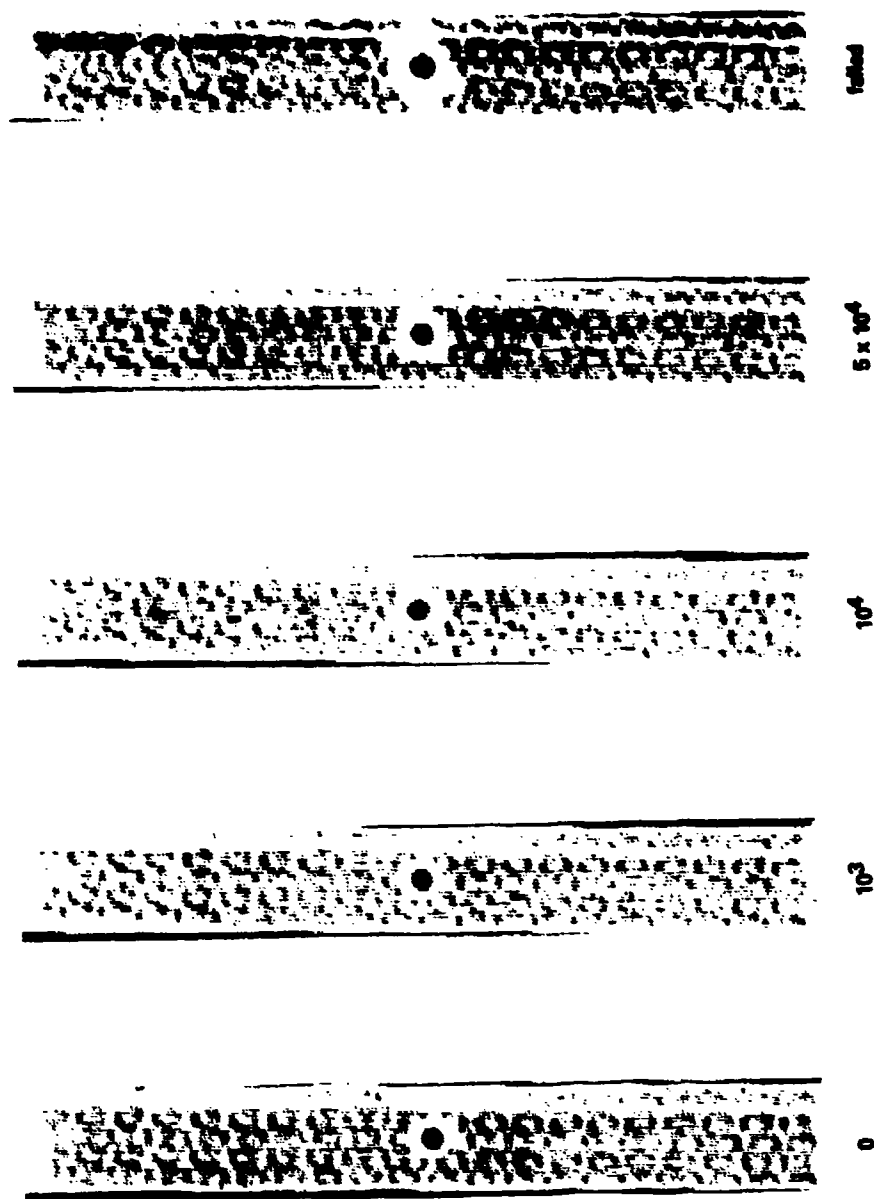


Fig 40 Ultraonic C-scans of a woven hole coupon with layup A (0.90) tested in reversed axial fatigue at the stress level giving a mean life of 100000 cycles. Left to right, scans after: 0 cycles at 1 dB steps, 10000 cycles at 1 dB steps, 10000 cycles at 1 dB steps, 50000 cycles at 1 dB steps, failure. Note the light line on the right side of the scans was due to a surface effect

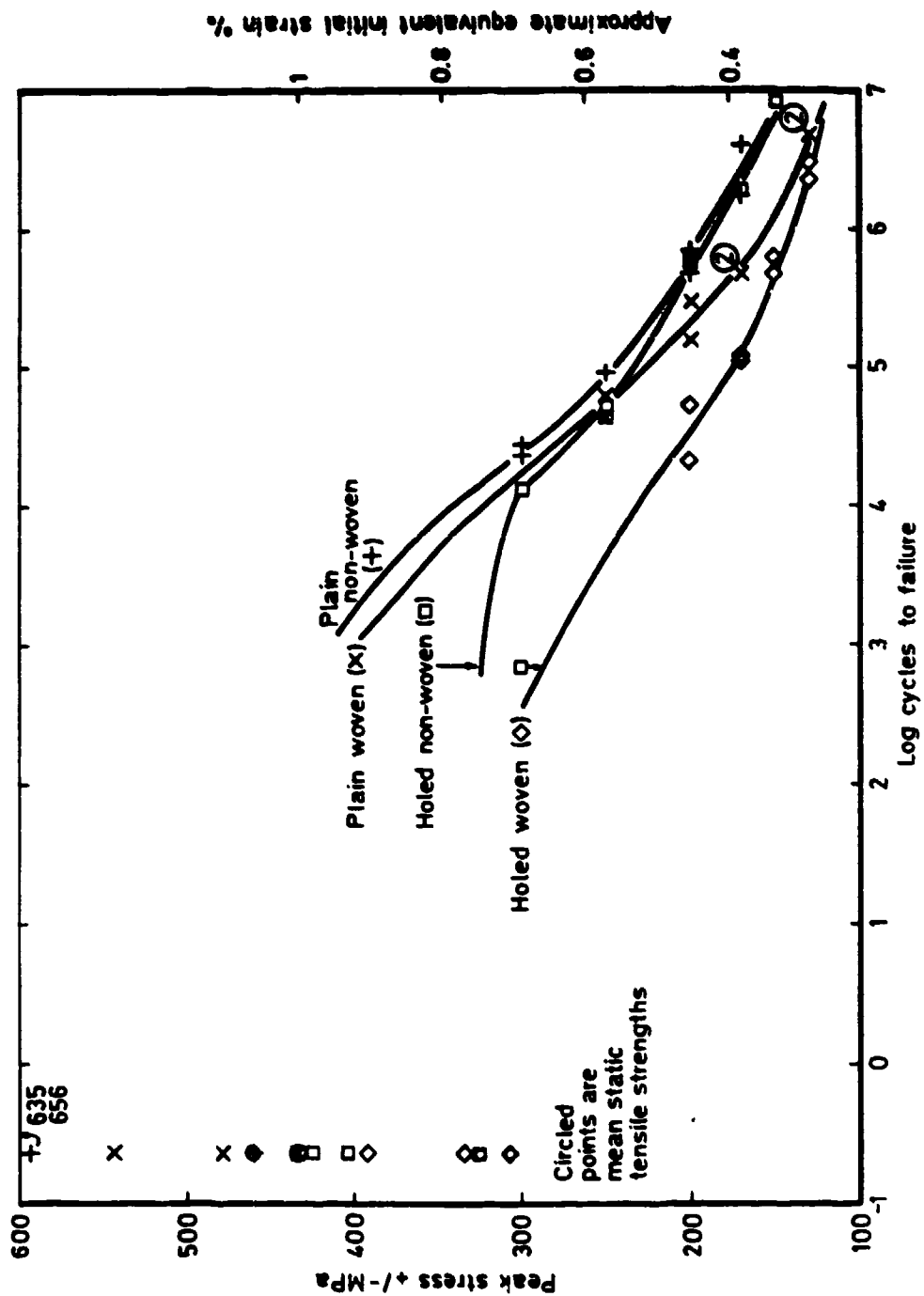


Fig 41 S-N plots of reversed axial fatigue data for layout C ($\pm 45, 0, 90$). Both tensile and compressive static data are presented at the 0.25 cycle point. Vertical arrows denote run up failures

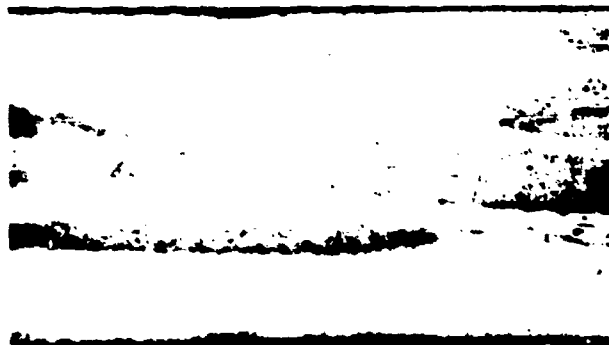
Fig 42



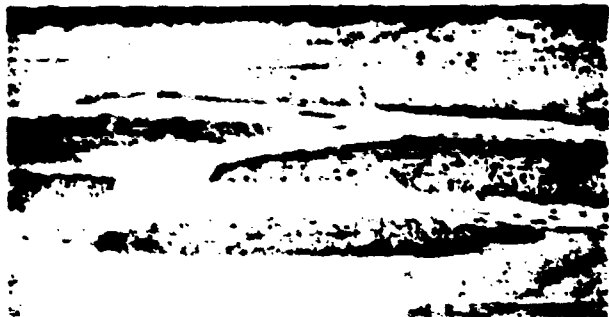
Fig 42 Optical micrographs of non-woven plain coupons with layup C ($\pm 45,0,90$) tested in reversed axial fatigue at the stress level giving a mean life of 100000 cycles. Top left to bottom right, micrographs after: 1000 cycles, 50000 cycles, 150000 cycles, 200000 cycles



0



10⁴



failure

Fig 43 Optical micrographs of woven plain coupons with layout C (1.45, 0.90) tested in reversed mild fatigue at the stress level giving a mean life of 100000 cycles. Left to right, micrographs after: 0 cycle, 10000 cycle, failure

Fig 44

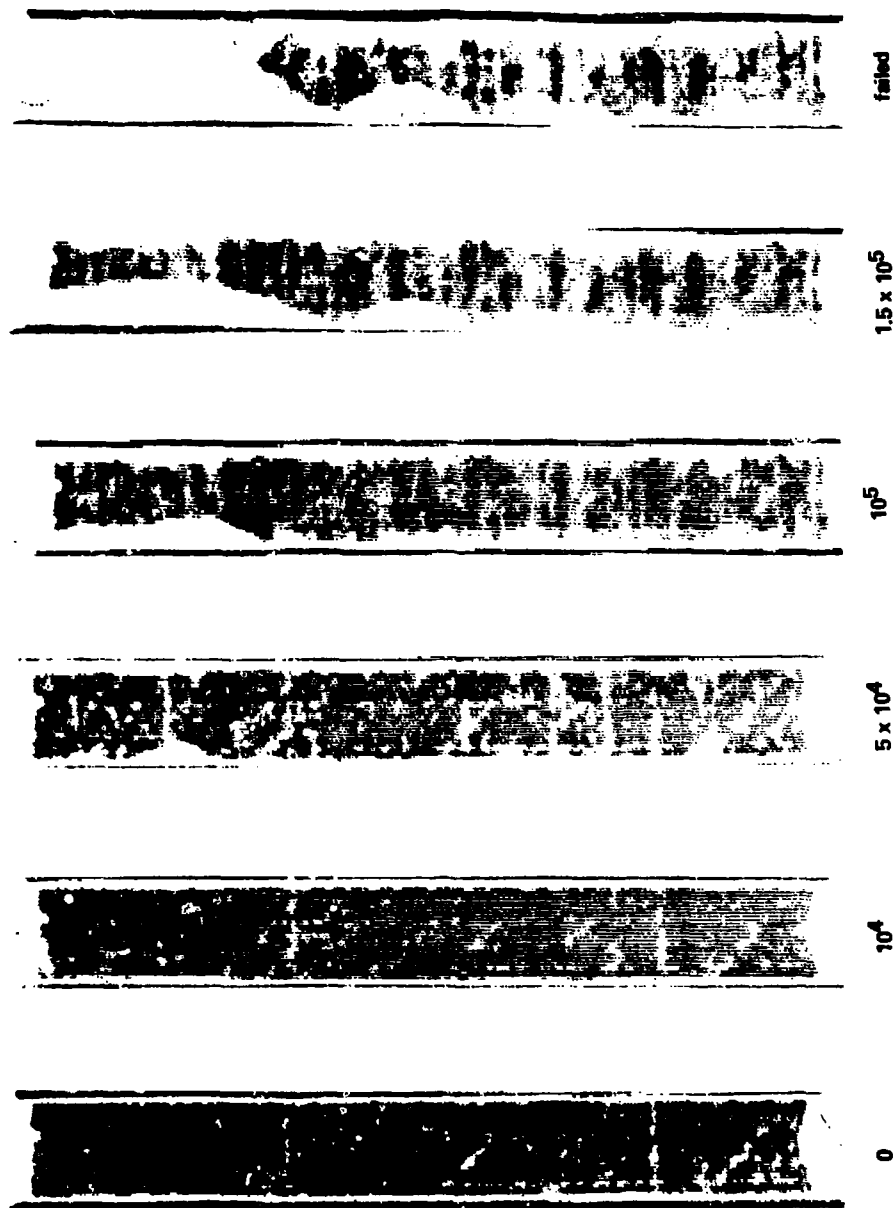


Fig 44 Ultrasonic C-scans of a non-woven plain coupon with layup C ($\pm 45, 0, 90$) tested in reversed axial fatigue at the stress level giving a mean life of 100000 cycles. Left to right, scans after: 0 cycles at 1 dB steps, 10000 cycles at 1 dB steps, 50000 cycles at 1 dB steps, 100000 cycles at 1 dB steps, 150000 cycles at 1 dB steps, failure

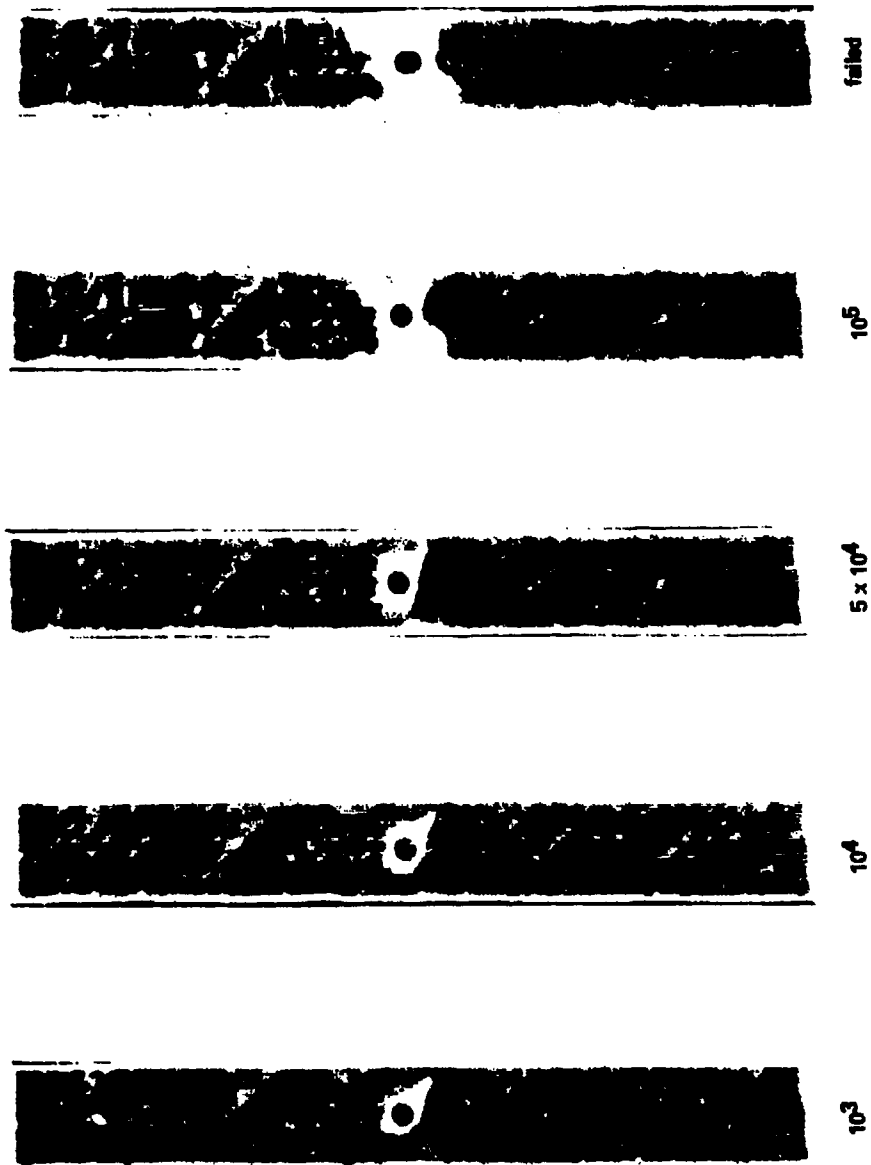


Fig 45

Fig 45 Ultrasonic C-scan of a non-woven holed coupon with layup C (±45, 0, 90) tested in reversed axial fatigue at the stress level giving a mean life of 100,000 cycles. Left to right, scans after: 1000 cycles at 1 dB steps, 10,000 cycles at 1 dB steps, 50,000 cycles at 1 dB steps, 100,000 cycles at 1 dB steps, failure

Fig 46

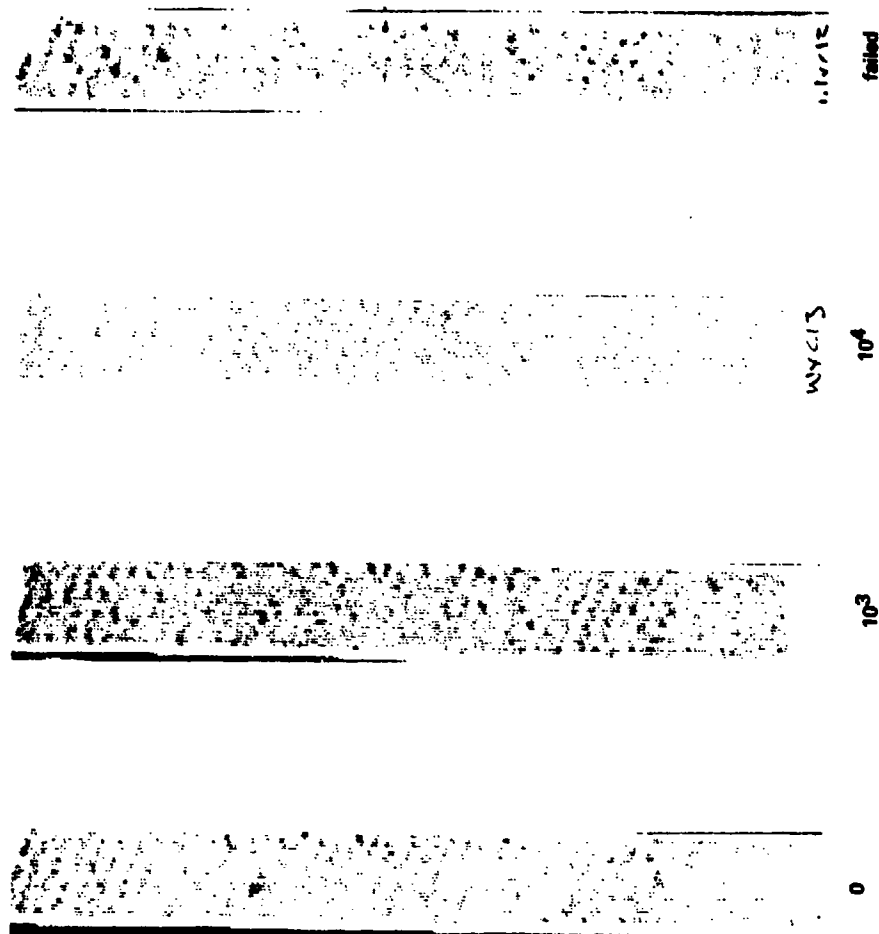


Fig 46 Ultrasonic C-scans of a woven plain coupon with layup C ($\pm 45,0,90$) tested in reversed axial fatigue at the stress level giving a mean life of 100000 cycles. Left to right, scans after, 0 cycles at 1 dB steps, 1000 cycles at 1 dB steps, 10000 cycles at 1 dB steps, failure

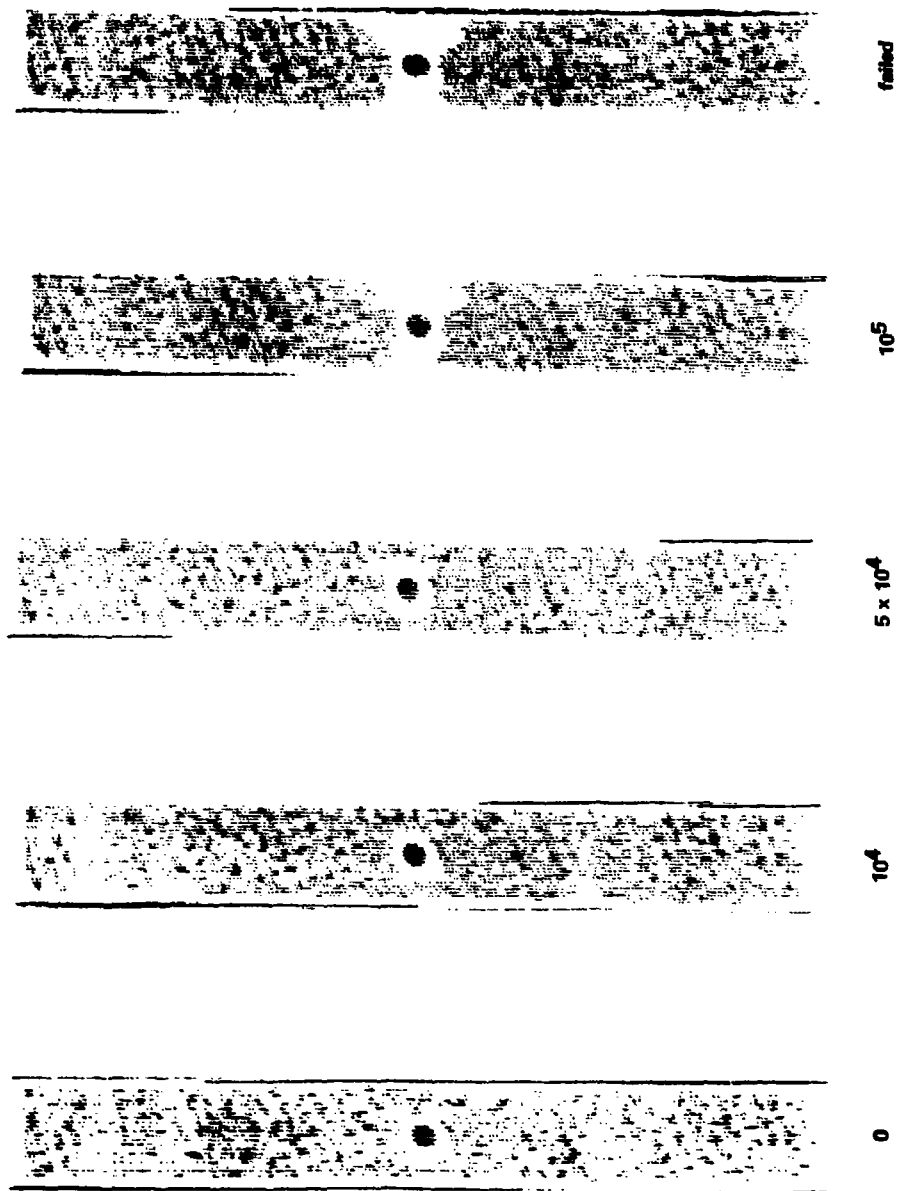


Fig 47 Ultrasonic C-scans of a woven holed coupon with layup C ($\pm 45, 0, 90$) tested in reversed axial fatigue at the stress level giving a mean life of 100,000 cycles. Left to right, scans after: 0 cycles at 1 dB steps, 10,000 cycles at 1 dB steps, 50,000 cycles at 1 dB steps, 100,000 cycles at 1 dB steps, failure

Fig 48

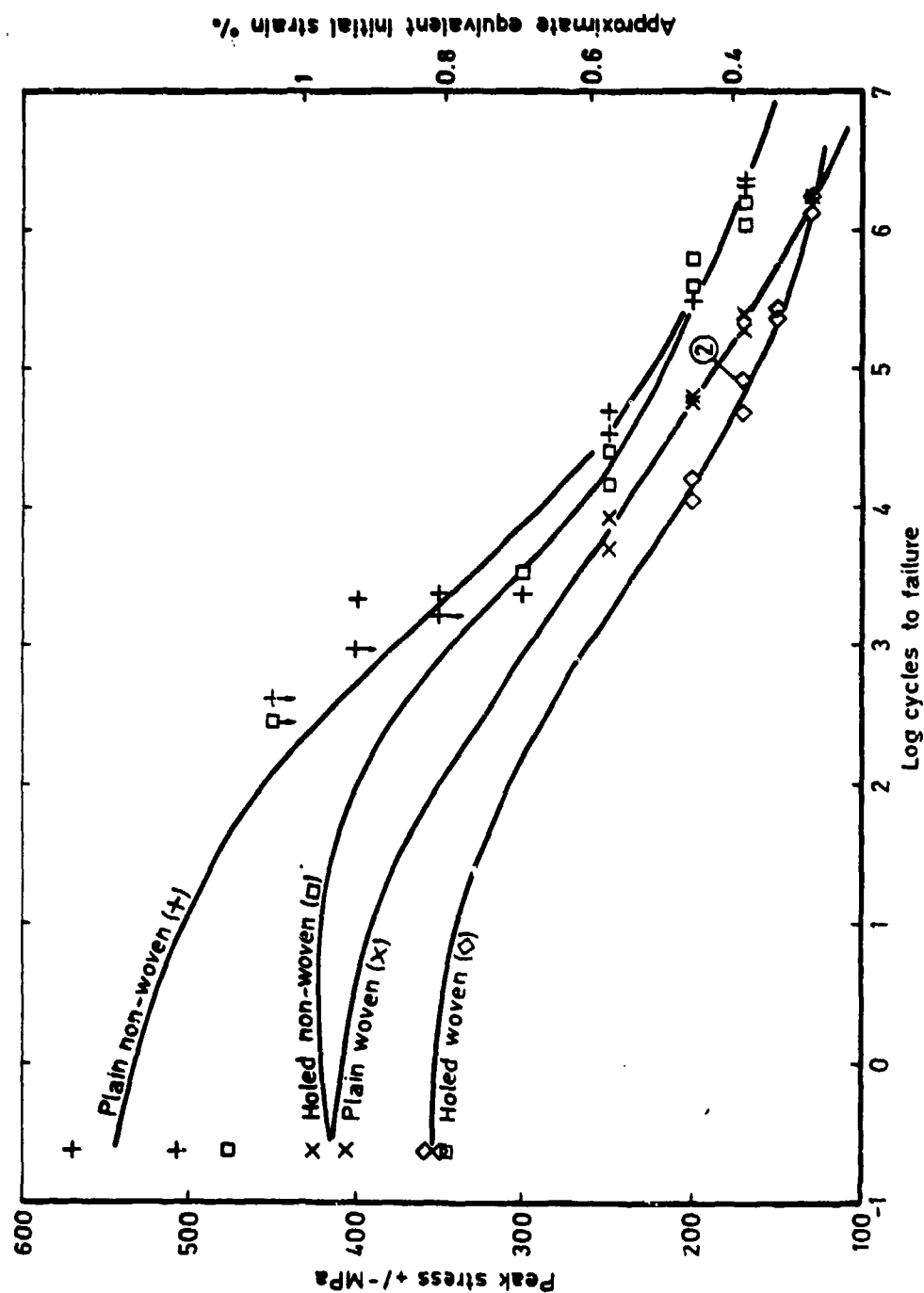
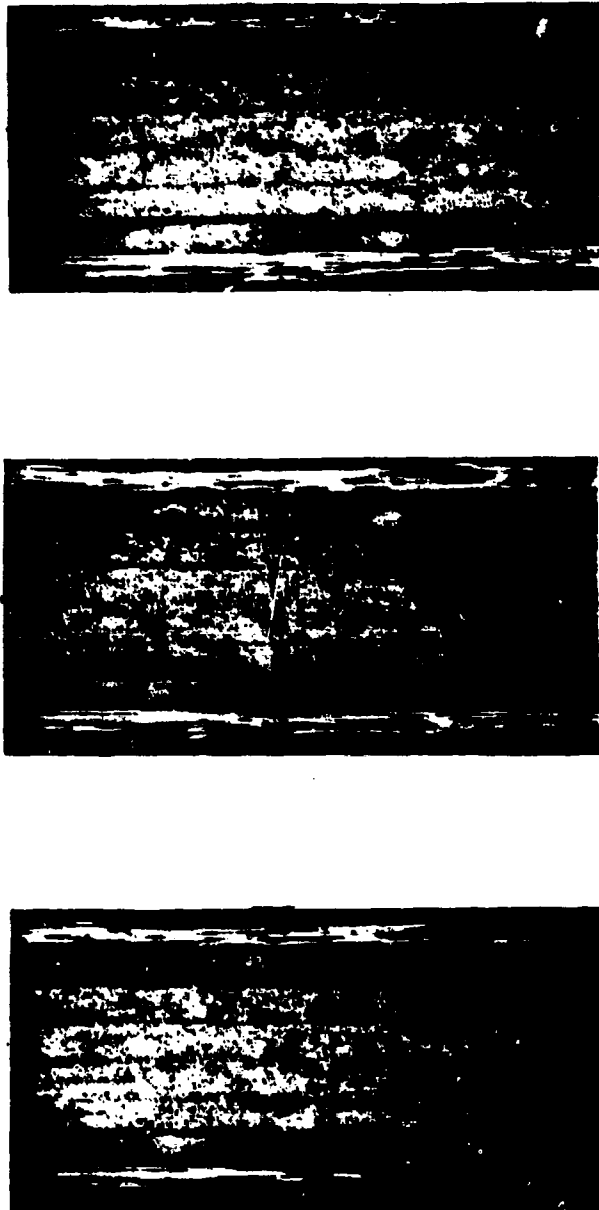


Fig 48 S-N plots of reversed axial fatigue data for layup D (0,90,45). Vertical arrows denote run up failures



10^5

10^4

10^3

Fig 49

Fig 49 Optical micrographs of non-woven plain coupons with layup D (0.90, ±.45) tested in reversed axial fatigue at the stress level giving a mean life of 100000 cycles. Left to right, micrographs after: 1000 cycles, 10000 cycles, 100000 cycles

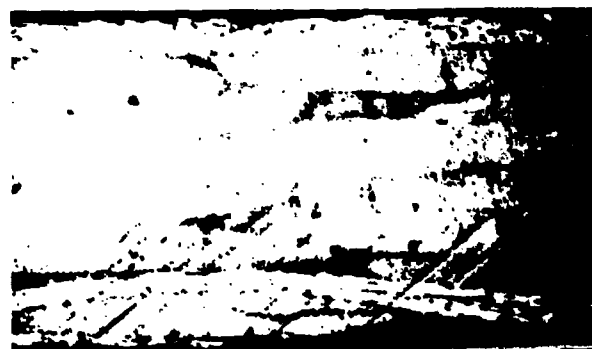
Fig 50



Failed



5×10^4



0

Fig 50 Optical micrographs of woven plain coupons with layup D (0,90, ±45) tested in reversed axial fatigue at the stress level giving a mean life of 100000 cycles. Left to right, micrographs after: 0 cycles, 50000 cycles, failure

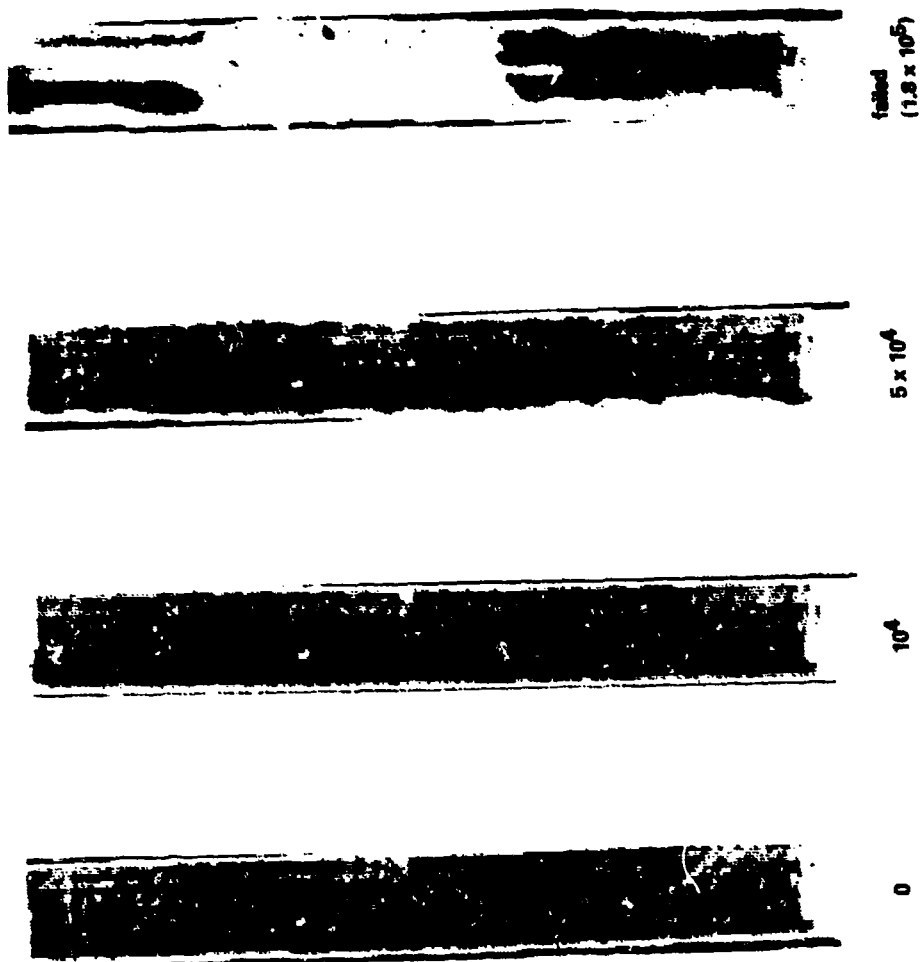


Fig 51 Ultrasonic C-scans of a non-woven plain coupon with layout D (0.90 ± 45) tested in reversed axial fatigue at the stress level giving a mean life of 100,000 cycles. Left to right, scans after: 0 cycles at 1 dB steps, 10,000 cycles at 1 dB steps, 50,000 cycles at 1 dB steps, 180,000 cycles at 1 dB — failure

Fig 52

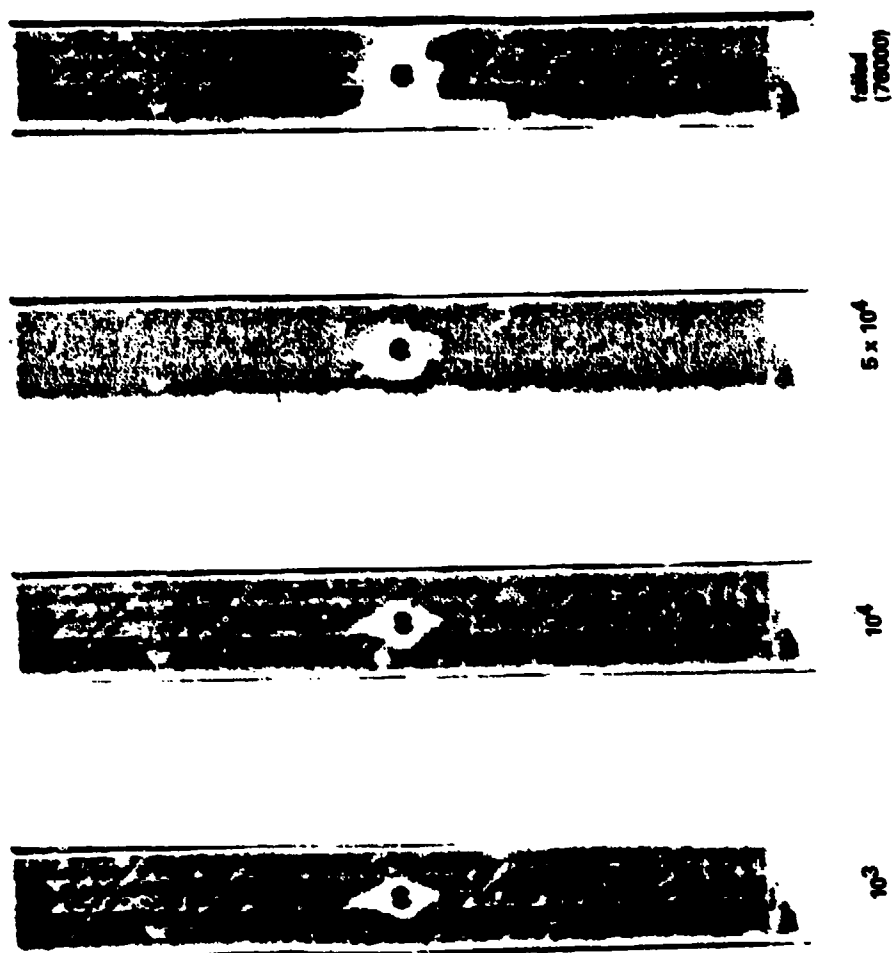


Fig 52 Ultrasonic C-scans of a non-woven holed coupon with layup D (0.90 \pm 46) tested in reversed axial fatigue at the stress level giving a mean life of 100000 cycles. Left to right, scans after: 1000 cycles at 1 dB steps, 10000 cycles at 1 dB steps, 50000 cycles at 1 dB steps, 76000 cycles at 1 dB steps, failure

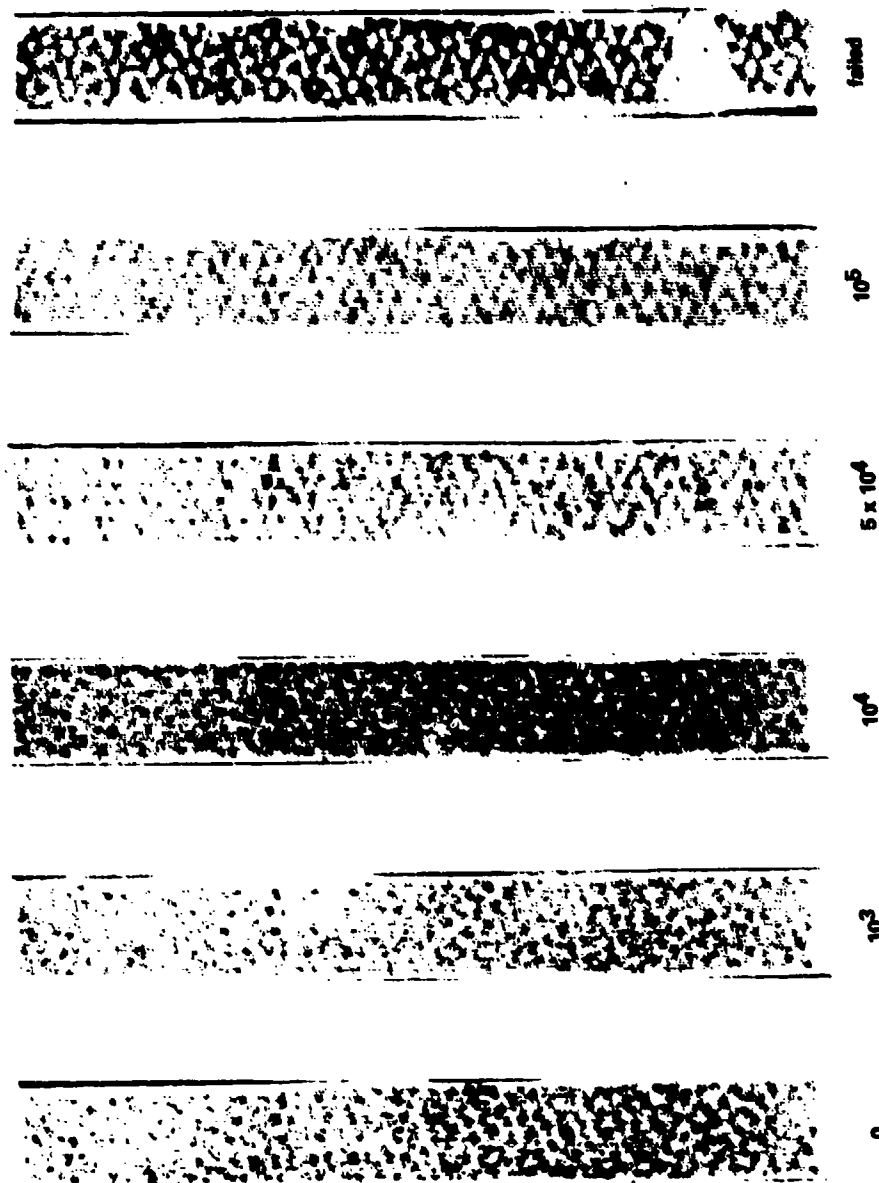


Fig 53 Ultrasonic C-scans of a woven plain coupon with layup D (0, 90, ± 45) tested in reversed axial fatigue at the stress level giving a mean life of 100,000 cycles. Left to right, scans after: 0 cycles at 1 dB steps, 1000 cycles at 1 dB steps, 10,000 cycles at 1 dB steps, 50,000 cycles at 1 dB steps, 100,000 cycles at 1 dB steps, failure

Fig 54

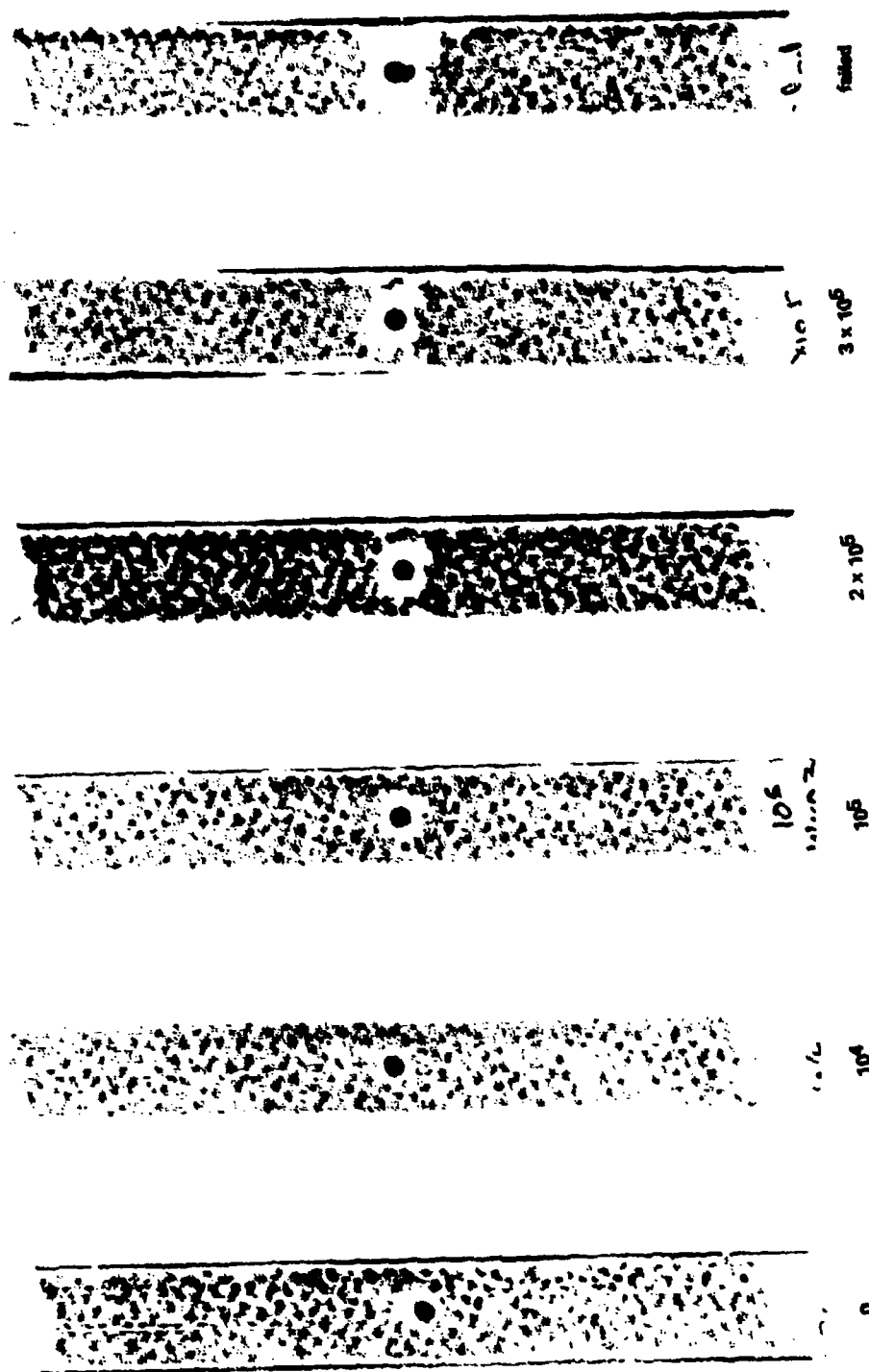


Fig 54 Ultrasonic C-scans of a woven holed coupon with layout D (0.90, \pm .45) tested in reversed axial fatigue at the stress level giving a mean life of 100,000 cycles. Left to right, scans after: 0 cycles at 1 dB steps, 10,000 cycles at 1 dB steps, 100,000 cycles at 1 dB steps, 200,000 cycles at 1 dB steps, 300,000 cycles at 1 dB steps, failure

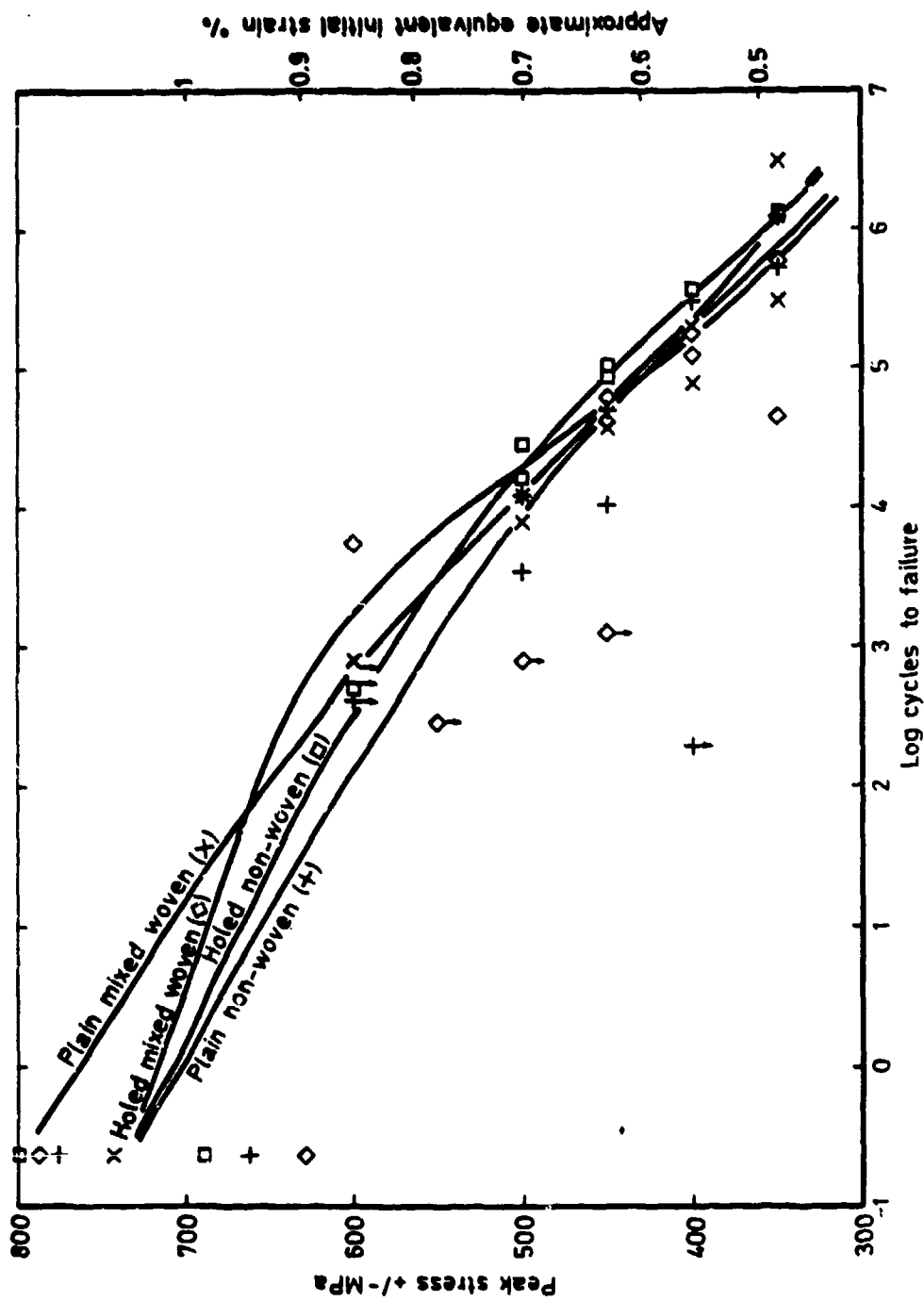


Fig 55

Fig 55 S-N plots of reversed axial fatigue data for layout E (±45,02). Vertical arrows denote run up failures

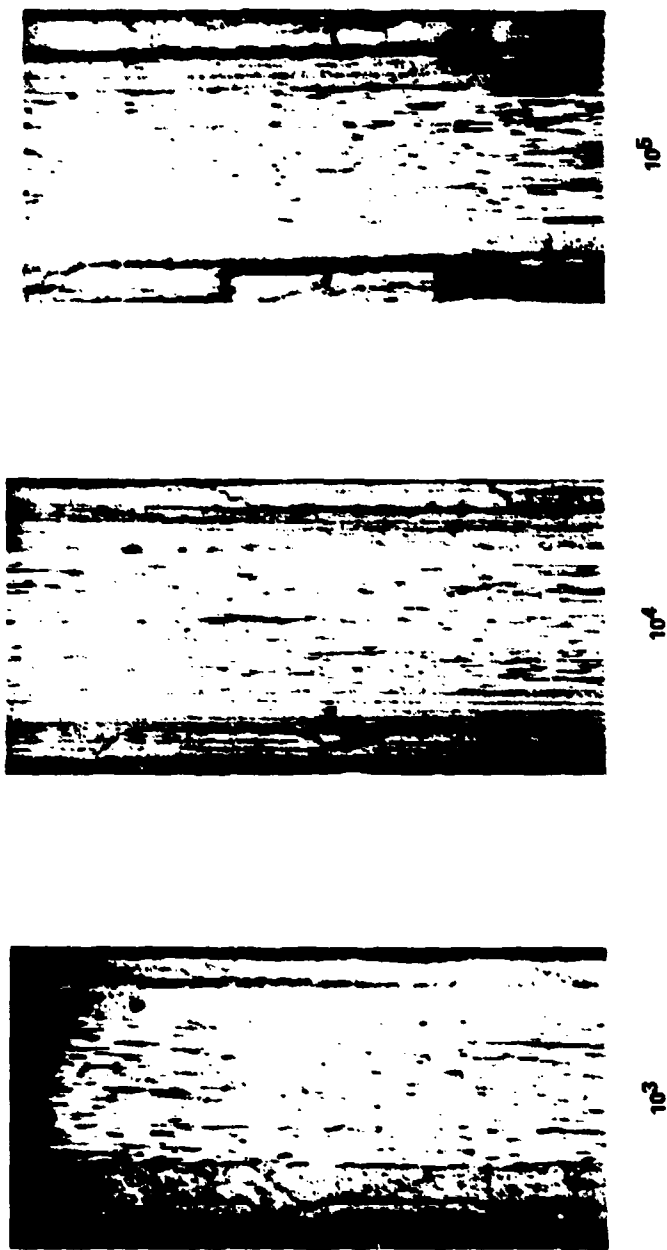
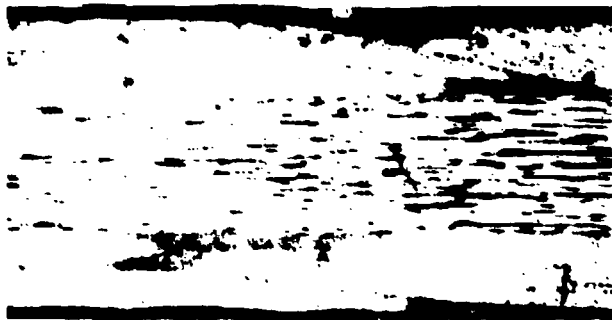
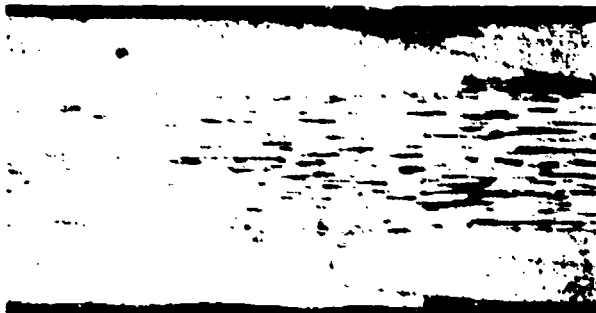


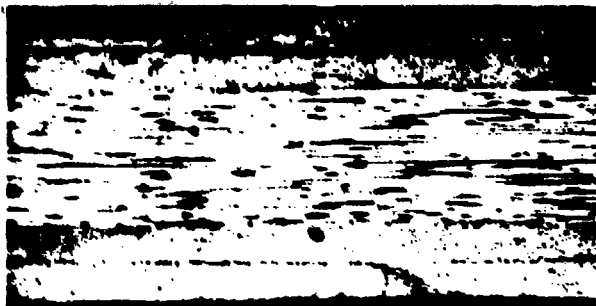
Fig 56 Optical micrographs of non-woven plain coupons with layout E ($\pm 45,02$) tested in reversed axial fatigue at the stress level giving a mean life of 100000 cycles. Left to right, micrographs after: 1000 cycles, 100000 cycles, 100000 cycles



10⁴



5 x 10⁴



10⁵

Fig 57 Optical micrographs of woven plain coupons with layup E ($\pm 45, 02$) tested in reversed axial fatigue at the stress level giving a mean life of 100000 cycles. Left to right, micrographs after: 10000 cycles, 50000 cycles, 100000 cycles

Fig 57

Fig 58

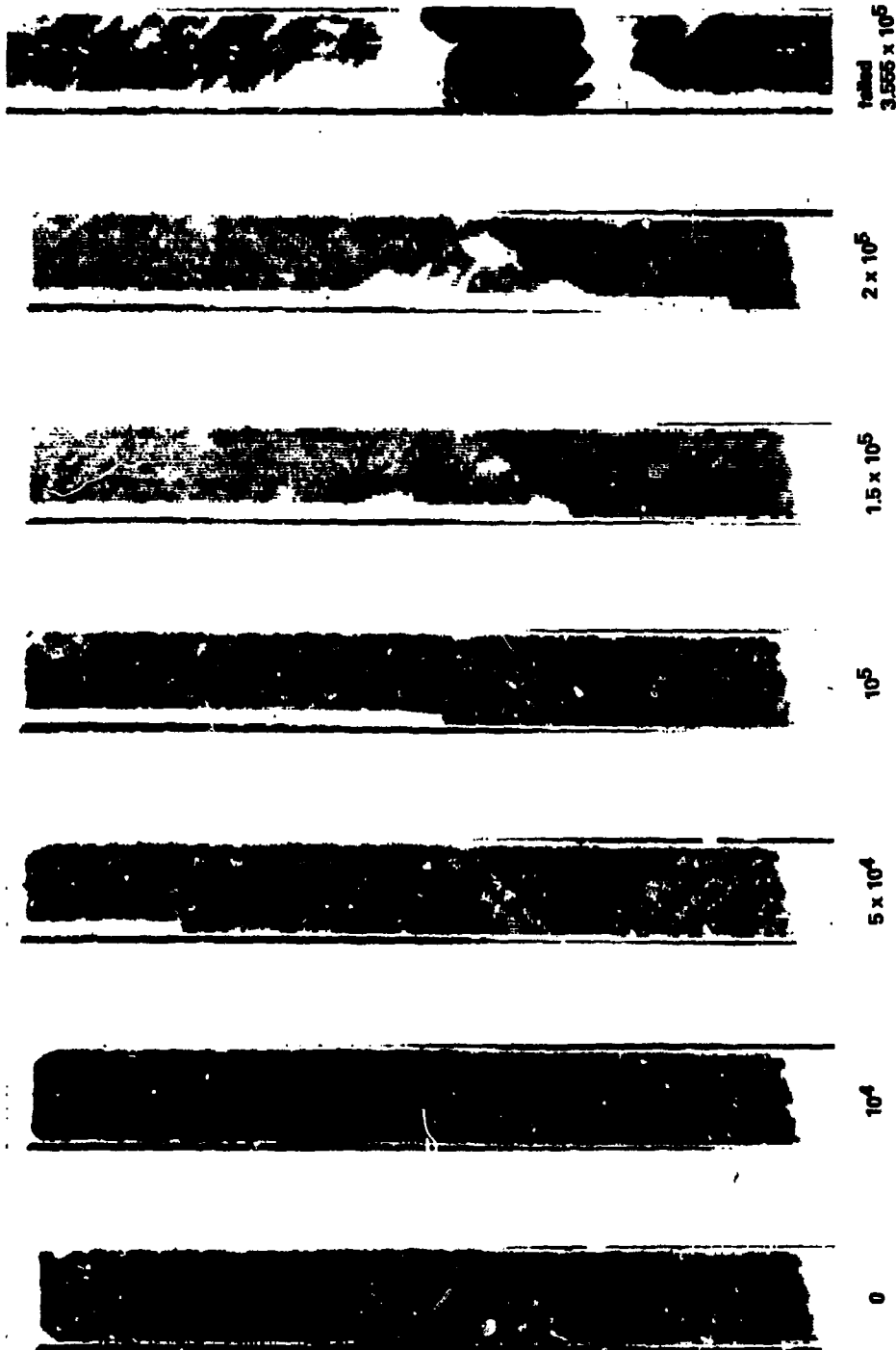


Fig 58 Ultrasonic C-scans of a non-woven plain coupon with layup E ($\pm 45, 02$) tested in reversed axial fatigue at the stress level giving a mean life of 100000 cycles. Left to right, scans after: 0 cycles at 1 dB steps, 10000 cycles at 1 dB steps, 50000 cycles at 1 dB steps, 100000 cycles at 1 dB steps, 150000 cycles at 1 dB steps, 200000 cycles at 1 dB steps, 355500 cycles at 1 dB steps — failure

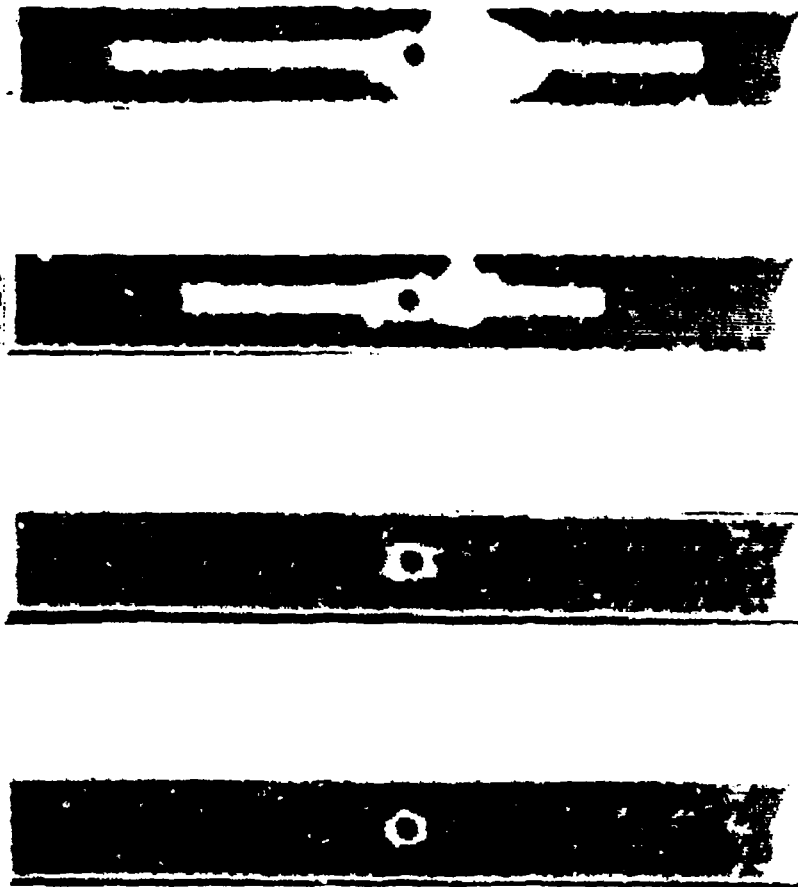


Fig 59 Ultrasonic C-scans of a non-woven holed coupon with layout E (1-45, 02) tested in reversed axial fatigue at the stress level giving a mean life of 100,000 cycles. Left to right, scans after: 0 cycles at 1 dB steps, 1000 cycles at 1 dB steps, 10,000 cycles at 1 dB steps, 16,400 cycles at 1 dB steps -- failure

Fig 60

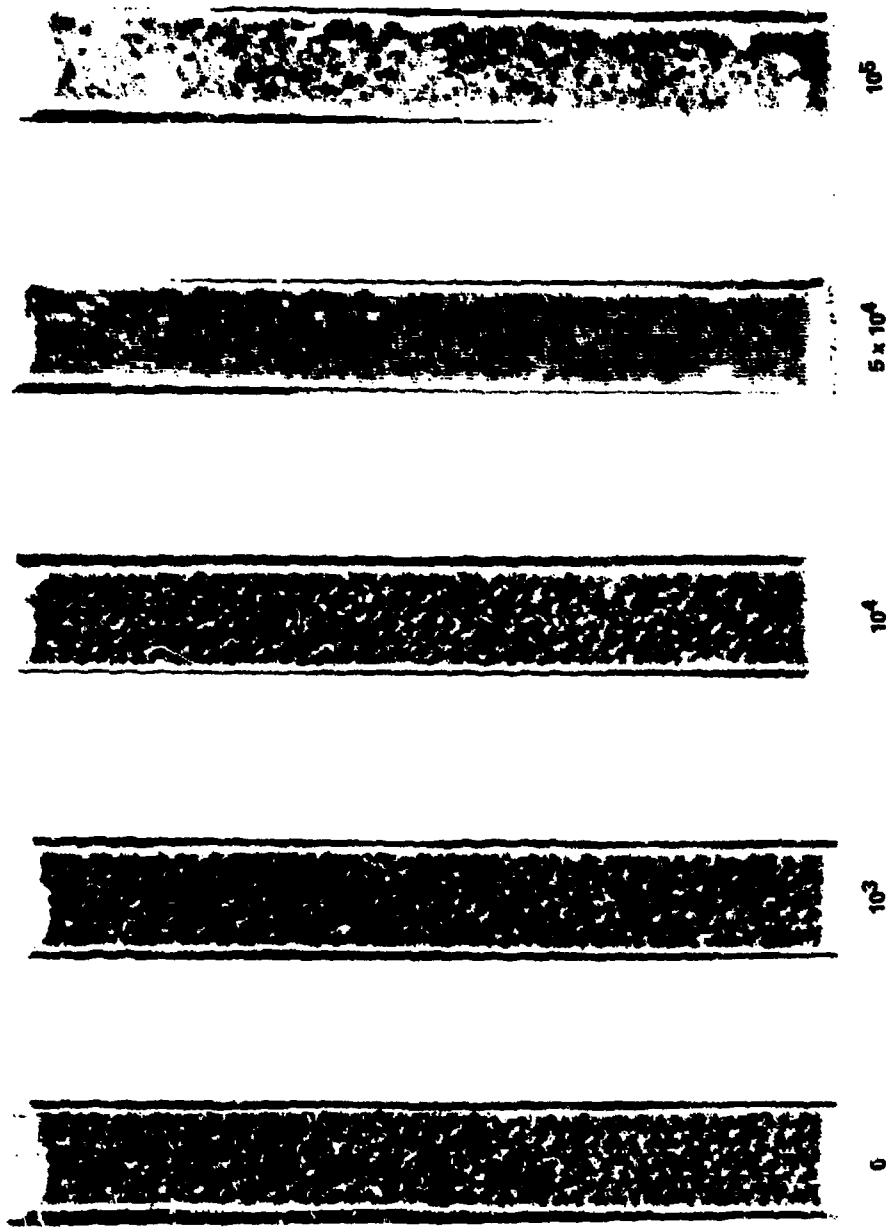
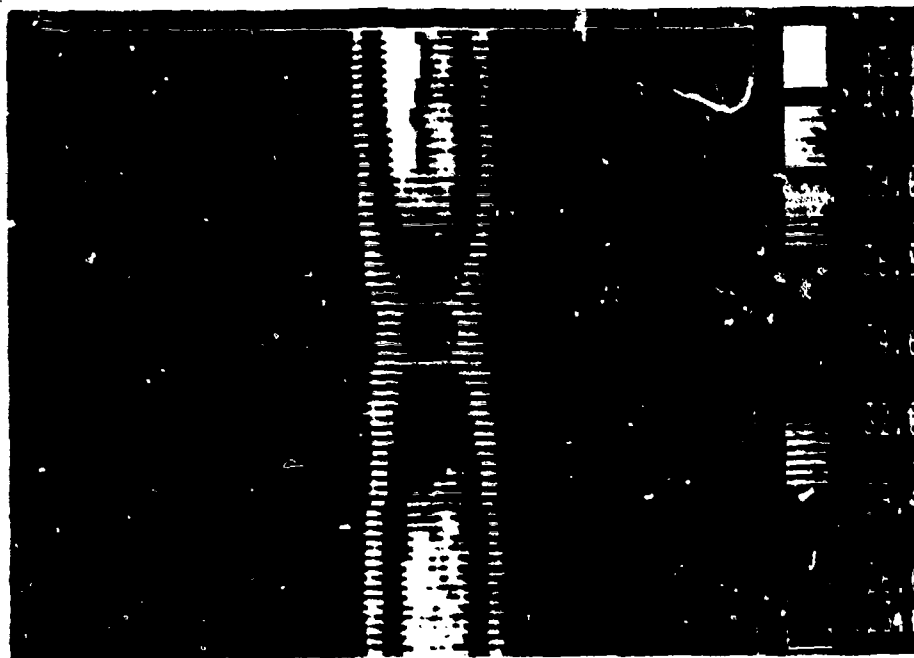


Fig 60 Ultrasonic C-scans of a woven plain coupon with layup E (-45,02) tested in reversed axial fatigue at the stress level giving a mean life of 100,000 cycles. Left to right, scans after: 0 cycles at 1 dB steps, 1000 cycles at 1 dB steps, 10000 cycles at 1 dB steps, 50000 cycles at 1 dB steps, 100000 cycles at 1 dB steps



↑ Surface
temperature
°C

Fig 61 Infra-red thermogram of a woven hole coupon with layup E ($\pm 45,02$) tested in reversed axial fatigue at ± 400 MPa after 4000 cycles

REPORT DOCUMENTATION PAGE

Overall security classification of this page

UNCLASSIFIED

As far as possible this page should contain only unclassified information. If it is necessary to enter classified information, the box above must be marked to indicate the classification, e.g. Restricted, Confidential or Secret.

1. DRIC Reference (to be added by DRIC)	2. Originator's Reference RAE TR85059	3. Agency Reference N/A	4. Report Security Classification/Marking UNCLASSIFIED
5. DRIC Code for Originator 7673000W	6. Originator (Corporate Author) Name and Location Royal Aircraft Establishment, Farnborough, Hants, UK		
5a. Sponsoring Agency's Code N/A	6a. Sponsoring Agency (Contract Authority) Name and Location N/A		
7. Title A comparison of the fatigue performance of woven and non-woven CFRP laminates			
7a. (For Translations) Title in Foreign Language			
7b. (For Conference Papers) Title, Place and Date of Conference			
8. Author 1. Surname, Initials Curtis, P.T.	9a. Author 2 Moore, B.B.	9b. Authors 3, 4	10. Date June 1985
			Pages 98
			Refs. 20
11. Contract Number N/A	12. Period N/A	13. Project	14. Other Reference Nos.
15. Distribution statement (a) Controlled by - DRIC (b) Special limitations (if any) -			
16. Descriptors (Keywords) (Descriptors marked * are selected from TEST) Fatigue. Carbon fibre. Laminates. Woven fabric.			
17. Abstract Static and fatigue tests were carried out at room temperature on CFRP laminates with five lay-ups, of both woven and non-woven CFRP. S-N diagrams were produced for both zero-tension and reversed axial loading. Damage development was monitored by optical microscopy, ultrasonic C-scanning, video recording and infra-red thermography. Carbon fibre reinforced plastics made with woven fabric rather than non-woven material, had significantly poorer static and fatigue performance than non-woven material, due to distortion of the load carrying 0° fibres. When woven fabric was orientated at 45° to the load direction the tensile static and fatigue performance was slightly better than in non-woven ±45° material. Replacing the ±45° layers of a (±45/0) laminate with woven fabric had little effect on the static or fatigue strength. non-woven material, notched coupons under fatigue loading did not show the notch sensitivity that was so significant under static loading. However in woven material, because of the additional fatigue degradation processes associated with row crossover points in the weave, holed coupons never quite achieved notch insensitivity in fatigue.			